

การปรับปรุงตัวรองรับไทเทเนียมไดออกไซด์สำหรับตัวเร่งปฏิกิริยา Pd/TiO₂
ในปฏิกิริยาไฮโดรจิเนชันของเฮกไซนอลและปฏิกิริยาออกซิเดชันของเบนซิลแอลกอฮอล์



นางสาวพัชรภรณ์ วีระชนะศักดิ์

จุฬาลงกรณ์มหาวิทยาลัย
CHULALONGKORN UNIVERSITY

วิทยานิพนธ์นี้เป็นส่วนหนึ่งของการศึกษาตามหลักสูตรปริญญาวิทยาศาสตรดุษฎีบัณฑิต

สาขาวิชาวิศวกรรมเคมี ภาควิชาวิศวกรรมเคมี

คณะวิศวกรรมศาสตร์ จุฬาลงกรณ์มหาวิทยาลัย

บทคัดย่อและแฟ้มข้อมูลฉบับเต็มของวิทยานิพนธ์ตั้งแต่ปีการศึกษา 2554 ที่ให้บริการในคลังปัญญาจุฬาฯ (CUIR)

ปีการศึกษา 2556

เป็นแฟ้มข้อมูลของนิสิตที่ส่งมาขึ้นทะเบียนที่สำนักงานบัณฑิตวิทยาลัย

ลิขสิทธิ์ของจุฬาลงกรณ์มหาวิทยาลัย

The abstract and full text of theses from the academic year 2011 in Chulalongkorn University Intellectual Repository (CUIR) are the thesis authors' files submitted through the University Graduate School.

MODIFICATION OF TiO₂ SUPPORTS FOR Pd/TiO₂ CATALYSTS IN HYDROGENATION
OF HEXYNOL AND OXIDATION OF BENZYL ALCOHOL

Miss Patcharaporn Weerachawanasak



A Dissertation Submitted in Partial Fulfillment of the Requirements
for the Degree of Doctor of Engineering Program in Chemical Engineering

Department of Chemical Engineering

Faculty of Engineering

Chulalongkorn University

Academic Year 2013

Copyright of Chulalongkorn University

พีชราภรณ์ วีระชวณะศักดิ์ : การปรับปรุงตัวรองรับไทเทเนียมไดออกไซด์สำหรับตัวเร่งปฏิกิริยา Pd/TiO₂ ในปฏิกิริยาไฮโดรจิเนชันของเฮกไซนอลและปฏิกิริยาออกซิเดชันของเบนซิลแอลกอฮอล์. (MODIFICATION OF TiO₂ SUPPORTS FOR Pd/TiO₂ CATALYSTS IN HYDROGENATION OF HEXYNOL AND OXIDATION OF BENZYL ALCOHOL) อ.ที่ปรึกษาวิทยานิพนธ์หลัก: รศ. ดร.จูงใจ ปั่นประณต , หน้า.

ศึกษาลักษณะพื้นผิวของตัวรองรับไทเทเนียมไดออกไซด์ที่ทำการปรับปรุงด้วยสารประกอบสามอะมิโนโพรพิลไตรเอทอกซีไซเลนหรือ APTES ที่ความเข้มข้นแตกต่างกัน ผลการวิเคราะห์ด้วยเทคนิคเอกซเรย์โฟโตอิเล็กตรอนสเปกโทรสโคปีและกล้องจุลทรรศน์อิเล็กตรอนแบบส่องกราดพบว่า การจัดเรียงตัวแบบชั้นเดียวของ APTES บนตัวรองรับไทเทเนียมไดออกไซด์จะเกิดขึ้นเมื่อความเข้มข้นของ APTES เท่ากับ 0.1 มิลลิโมลาร์ ต่อ 1.5 กรัมของไทเทเนียมไดออกไซด์ เมื่อความเข้มข้นของ APTES มีค่ามากเกินไป (1, 10 มิลลิโมลาร์) จะทำให้เกิดการจัดเรียงตัวแบบหลายชั้นของ APTES และเกิดการเกาะของหมู่อะมิโนบนพื้นผิวของไทเทเนียมไดออกไซด์มากกว่าการให้หมู่อะมิโนอิสระ นอกจากนี้งานวิจัยนี้ยังศึกษาคุณลักษณะของตัวเร่งปฏิกิริยาแพลเลเดียมบนตัวรองรับไทเทเนียมไดออกไซด์ที่ไม่ได้ปรับปรุงและที่ปรับปรุงพื้นผิวด้วย APTES ที่เตรียมด้วยวิธีแตกต่างกัน 3 วิธีได้แก่ วิธีการพอกพูนโดยไม่ใช้ไฟฟ้า วิธีอัลตราโซนิก และวิธีการยึดเกาะของอนุภาคคอลลอยด์ พบว่าตัวเร่งปฏิกิริยาแพลเลเดียมบนตัวรองรับไทเทเนียมไดออกไซด์ที่ปรับปรุงพื้นผิวด้วย APTES ความเข้มข้น 0.1 มิลลิโมลาร์ ซึ่งเตรียมด้วยวิธีการพอกพูนแบบไม่ใช้ไฟฟ้าให้ประสิทธิภาพในการเร่งปฏิกิริยาสูงที่สุดทั้งในปฏิกิริยาออกซิเดชันแบบเลือกเกิดในวัฏภาคของเหลวของเบนซิลแอลกอฮอล์และปฏิกิริยาไฮโดรจิเนชันแบบเลือกเกิดในวัฏภาคของเหลวของ 3-เฮกไซน์-1-ออล ทั้งนี้เป็นผลเนื่องมาจากการมีปริมาณของโลหะแพลเลเดียมบนพื้นผิวดังกล่าวที่สูง รวมถึงการมีโลหะ Pd⁰ และ PdO_x (1 ≤ x ≤ 2) จะให้ค่าการเร่งปฏิกิริยาออกซิเดชันที่สูง เพราะโลหะ Pd⁰ จะมีปริมาณเพิ่มมากขึ้นเมื่อเกิด in-situ ริดักชันของ PdO_x จากการดูดซับเบนซิลแอลกอฮอล์ นอกจากนี้ยังพบว่าอัตราการเกิดปฏิกิริยาไฮโดรจิเนชันของตัวเร่งปฏิกิริยาแพลเลเดียมบนตัวรองรับไทเทเนียมไดออกไซด์ที่ปรับปรุงพื้นผิวด้วย APTES ซึ่งเตรียมด้วยวิธีการพอกพูนแบบไม่ใช้ไฟฟ้าและวิธีอัลตราโซนิกจะมีค่าเพิ่มสูงขึ้นเมื่อมีอิเล็กตรอนเคลื่อนที่จากหมู่อะมิโนไปยังโลหะแพลเลเดียม และสำหรับตัวเร่งปฏิกิริยาแพลเลเดียมบนตัวรองรับไทเทเนียมไดออกไซด์ที่เตรียมด้วยวิธีอัลตราโซนิกแบบรีดิวซ์โดยใช้ก๊าซไฮโดรเจน พบว่าแพลเลเดียมที่มีขนาดเล็กและใกล้เคียงกันสามารถเกิดอันตรกิริยาที่แข็งแรงระหว่างโลหะและตัวรองรับได้เมื่อทำการรีดิวซ์ที่อุณหภูมิ 500 องศาเซลเซียส ในขณะที่ตัวเร่งปฏิกิริยาแพลเลเดียมบนตัวรองรับไทเทเนียมไดออกไซด์ที่เตรียมด้วยวิธีเคลือบฝังจะทำให้เกิดการรวมตัวกันของแพลเลเดียมขนาดใหญ่ขึ้นแทนการเกิดอันตรกิริยาที่แข็งแรงระหว่างโลหะและตัวรองรับ

ภาควิชา วิศวกรรมเคมี

ลายมือชื่อนิสิต

สาขาวิชา วิศวกรรมเคมี

ลายมือชื่อ อ.ที่ปรึกษาวิทยานิพนธ์หลัก

ปีการศึกษา 2556

5171851921 : MAJOR CHEMICAL ENGINEERING

KEYWORDS: TIO₂ / 3-(AMINOPROPYL)TRIETHOXSILANE / OXIDATION OF BENZYL ALCOHOL / HYDROGENATION OF 3-HEXYN-1-OL / PD/TIO₂ CATALYST

PATCHARAPORN WEERACHAWANASAK: MODIFICATION OF TiO₂ SUPPORTS FOR Pd/TiO₂ CATALYSTS IN HYDROGENATION OF HEXYNOL AND OXIDATION OF BENZYL ALCOHOL. ADVISOR: ASSOC. PROF. JOONGJAI PANPRANOT, Ph.D., pp.

The characteristics of surface modification of TiO₂ support with various concentrations of 3-(aminopropyl)triethoxysilane (APTES) were investigated. As revealed by X-ray photoelectron spectroscopy (XPS) and scanning electron microscopy (SEM) results, monolayer APTES grafting was obtained using 0.1mM of APTES on 1.5 g of TiO₂ support. Excess APTES concentrations (e.g. 1, 10 mM) resulted in both multilayer and reversed attachment, which NH₂-groups attached on TiO₂ surface rather than giving free NH₂ termination. In addition, three different preparation methods namely electroless deposition (ED), sonochemical (SN), and sol immobilization (IM) were used to prepare Pd catalysts supported on the TiO₂ and APTES modified TiO₂. The 1%Pd/TiO₂-0.1APTES catalysts prepared by ED exhibited the best catalytic performances in both liquid-phase selective oxidation of benzyl alcohol and liquid-phase selective hydrogenation of 3-hexyn-1-ol because high amounts of Pd were deposited on catalyst surface. In addition, the presence of both metallic Pd⁰ and PdO_x (1 ≤ x ≤ 2) gave high catalytic activity in the benzyl alcohol oxidation, suggesting the formation of highly metallic Pd⁰ sites via the in-situ reduction of PdO/PdO₂ by the adsorbed benzyl alcohol. Moreover, the hydrogenation rate was found to increase when electron donating from NH₂ termination of APTES molecules to the metallic Pd⁰ species occurred in case of Pd supported on APTES modified TiO₂ catalysts derived by ED and SN methods. For 1%Pd/TiO₂(S) catalyst prepared by the sonochemical method with H₂ reduction, the SMSI effect occurred during high temperature reduction at 500 °C whereas the conventional catalyst derived by incipient wetness impregnation method showed the absence of SMSI and sintering of metallic Pd⁰ particles was observed instead.

Department: Chemical Engineering Student's Signature

Field of Study: Chemical Engineering Advisor's Signature

Academic Year: 2013

ACKNOWLEDGEMENTS

I would like to express my sincere thanks to my thesis advisor, Associate Professor Dr. Joongjai Panpranot for her invaluable help and constant encouragement throughout the course of this research. I am most grateful for her teaching and advice. I would not have achieved this far and this thesis would not have been completed without all the support that I have always received from her.

I also would like to thank my committee members, Associate Professor Dr. Anongnat Somwangthanaroj, Associate Professor Dr. Bunjerd Jongsomjit, Dr. Akawat Sirisuk, and Assistant Professor Dr. Okorn Mekasuwandumrong, for serving as my committee members even at hardship. I also want to thank you for letting my defense be an enjoyable moment, and for your brilliant comments and suggestions.

In addition, I am grateful for Professor. Graham J. Hutching of Cardiff Catalysis Institute, School of Chemistry, Cardiff University for suggestions and all his help.

I also would like to thanks for Professor. Masahiko Arai and Dr. Shin-Ichiro Fujita for providing my assistance to conduct research at the Graduate School of Engineering, Hokkaido University.

I also would like to thank the financial supports from the Royal Golden Jubilee Ph.D. scholarship from Thailand Research Fund, and Chulalongkorn University.

Finally, I most gratefully acknowledge my parents, my family and my friends for all their support throughout the period of this research.

CHULALONGKORN UNIVERSITY

CONTENTS

| | Page |
|--|------|
| THAI ABSTRACT | iv |
| ENGLISH ABSTRACT | v |
| ACKNOWLEDGEMENTS | vi |
| CONTENTS | vii |
| LIST OF TABLES | xii |
| LIST OF FIGURES | xiv |
| CHAPTER I INTRODUCTION | 1 |
| 1.1 Rational..... | 1 |
| 1.2 Research objectives | 4 |
| 1.3 Research scopes | 5 |
| 1.4 Research methodology | 7 |
| CHAPTER II THEORY | 9 |
| 2.1 Titanium dioxide (TiO ₂)..... | 9 |
| 2.1.1 Applications of TiO ₂ | 10 |
| 2.2 Palladium..... | 13 |
| 2.3 Electroless deposition | 15 |
| 2.4 Hydrogenation of alkyne..... | 17 |
| 2.5 Benzyl alcohol oxidation | 22 |
| CHAPTER III LISTERATURE REVIEWS..... | 24 |
| 3.1 Supported Pd catalyst in liquid-phase hydrogenation | 24 |
| 3.2 Supported Pd catalyst in alcohol oxidation..... | 28 |
| 3.3 Role of TiO ₂ in the selective hydrogenation and oxidation | 29 |
| 3.4 Modification of TiO ₂ with 3-(aminopropyl)triethoxysilane (APTES) | 34 |
| CHAPTER IV EXPERIMENTAL..... | 38 |
| 4.1 Surface modification of TiO ₂ support with APTES | 38 |
| 4.2 Preparation of Pd supported on TiO ₂ catalysts..... | 39 |
| 4.2.1 Electroless deposition (ED)..... | 40 |

| | Page |
|--|------|
| 4.2.2 Sonochemical (SN, S)..... | 41 |
| 4.2.3 Sol immobilization (IM)..... | 43 |
| 4.2.4 Incipient wetness impregnation (I)..... | 44 |
| 4.3 Reaction study..... | 45 |
| 4.3.1 The liquid-phase selective hydrogenation of 3-hexyn-1-ol to cis-3-hexen-1-ol procedure..... | 45 |
| 4.3.2 The liquid-phase selective hydrogenation of phenylacetylene to styrene procedure..... | 47 |
| 4.3.3 The solvent-free selective oxidation of benzyl alcohol to benzaldehyde procedure..... | 49 |
| 4.4 Characterization techniques | 51 |
| 4.4.1 X-ray Diffraction (XRD)..... | 51 |
| 4.4.2 N ₂ Physisorption..... | 51 |
| 4.4.3 X-ray Photoelectron Spectroscopy (XPS) | 52 |
| 4.4.4 Scanning Electron Microscope (SEM)..... | 52 |
| 4.4.5 Transmission Electron Microscopy (TEM)..... | 52 |
| 4.4.6 Fourier Transform Infrared Spectroscopy (FTIR)..... | 53 |
| 4.4.7 CO-Pulse Chemisorption..... | 53 |
| 4.4.8 Inductive Coupled Plasma Optical Emission Spectrometer (ICP-OES)..... | 53 |
| CHAPTER V RESULTS AND DISCUSSION | 55 |
| Part I Surface modification of TiO ₂ supports with 3-(aminopropyl)triethoxysilane (APTES)..... | 56 |
| 5.1 The characteristics and properties of TiO ₂ and APTES modified TiO ₂ supports . 56 | |
| 5.1.1 N ₂ -physisorption..... | 56 |
| 5.1.2 X-Ray Diffraction (XRD)..... | 56 |
| 5.1.3 Fourier Transform Infrared Spectroscopy (FTIR)..... | 59 |
| 5.1.4 X-ray photoelectron spectroscopy (XPS)..... | 61 |
| 5.1.5 Scanning Electron Microscopy (SEM) | 66 |

| | |
|--|-----|
| Part II Comparative study the effect of catalysts preparation methods..... | 71 |
| 5.2 The characteristics and catalytic properties of 1%Pd/TiO ₂ catalysts prepared by electroless deposition method..... | 71 |
| 5.2.1 Catalyst characterizations..... | 71 |
| 5.2.1.1 X-ray diffraction (XRD)..... | 71 |
| 5.2.1.2 Transmission electron microscopy (TEM)..... | 73 |
| 5.2.1.3 X-ray photoelectron spectroscopy (XPS) | 76 |
| 5.2.1.4 Fourier transforms infrared spectroscopy (FTIR)..... | 79 |
| 5.2.2 The catalytic activity of 1%Pd/TiO ₂ catalysts prepared by electroless deposition in the solvent-free selective oxidation of benzyl alcohol. | 81 |
| 5.2.3 Catalytic activity of 1%Pd/TiO ₂ catalysts prepared by electroless deposition method in the liquid phase selective hydrogenation of 3-hexyn-1-ol..... | 85 |
| 5.3 The characteristics and catalytic properties of 1%Pd/TiO ₂ catalysts prepared by sonochemical method..... | 89 |
| 5.3.1 Catalyst characterizations..... | 89 |
| 5.3.1.1 X-ray diffraction (XRD)..... | 89 |
| 5.3.1.2 Transmission electron microscopy (TEM)..... | 91 |
| 5.3.1.3 X-ray photoelectron spectroscopy (XPS) | 94 |
| 5.3.1.4 Fourier transforms infrared spectroscopy (FTIR)..... | 97 |
| 5.3.2 Reaction study in the solvent-free selective oxidation of benzyl alcohol to benzaldehyde..... | 99 |
| 5.3.3 Reaction study in the liquid phase selective hydrogenation of 3-hexyn-1-ol to cis-3-hexen-1-ol..... | 102 |
| 5.4 The characteristics and catalytic properties of 1%Pd/TiO ₂ catalysts prepared by sol immobilization method | 106 |
| 5.4.1 Catalyst characterizations..... | 106 |
| 5.4.1.1 X-ray diffraction (XRD)..... | 106 |
| 5.4.1.2 Transmission electron microscopy (TEM)..... | 108 |

| | Page |
|--|------|
| 5.4.1.3 X-ray photoelectron spectroscopy (XPS) | 110 |
| 5.4.2 Reaction study in the solvent-free selective oxidation of benzyl alcohol to benzaldehyde | 113 |
| 5.4.3 Reaction study in the liquid phase selective hydrogenation of 3-hexyn-1-ol to cis-3-hexen-1-ol | 116 |
| 5.5 Comparative study the catalytic behavior for 1%Pd/TiO ₂ catalysts prepared by three different preparation methods | 120 |
| 5.5.1 The Pd supported on non-modified TiO ₂ catalysts | 120 |
| 5.5.1.1 Reaction study in solvent-free selective oxidation of benzyl alcohol to benzaldehyde | 120 |
| 5.5.1.2 Reaction study in the liquid phase selective hydrogenation of 3-hexyn-1-ol to cis-3-hexen-1-ol | 126 |
| 5.5.2 The Pd supported on APTES modified TiO ₂ catalysts | 130 |
| 5.5.2.1 Reaction study in solvent-free selective oxidation of benzyl alcohol to benzaldehyde | 130 |
| Part III Comparative study the characteristics and catalytic properties of 1%Pd/TiO ₂ catalysts prepared by sonochemical method with H ₂ reduction and incipient wetness impregnation method | 137 |
| 5.6 The characteristics and catalytic properties of 1%Pd/TiO ₂ catalysts prepared by sonochemical with H ₂ reduction and incipient wetness impregnation method | 137 |
| 5.6.1 Catalyst characterizations | 138 |
| 5.6.1.1 X-ray diffraction (XRD) | 138 |
| 5.6.1.2 Transmission electron microscopy (TEM) | 139 |
| 5.6.1.3 CO pulse chemisorption | 142 |
| 5.6.1.4 X-Ray photoelectron spectroscopy (XPS) | 143 |
| 5.6.2 Catalytic performance of 1%Pd/TiO ₂ (l) and 1%Pd/TiO ₂ (s) catalysts in the liquid phase selective hydrogenation of phenylacetylene to styrene | 146 |
| CHAPTER VI CONCLUSIONS AND RECOMMENDATIONS | 148 |
| 6.1 Conclusions | 148 |

| | Page |
|---------------------------|------|
| 6.2 Recommendations | 150 |
| REFERENCES | 151 |
| VITA..... | 182 |



จุฬาลงกรณ์มหาวิทยาลัย
CHULALONGKORN UNIVERSITY

LIST OF TABLES

| | |
|--|----|
| Table 2.1 Physical properties of palladium..... | 14 |
| Table 4.1 Chemicals used in modification of TiO ₂ supports | 39 |
| Table 4.2 Chemicals used in sensitization process for electroless deposition..... | 41 |
| Table 4.3 The chemical compositions of Pd electroless plating bath | 41 |
| Table 4.4 Chemicals used for 1%Pd/TiO ₂ catalysts prepared by sonochemical | 43 |
| Table 4.5 Chemicals used for 1%Pd/TiO ₂ catalysts prepared by sol immobilization.. | 44 |
| Table 4.6 Chemicals used for 1%Pd/TiO ₂ catalysts prepared by incipient wetness impregnation..... | 45 |
| Table 4.7 The operating conditions of gas chromatography (GC2014)..... | 46 |
| Table 4.8 Chemicals used in the liquid-phase hydrogenation of 3-hexyn-1-ol..... | 47 |
| Table 4.9 The operating conditions of gas chromatography (GC14B)..... | 48 |
| Table 4.10 Chemicals used in the liquid-phase hydrogenation of phenylacetylene... | 48 |
| Table 4.11 The operating conditions for gas chromatography (GC Varian star 3800 cx) | 50 |
| Table 4.12 Chemicals used in solvent-free liquid-phase selective oxidation of benzyl alcohol | 50 |
| Table 5.1 The peak position of anatase (101) TiO ₂ , d-spacing, lattice parameters and average crystallite size of TiO ₂ and APTES modified TiO ₂ supports | 58 |
| Table 5.2 The binding energy and surface compositions of TiO ₂ and APTES modified TiO ₂ supports..... | 66 |
| Table 5.3 The peak position of anatase (101) TiO ₂ , d-spacing and the lattice parameters of TiO ₂ for 1%Pd/TiO ₂ catalysts prepared by electroless deposition method. | 73 |

| | |
|--|-----|
| Table 5.4 Surface compositions and the relative abundance of Pd species of 1%Pd/TiO ₂ catalysts prepared by electroless deposition | 78 |
| Table 5.5 Solvent-free liquid-phase selective oxidation of benzyl alcohol to benzaldehyde for 1%Pd/TiO ₂ catalysts prepared by electroless deposition method at 7h. | 84 |
| Table 5.6 The peak position of anatase (101) TiO ₂ , d-spacing and the lattice parameters of TiO ₂ for 1%Pd/TiO ₂ catalysts prepared by sonochemical method. | 90 |
| Table 5.7 Surface compositions and the relative abundance of Pd species of 1%Pd/TiO ₂ catalysts prepared by sonochemical method | 96 |
| Table 5.8 Solvent-free selective oxidation of benzyl alcohol to benzaldehyde for 1%Pd/TiO ₂ catalysts prepared by sonochemical method at 7h..... | 101 |
| Table 5.9 The peak position of anatase (101) TiO ₂ , d-spacing and the lattice parameters of TiO ₂ for 1%Pd/TiO ₂ catalysts prepared by sol immobilization method. | 107 |
| Table 5.10 Surface compositions and the relative abundance of Pd species of 1%Pd/TiO ₂ catalysts prepared by sol immobilization method | 112 |
| Table 5.11 Solvent-free selective oxidation of benzyl alcohol to benzaldehyde for 1%Pd/TiO ₂ catalysts prepared by sol immobilization method at 7h. | 115 |
| Table 5.12 The XPS results of TiO ₂ and 1%Pd/TiO ₂ catalysts reduced at 40 and 500°C | 144 |
| Table 6.1 The characteristics of 1%Pd/TiO ₂ catalysts prepared by different methods | 148 |

LIST OF FIGURES

| | |
|--|----|
| Figure 2.1 Crystal structures of (a) anatase, (b) brookite, and (c) rutile..... | 9 |
| Figure 2.2 General reaction pathways of 3-hexyn-1-ol hydrogenation..... | 21 |
| Figure 2.3 General reaction pathways of benzyl alcohol oxidation..... | 23 |
| Figure 4.1 Structure of 3-(aminopropyl)triethoxysilane (APTES)..... | 39 |
| Figure 4.2 The schematic diagram of the liquid-phase hydrogenation system..... | 49 |
| Figure 4.3 The schematic diagram of the liquid-phase oxidation system..... | 51 |
| Figure 5.1 N ₂ adsorption-desorption isotherm of pristine TiO ₂ support..... | 57 |
| Figure 5.2 The XRD patterns of pristine TiO ₂ and APTES modified TiO ₂ supports..... | 58 |
| Figure 5.3 FTIR spectra of pristine TiO ₂ and APTES modified TiO ₂ supports with various concentrations of APTES..... | 60 |
| Figure 5.4 The XPS spectra of (a) Ti 2p, (b) O 1s for TiO ₂ and APTES modified TiO ₂ supports..... | 64 |
| Figure 5.5 The XPS spectra of (c) N 1s, and (d) Si 2p for TiO ₂ and APTES modified TiO ₂ supports..... | 65 |
| Figure 5.6 SEM micrographs with the quantitative line scan analysis of (a) TiO ₂ - 0.1APTES and (b) TiO ₂ -10APTES..... | 68 |
| Figure 5.7 SEM quantitative line scan of Si contents on TiO ₂ -0.1APTES and TiO ₂ - 10APTES..... | 69 |
| Figure 5.8 The features of APTES attachment modes with various APTES concentrations..... | 70 |
| Figure 5.9 The XRD patterns of 1%Pd/TiO ₂ catalysts prepared by electroless deposition method..... | 72 |

| | |
|---|----|
| Figure 5.10 TEM micrographs and Pd particles size distributions of 1%Pd/TiO ₂ catalysts prepared by electroless deposition method (a) 1%Pd/TiO ₂ -ED, (b) 1%Pd/TiO ₂ -0.1APTES-ED, (c) 1%Pd/TiO ₂ -1APTES-ED, and (d) 1%Pd/TiO ₂ -10APTES-ED | 74 |
| Figure 5.11 The XPS spectra of Pd 3d for 1%Pd/TiO ₂ catalysts prepared by electroless deposition method | 77 |
| Figure 5.12 FTIR spectra of pristine TiO ₂ and 1%Pd/TiO ₂ catalysts prepared by electroless deposition method | 80 |
| Figure 5.13 The mechanism for <i>in-situ</i> reduction of PdO _x to metallic Pd ⁰ by hydrogen spillover from the benzyl alcohol during the benzyl alcohol oxidation. . | 83 |
| Figure 5.14 Conversion of 3-hexyn-1-ol for 1%Pd/TiO ₂ catalysts prepared by electroless deposition with different reaction times | 87 |
| Figure 5.15 Selectivity of cis-3-hexen-1-ol for 1%Pd/TiO ₂ catalysts prepared by electroless deposition with different reaction times | 87 |
| Figure 5.16 The catalytic performance for 1%Pd/TiO ₂ catalysts prepared by electroless depositions in the liquid phase selective hydrogenation of 3-hexyn-1-ol | 88 |
| Figure 5.17 The XRD patterns of 1%Pd/TiO ₂ catalysts prepared by sonochemical method | 90 |
| Figure 5.18 TEM micrographs and Pd particles size distributions of 1%Pd/TiO ₂ catalysts prepared by sonochemical method (a) 1%Pd/TiO ₂ -SN, (b) 1%Pd/TiO ₂ -0.1APTES-SN, (c) 1%Pd/TiO ₂ -1APTES-SN, and (d) 1%Pd/TiO ₂ -10APTES-SN | 92 |

| | | |
|-------------|--|-----|
| Figure 5.19 | The XPS spectra of Pd 3d for 1%Pd/TiO ₂ catalysts prepared by sonochemical method..... | 95 |
| Figure 5.20 | FTIR spectra of pristine TiO ₂ and 1%Pd/TiO ₂ catalysts prepared by sonochemical method..... | 98 |
| Figure 5.21 | Conversion of 3-hexyn-1-ol for 1%Pd/TiO ₂ catalysts prepared by sonochemical method with different reaction times..... | 104 |
| Figure 5.22 | Selectivity of cis-3-hexen-1-ol for 1%Pd/TiO ₂ catalysts prepared by sonochemical method with different reaction times..... | 104 |
| Figure 5.23 | The catalytic performance for 1%Pd/TiO ₂ catalysts prepared by sonochemical in the liquid phase selective hydrogenation of 3-hexyn-1-ol..... | 105 |
| Figure 5.24 | The XRD patterns of 1%Pd/TiO ₂ catalysts prepared sol immobilization method..... | 107 |
| Figure 5.25 | TEM micrographs and Pd particles size distributions of 1%Pd/TiO ₂ catalysts prepared by sol immobilization method (a) 1%Pd/TiO ₂ -IM, (b) 1%Pd/TiO ₂ -0.1APTES-IM, and (c) 1%Pd/TiO ₂ -10APTES-IM..... | 109 |
| Figure 5.26 | The XPS spectra of Pd 3d for 1%Pd/TiO ₂ catalysts prepared by sol immobilization method..... | 111 |
| Figure 5.27 | Conversion of 3-hexyn-1-ol for 1%Pd/TiO ₂ catalysts prepared by sol immobilization method with different reaction times..... | 118 |
| Figure 5.28 | Selectivity of cis-3-hexen-1-ol for 1%Pd/TiO ₂ catalysts prepared by sol immobilization method with different reaction times..... | 118 |

| | | |
|-------------|---|-----|
| Figure 5.29 | The catalytic performance for 1%Pd/TiO ₂ catalysts prepared by sol immobilization method in the liquid phase selective hydrogenation of 3-hexyn-1-ol | 119 |
| Figure 5.30 | Conversion of benzyl alcohol as a function of reaction time for 1%Pd/TiO ₂ catalysts | 124 |
| Figure 5.31 | Selectivity of benzaldehyde as a function of reaction time for 1%Pd/TiO ₂ catalysts | 124 |
| Figure 5.32 | Selectivity of toluene as a function of reaction time for 1%Pd/TiO ₂ catalysts | 125 |
| Figure 5.33 | Conversion of 3-hexyn-1-ol as a function of reaction time for 1%Pd/TiO ₂ catalysts | 128 |
| Figure 5.34 | Selectivity of cis-3-hexen-1-ol as a function of reaction time for 1%Pd/TiO ₂ catalysts | 128 |
| Figure 5.35 | The catalytic performance of 1%Pd/TiO ₂ catalysts in the liquid phase selective hydrogenation of 3-hexyn-1ol..... | 129 |
| Figure 5.36 | Conversion of benzyl alcohol as a function of reaction time for 1%Pd/TiO ₂ -0.1APTES catalysts..... | 132 |
| Figure 5.37 | Selectivity of benzaldehyde as a function of reaction time for 1%Pd/TiO ₂ -0.1APTES catalysts..... | 133 |
| Figure 5.38 | Selectivity of toluene as a function of reaction time for 1%Pd/TiO ₂ -0.1APTES catalysts | 133 |
| Figure 5.39 | Conversion of 3-hexyn-1-ol as a function of reaction time for APTES modified 1%Pd/TiO ₂ catalysts | 135 |

| | | |
|--------------|---|-----|
| Figure 5.40 | Selectivity of cis-3-hexen-1-ol as a function of reaction time for APTES modified 1%Pd/TiO ₂ catalysts..... | 136 |
| Figure 5. 41 | The catalytic performance of 1%Pd/TiO ₂ -0.1APTES catalysts in the liquid- phase selective hydrogenation of 3-hexyn-1-ol | 136 |
| Figure 5.42 | The XRD patterns of TiO ₂ support and 1%Pd/TiO ₂ catalysts | 138 |
| Figure 5.43 | TEM micrographs of (a) 1%Pd/TiO ₂ (l)-R40, (b) 1%Pd/TiO ₂ (l)-R500, (c) 1%Pd/TiO ₂ (S)-R40, and (d) 1%Pd/TiO ₂ (S)-R500 catalysts | 140 |
| Figure 5.44 | Particle sizes distribution of (a) 1%Pd/TiO ₂ (l) and (b) 1%Pd/TiO ₂ (S) catalysts..... | 141 |
| Figure 5.45 | The CO chemisorption results for 1%Pd/TiO ₂ (l) and 1%Pd/TiO ₂ (S) catalysts | 142 |
| Figure 5.46 | The Pd 3d XPS spectra of (a) 1%Pd/TiO ₂ (l) and (b) 1%Pd/TiO ₂ (S)..... | 145 |
| Figure 5.47 | The conversion of phenylacetylene for 1%Pd/TiO ₂ (l) and 1%Pd/TiO ₂ (S) catalysts as a function of reaction time..... | 147 |
| Figure 5.48 | The selectivity of styrene for 1%Pd/TiO ₂ (l) and 1%Pd/TiO ₂ (S) catalysts as a function of reaction time. | 147 |

CHAPTER I

INTRODUCTION

1.1 Rational

The liquid-phase selective hydrogenation of alkyne to alkene remains one of the most intensely studied fields of research in catalysis, particularly in the field of fine chemical productions and pharmaceuticals [1, 2]. Many intermediate valuable compounds can be produced or the undesired compounds can be removed using this reaction [3, 4]. Generally, liquid-phase selective hydrogenation can be performed in batch type slurry process or continuous flow process but a large number of these reactions are carried out using batch type operation. The main goal of this reaction is to obtain the highest alkenes selectivity with high activity in alkynes hydrogenation.

The liquid-phase selective oxidation of alcohol to the corresponding aldehyde is an importance transforming functional groups in organic synthesis, especially for primary alcohol [5, 6]. The corresponding aldehydes or ketones are both valuable intermediates and high value products for the pharmaceuticals, agrochemicals, and perfume industries [7]. Traditionally, the oxidation of alcohol has been carried out using stoichiometric oxygen donors such as chromate or permanganate. However, recently using of environmentally benign oxidants (e.g. molecular oxygen) with the heterogeneous transition metal catalysts has been received more attention [8, 9].

Heterogeneous catalysts which prepared from the noble metals group VIII, especially for Pd metal, have received much interested in both liquid-phase selective hydrogenation of alkyne to alkene and liquid-phase selective oxidation of alcohol to aldehyde because they exhibit high catalytic activity and less agglomeration of active

species during chemical reaction, enable easy catalyst recovery and simplify catalyst handling. Additionally, the performance of noble metal catalysts has been found to be dependent on several factors such as liquid composition (substrate structure, solvent effect, etc.), catalyst nature (elemental composition, morphology, support effects, modifiers, etc.) and reaction conditions (temperature, pressure, etc.). For the liquid-phase selective hydrogenation of alkyne, the Pd catalysts have the unique ability to selectively hydrogenation [10]. As similar as for the liquid-phase selective oxidation of alcohol, Pd catalysts have attracted considerable attention because they show the superior catalytic performance relative to non-noble metals [11], including they can catalyze aerobic oxidation of both primary and secondary alcohols.

Several supports have been used for catalyst preparations such as SiO_2 [12, 13], Al_2O_3 [14-17], carbon [18, 19], mesostructure silica [6, 20] or TiO_2 [4, 21-24]. However, it is well known that TiO_2 is a reducible metal oxide support and it shows the strong interaction with group VIII noble metals than other metal oxide such as SiO_2 or Al_2O_3 [4, 25-28]. In this case, the catalytic performance in hydrogenation can be improved. Although, the effect of strong metal-support interaction (SMSI) was not much reported in selective oxidation of alcohol, Pd supported on TiO_2 catalyst also exhibited the good catalytic performance in selective oxidation of alcohol. Therefore, Pd supported on TiO_2 catalyst has attracted much attention for both reactions, selective hydrogenation of alkyne and selective oxidation of alcohol.

Titanium dioxide or TiO_2 is a versatile material used as pigment, UV-filter, coating, catalyst or catalyst support. For catalyst support, it exhibits attractive characteristics such as chemical stability, non-toxicity, environmental friendly and low cost. Generally, TiO_2 has three main crystal structures e.g. anatase, rutile and

brookite, and each structure exhibits different physical properties. Yuanzhi Li and co-worker [28] reported that Pd supported on anatase-TiO₂ manifested the strong-metal support interaction (SMSI) easier than Pd supported on rutile-TiO₂. In this case, the Pd/TiO₂ catalysts with SMSI were found to exhibit higher selectivity for anatase -TiO₂ supported Pd catalyst than rutile-TiO₂ supported one. Therefore, TiO₂-anatase has been extensively used as catalyst support. Moreover, in my previous work the effect of anatase-TiO₂ crystallite sizes on the SMSI was investigated in the liquid-phase selective hydrogenation of phenylacetylene [4, 27]. It was found that reduction with H₂ at high temperature (500°C) resulted in the SMSI for the nano-sized TiO₂ supported Pd catalyst but not for the micron-sized TiO₂ supported one. The SMSI appeared to be necessary for high catalytic performance of the Pd/TiO₂ catalysts in the liquid-phase selective hydrogenation of phenylacetylene to styrene. However, high metal dispersion is an important factor affecting catalytic activity in the liquid-phase hydrogenation. From our knowledge, the Pd supported on micron-TiO₂ showed low Pd dispersion, sintering of Pd metal and absented of SMSI effect at high temperature reduction. Thus, the improvement of metal catalysts dispersion on the micron-sized TiO₂ is necessary for the liquid-phase selective hydrogenation.

Generally, support modification is used for changing surface properties of support such as surface area, surface defect, surface acidity or basicity of the support, etc., which results in dispersion of active metal catalyst. Both of organic and inorganic compounds have been used for support modification. Nevertheless, the modification of TiO₂ support with organometallic compounds various functional groups has attracted wide attention. Because of different functional groups on TiO₂ surface affects to weak or strong interaction of subsequent binding metal. There are

many functional groups which used to modify the metal oxide supports such as phosphonate, carboxylate or amine. Among of these, amine functional group is frequently used to modify the metal oxide supports. Terminal amine is generally obtained from silane coupling agents such as 3-(aminopropyl)triethoxysilane (APTES), 3-(aminopropyl)diethoxysilane (APDES), or 3-(aminopropyl)monoethoxysilane (APMES) etc. APTES is one of the most typical agent that use to modify on metal oxide because APTES tends to organize on oxide surface into self-assembled monolayer and free amine groups give high binding affinity to stabilize metal nanoparticles [29-31]. Nevertheless, the APTES attachment on TiO_2 to promote the dispersion of Pd catalyst has not been investigated. Furthermore, particular problem related to APTES modification is its tendency to form multilayer instead of monolayer and it can be occurred reverse attachment on the surface of metal oxide.

1.2 Research objectives

1. To investigate the characteristics of surface modification of TiO_2 supports with 3-(aminopropyl)triethoxysilane (APTES) by post synthesis grafting method.
2. To investigate the characteristics and catalytic properties of Pd supported on APTES modified- TiO_2 catalysts prepared by electroless deposition (ED), sonochemical (SN), and sol immobilization (IM) methods in the liquid-phase selective hydrogenation of 3-hexyn-1-ol to cis-3-hexen-1-ol and the solvent free liquid-phase selective oxidation of benzyl alcohol to benzaldehyde.
3. To investigate the characteristics and catalytic properties of Pd supported on TiO_2 catalysts prepared by sonochemical method with H_2 reduction

compared with that one prepared by incipient wetness impregnation method in the liquid-phase selective hydrogenation of phenylacetylene to styrene.

1.3 Research scopes

Part I, II

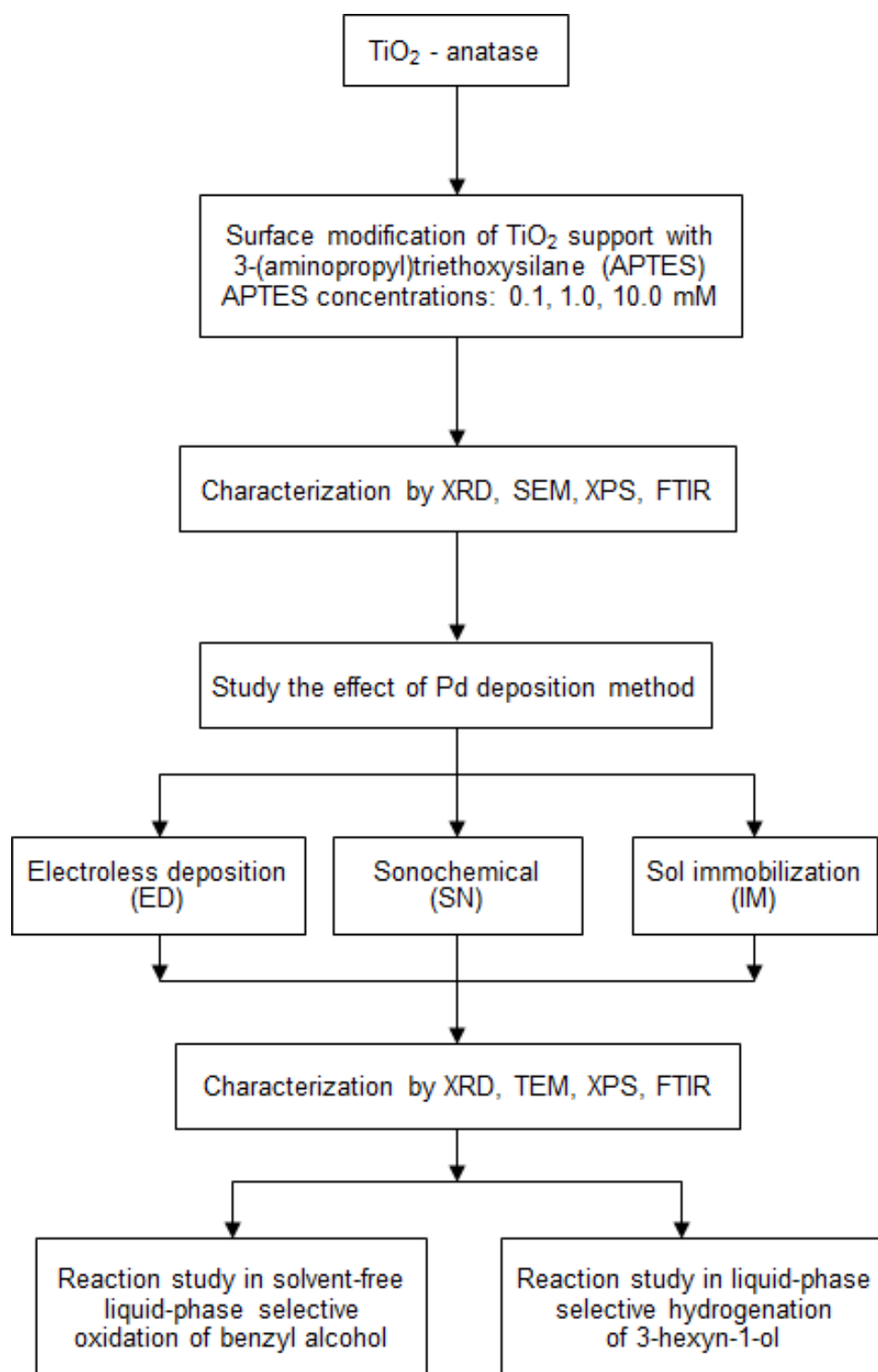
1. Commercial TiO_2 support available from Sigma-Aldrich has been used in this research.
2. The TiO_2 support was modified by APTES under various concentrations of APTES 0.1, 1, and 10 mM by post synthesis grafting method.
3. Pd catalysts supported on the APTES modified TiO_2 were prepared by different preparation methods, electroless deposition, sonochemical and sol immobilization methods with Pd loading ca. 1% by weight.
4. The APTES modified TiO_2 supports and all 1%Pd/ TiO_2 catalysts were characterized by several techniques such as X-ray diffraction (XRD), Fourier transforms infrared spectroscopy (FTIR), inductively coupled plasma (ICP), scanning electron microscopy (SEM), transmission electron microscopy (TEM), and X-ray photoelectron spectroscopy (XPS).
5. The catalytic performances of all 1%Pd/ TiO_2 catalysts were evaluated in both reactions. The first one is the liquid-phase selective hydrogenation of 3-hexyn-1-ol to cis-3-hexen-1-ol using 100 ml stainless steel autoclave reactor and the second one is the solvent free liquid-phase selective oxidation of benzyl alcohol to benzaldehyde using 50 ml glass stirred reactor.

Part III

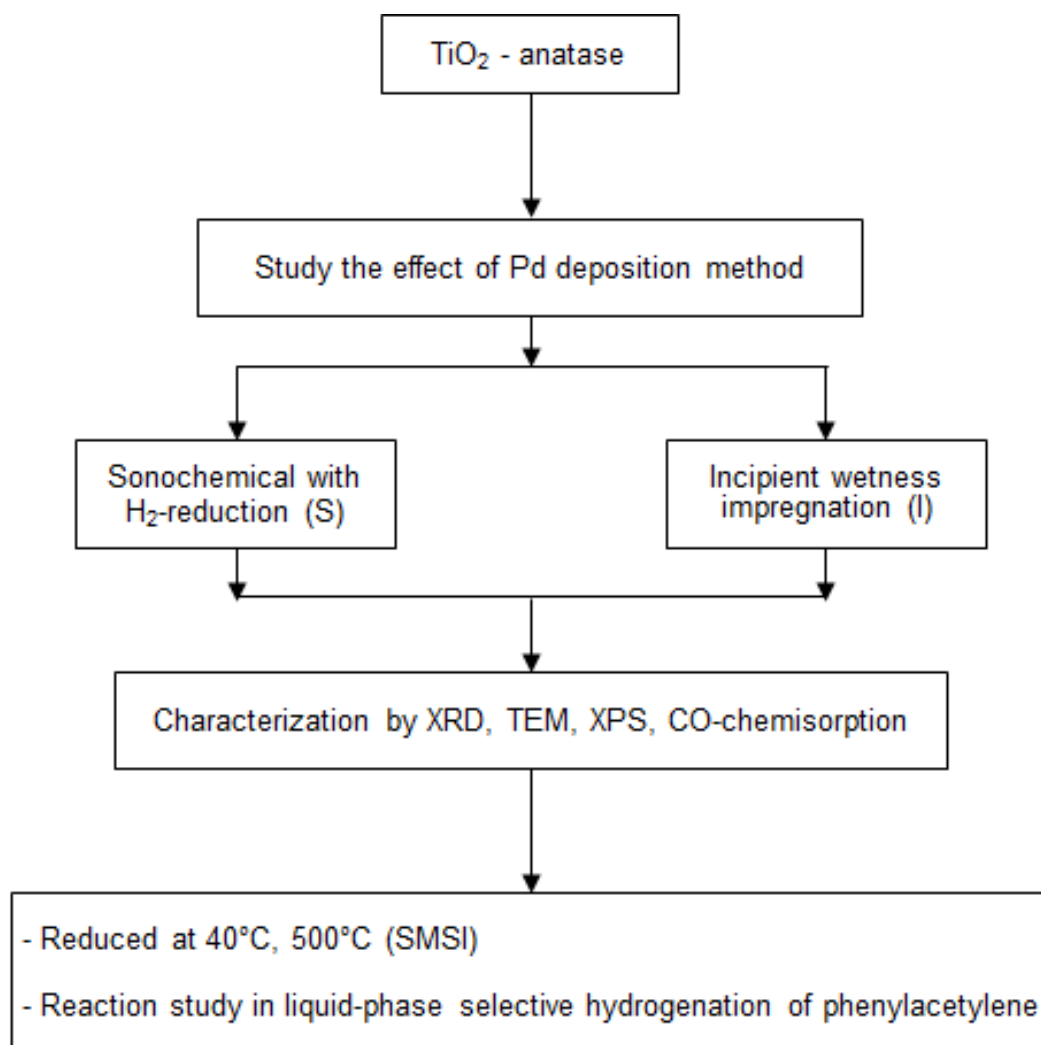
1. Pd supported on TiO_2 catalysts were prepared by sonochemical with H_2 reduction and incipient wetness impregnation method with Pd loading ca. 1% by weight.
2. All 1%Pd/ TiO_2 catalysts were characterized by several techniques such as X-ray diffraction (XRD), CO pulse chemisorption, transmission electron microscopy (TEM), and X-ray photoelectron spectroscopy (XPS).
3. The catalytic performances of all 1%Pd/ TiO_2 catalysts were evaluated the liquid-phase selective hydrogenation of phenylacetylene to styrene using 50 ml stainless steel autoclave reactor.

1.4 Research methodology

Part I, II



Part III



CHAPTER II

THEORY

2.1 Titanium dioxide (TiO₂)

Titanium dioxide, titanium (IV) oxide or well-known as titania is the naturally occurring oxide of titanium. Its chemical formula is TiO₂. There are three major different crystalline structures, anatase (tetragonal), rutile (tetragonal) and brookite (orthorhombic). Their crystalline structures are illustrated in **Figure 2.1**. Rutile is the most thermally stability form. Anatase and brookite tend to be more stable at lower temperatures and they transformed to rutile with upon heating. The transformation from anatase to rutile is accompanied by the evolution of ca. 12.6 kJ/mol (3.01 kcal/mol), but the rate of transformation is greatly affected by temperature and by the presence of other substance which may either catalyze or inhibit the reaction. The change is not reversible; ΔG for the change from anatase to rutile is always negative. While anatase and rutile TiO₂ have been extensively studied and used in many aspects, brookite TiO₂ is scarce and difficult to purify.

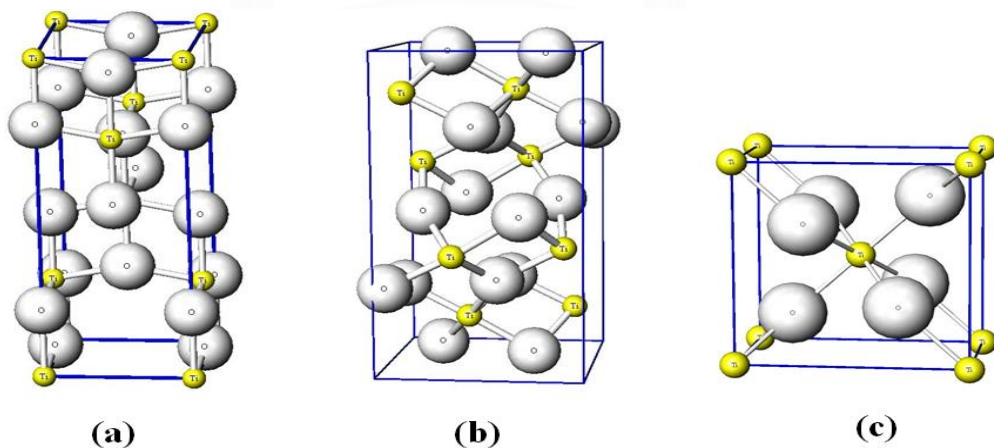


Figure2. 1 Crystal structures of (a) anatase, (b) brookite, and (c) rutile

Both of rutile and anatase forms have a structure belonging to tetragonal crystal system but they are not isomorphous. The two tetragonal crystal types are more common because they are easy to make. Anatase occurs usually in near-regular octahedral, and rutile forms slender prismatic crystal, which are frequently twinned.

2.1.1 Applications of TiO₂

In the last decade, titanium dioxide is one of the most important materials for several industrials such as using as white pigment (e.g. cosmetics or plights), gas sensor, solar cell, corrosion protective coating, photocatalyst, catalyst support and etc. The major applications are demonstrated follow these topics.

- Pigment

Titanium dioxide is the most widely used white pigment because of its brightness and very high refractive index ($n = 2.7$), in which it is surpassed only by a few other materials. Approximately 4 million tons of pigmentary TiO₂ are consumed annually worldwide. When deposited as a thin film, its refractive index and colour make it an excellent reflective optical coating for dielectric mirrors. TiO₂ is also an effective opacifier in powder form, where it is employed as a pigment to provide whiteness and opacity to products such as paints, coatings, plastics, papers, inks, foods, medicines (i.e. pills and tablets) as well as most toothpastes. Opacity is improved by optimal sizing of the titanium dioxide particles.

Used as a white food coloring. Titanium dioxide is often used to whiten skimmed milk; this has been shown statistically to increase skimmed milk's palatability [32]. In cosmetic and skin care products, titanium dioxide is used both as a pigment and a thickener. It is also used as a tattoo pigment and in styptic pencils.

This pigment is used extensively in plastics and other applications for its UV resistant properties where it acts as a UV absorber, efficiently transforming destructive UV light energy into heat.

In ceramic glazes titanium dioxide acts as a pacifier and seeds crystal formation. Titanium dioxide is found in almost every sunscreen with a physical blocker because of its high refractive index, its strong UV light absorbing capabilities and its resistance to discoloration under ultraviolet light. This advantage enhances its stability and ability to protect the skin from ultraviolet light. Sunscreens designed for infants or people with sensitive skin are often based on titanium dioxide and/or zinc oxide, as these mineral UV blockers are believed to cause less skin irritation than chemical UV absorber ingredients. The titanium dioxide particles used in sunscreens have to be coated with silica or alumina, because titanium dioxide creates radicals in the photocatalytic reaction. These radicals are carcinogenic, and could damage the skin.

- Photocatalyst

Titanium dioxide, particularly in the anatase form, is a photocatalyst under ultraviolet light. Recently it has been found that TiO_2 , when spiked with nitrogen ions or doped with metal oxide like tungsten trioxide, is also a photocatalyst under visible and UV light. The strong oxidative potential of the positive holes oxidizes water to create hydroxyl radicals. It can also oxidize oxygen or organic materials directly. TiO_2 is thus added to paints, cements, windows, tiles, or other products for its sterilizing, deodorizing and anti-fouling properties and is used as a hydrolysis catalyst. It is also used in the Graetzel cell, a type of chemical solar cell.

The photocatalytic properties of titanium dioxide were discovered by Akira Fujishima in 1967 and published in 1972 [33, 34]. TiO_2 has potential for use in energy production: as a photocatalyst,

(1) TiO_2 can carry out hydrolysis; i.e., break water into hydrogen and oxygen. Were the hydrogen collected, it could be used as a fuel. The efficiency of this process can be greatly improved by doping the oxide with carbon.

(2) TiO_2 can also produce electricity when in nanoparticle form. Research suggests that by using these nanoparticles to form the pixels of a screen, they generate electricity when transparent and under the influence of light. If subjected to electricity on the other hand, the nanoparticles blacken, forming the basic characteristics of a LCD screen.

- Catalyst support

TiO_2 has been extensively used as catalyst support, particularly TiO_2 -anatase, since it exhibits a large number of attractive characteristic such as chemical stability, non-toxicity, low cost and high oxidation rates. Because heterogeneous catalysts consist of small metal clusters on the metal oxide support, many growth studies of metals on TiO_2 were performed. These metal/ TiO_2 systems often serve as a model for other metal/oxide surfaces. It is well known that the role of TiO_2 on catalytic activity is more complex than simple to increase catalyst surface area and interactions between the catalyst and TiO_2 may occur that lead to changes in reactivity and selectivity [35]. This change in catalytic properties has been attributed to the strong-metal support interaction effect (SMSI). It is the encapsulation of the metal particles by a reduced TiO_x overlayer.

Strong metal support interaction (SMSI) was found by Tauster et al in 1978. [36] SMSI is the loss of the metal's ability to chemisorb molecules which normally react without difficulty at metal surfaces: hydrogen and carbon monoxide [37]. Generally, the SMSI account for the changes in catalytic activity when the group VIII metals Fe, Ni, Rh, Pt, Pd, and Ir, supported on reducible oxides (TiO_2 , TaO_5 , CeO_2 , NbO , etc.), are reduced at elevated temperature. Furthermore, the effect of high reduction in hydrogen at high temperature is not to cause particle growth by sintering, so the loss of chemisorption capacity cannot be attributed to this. However transmission electron microscopy has revealed suggestions of alteration in the morphology of metal particles. Another notable feature of SMSI is that it is reversed by oxidizing conditions. Oxygen chemisorption is not suppressed, and any explanation of the effect must take account of this.

2.2 Palladium

Palladium is one of the six platinum group metal (the others being Pt, Rh, Ru, Ir, and Os). These metals commonly occur together in nature. These have similar chemical properties, but palladium has the lowest melting point and is the least dense of them. Palladium, as well as Pt, and sometimes Ir, is considered to be a precious and noble metal. Palladium does not tarnish in air at room temperature. Common oxidation states of palladium are 0, +1, +2 and +4. Although originally +3 was thought of as one of the fundamental oxidation states of palladium, there is no evidence for palladium occurring in the +3 oxidation state; this has been investigated via X-ray diffraction for a number of compounds, indicating a dimer of palladium(II) and palladium(IV) instead.

Palladium has unique catalytic properties in homogeneous and in heterogeneous reactions. In heterogeneous catalysis palladium is used for oxidation and hydrogenation reactions. One of the most remarkable properties of palladium is the ability to dissociate and dissolve hydrogen. Atomic hydrogen occupies the octahedral interstices between the Pd atoms of the cubic-closed packed metal. Palladium can absorb up to 900 times of its own volume of hydrogen at room temperature.

Table 2.1 Physical properties of palladium

| Property | Palladium |
|--------------------------------------|-----------------------|
| Atomic number | 46 |
| Atomic weight (g.mol ⁻¹) | 106.42 |
| Atomic radius (pm) | 137 |
| Density (g.cm ⁻³) | 12.023 |
| Electron configuration | [Kr] 4d ¹⁰ |
| Crystal structure | fcc |
| Melting point (K) | 1827 |

Palladium, the preferred metal of choice for alkynes selective hydrogenation, is normally used as a supported heterogeneous catalyst and frequently in presence of some form of additive to promote selectivity. Activity of palladium for hydrocarbon hydrogenation is based on the ability for the dissociative adsorption of hydrogen and chemisorption of unsaturated hydrocarbons. Palladium shows a strong deactivation behavior because of hydrocarbon and carbon deposits. For heterogeneous system in particular catalyst performance is strongly influence by,

firstly the ability to get reactant to the active sites, then to establish the optimum hydrogen-to-hydrocarbon surface coverage, and, finally, the rapid removal of the hydrogenated products.

2.3 Electroless deposition

Electroless deposition is an autocatalytic redox process in which metal ions are chemically reduced with an appropriate reducing agent at catalytic surface sites in the absence of any external electrical source leading to induce uniform metallic atoms deposited on substrate. This process has received more attention mainly due to its capability for metallization of non-conducting materials such as glass, ceramics and polymers. Nowadays, electroless deposition has been involved in many applications such as electronics industry and ceramic membrane etc. The advantages of electroless depositions are summarized as following:

- This process is simple and low cost.
- Uniform metals deposited on substrate can be obtained.
- The metallization can be occurred on non-conducting substrates.
- This process does not require the external electric sources.
- It gives a good adhesion between metal and substrate surface.

However, there are some disadvantages which can be observed in electroless deposition such as low deposition rate, metal loss, and difficult control of metal film thickness [38]. Generally, the conventional electroless deposition is consisted of three important processes, pretreating process, activation or sensitization process, and electroless plating process.

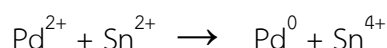
I. Pretreating process

In order to achieve good metal adhesion and control electroless plating, surface cleaning is an essential step, especially for non-conducting surface (plastics or ceramics). The composition of chemicals etching depended on the nature of substrate. Generally, alkaline and acid solutions are frequently used such as NaOH or HCl, etc. After pretreating process, the substrate surface which is not inherently catalytic, must be activated prior to electroless plating. Typically, Pd based catalysts are often used for the electroless metallization of dielectric materials and produce a seed layer of Pd on the surface.

II. Activation or sensitization process

A widely used Pd catalyst is based on combination of Sn and Pd chemistry. There are two conventional methods have been applied to catalyze the substrate surface. First one is a two-step process, which the substrate is placed in SnCl₂ solution following by activated in PdCl₂ solution. Second one is one-step process, which the mixture of SnCl₂-PdCl₂ colloidal solution is used for activation. However, the most extensively used system is the one-step process.

In this research, we used the one-step activation process for catalyst preparation. The Pd/Sn catalysts are prepared by mixing PdCl₂ with a large excess of SnCl₂ in HCl solution. The Pd²⁺ ions are reduced to metallic Pd⁰ by SnCl₂ via the following redox reaction.

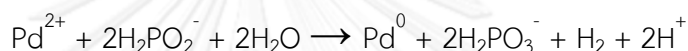


In this step, tin is not only acted as the reducing agent for Pd ions but it also stabilizes the small Pd nuclei via a strong Sn⁴⁺ adsorption [39]. The Pd nuclei

covering by Sn^{4+} species are distributed over the substrate surface, which become catalytically active for the successive deposition of a Pd metal layer.

III. Electroless plating process

For electroless plating process, the reducing metal ions by chemical reduction are deposited on substrate by control the pH of plating bath. In this research, Pd plating bath is used for prepared Pd/TiO₂ catalysts. Sodium hypophosphite was selected as reducing agent which used to reduce Pd²⁺ ions to metallic Pd⁰. The Pd²⁺ reduction by sodium hypophosphite can be written as following:



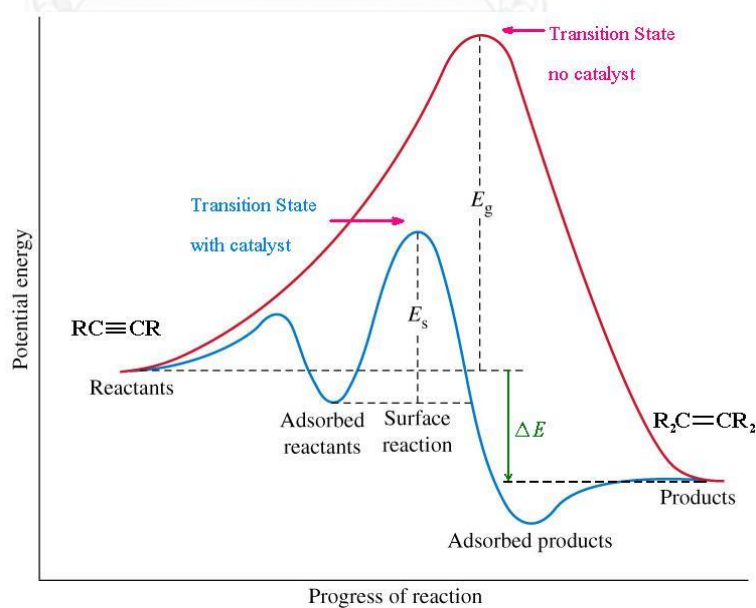
In addition, ammonium chloride (NH₄Cl) and ammonium hydroxide (NH₄OH) were used as a stabilizing agent and buffer solution for adjust the pH of electroless plating bath, respectively.

2.4 Hydrogenation of alkyne

Catalytic hydrogenation reaction is a well-known versatile reaction widely used in organic syntheses. Many functional groups contained in organic substrates can be hydrogenated to produce several useful compounds which has been used for wide applications such as monomers for production of various polymers, fats and oil for producing edible and no edible products, and intermediates used in pharmaceutical industry. Hydrogenation processes are often carried out in a small scale in batch reactor. Batch processes are usually most cost effective since the equipment need not to be dedicated to a single reaction. Typically the catalyst is powdered and slurries with reactant; a solvent is usually present to influence product selectivity and to adsorb the reaction heat liberated by the reaction. Since most hydrogenations

are highly exothermic, careful temperature control is required to achieve the desired selectivity and to prevent temperature runaway.

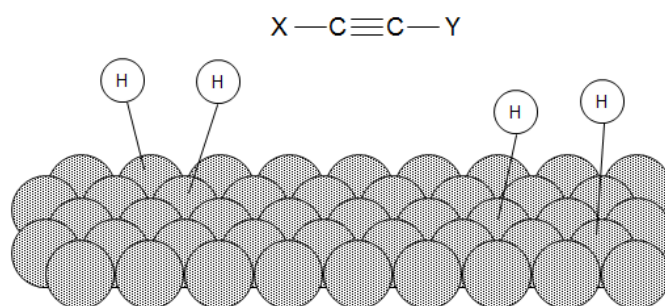
Selective hydrogenation of alkyne to alkene is an addition of hydrogen to a carbon-carbon triple bond in order to produce only alkene product. The overall effect of such an addition is the reductive removal of the triple bond functional group. The simplest source of two hydrogen atoms is molecular hydrogen (H_2), but mixing alkyne with hydrogen does not result in any discernable reaction. However, careful hydrogenation of alkyne proceeds exclusively to the alkene until the former is consumed, at which point the product alkene is very rapidly hydrogenated to an alkane. Although the overall hydrogenation reaction is exothermic, high activation energy prevents it from taking place under normal conditions. This restriction may be circumvented by the use of a catalyst, as shown in the following diagram.



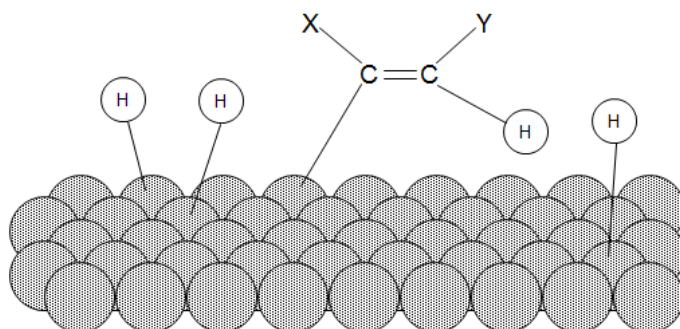
Catalysts are substances that change the rate (velocity) of a chemical reaction without being consumed or appearing as part of the product. Catalysts act by lowering the activation energy of reactions, but they do not change the relative potential energy of the reactants and products. Finely divided metals, such as platinum, palladium and nickel, are among the most widely used hydrogenation catalysts.

Selective hydrogenation of alkyne to alkene is the reaction which takes place on the surface of the metal catalyst. The mechanism of the reaction can be described in four steps:

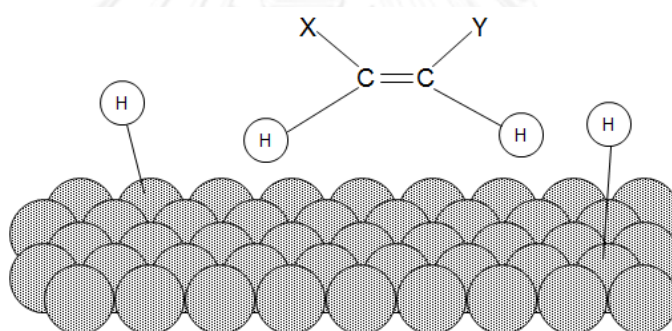
Step 1: Hydrogen molecules react with the metal atoms at the catalyst surface. The relatively strong H-H sigma bond is broken and replaced with two weak metal-H bonds.



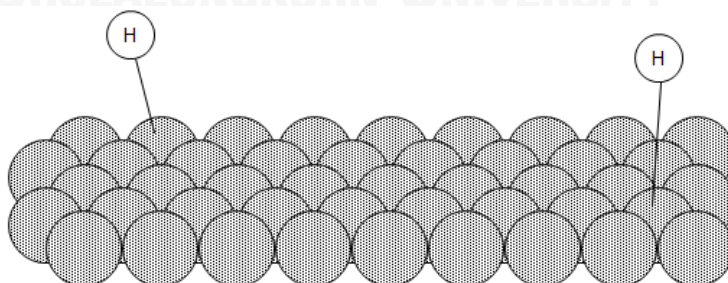
Step 2: The pi bond of the alkyne interacts with the metal catalyst weakening the bond. A hydrogen atom is transferred from the catalyst surface to one of the carbons of the triple bond.



Step 3: The pi bond of the alkyne interacts with the metal catalyst weakening the bond. A second hydrogen atom is transferred from the catalyst surface forming alkene product.



Step 4: The alkene is released from the catalyst's surface allowing the catalyst to accept additional hydrogen and alkene molecules.



In this research, the liquid-phase selective hydrogenation of 3-hexyn-1-ol was investigated. The selective hydrogenation of 3-hexyn-1-ol gives a valuable fragrance left alcohol, cis-3-hexen-1-ol. The general reaction pathways of 3-hexyn-1-ol are shown in Figure 2.2.

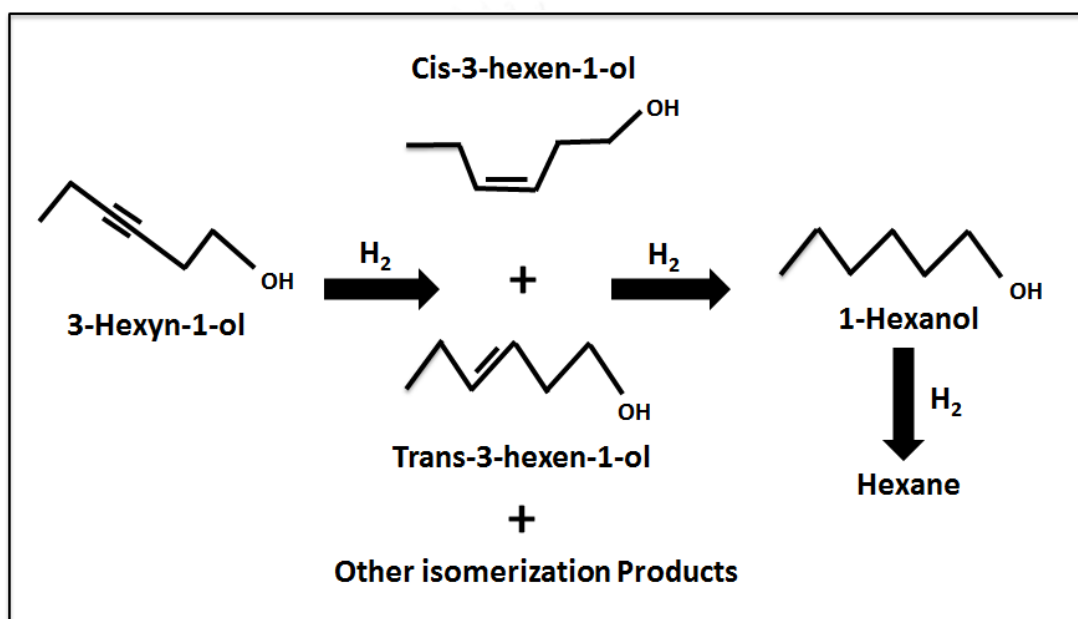


Figure 2.2 General reaction pathways of 3-hexyn-1-ol hydrogenation

First step, 3-hexyn-1-ol substrates can be hydrogenated to cis-3-hexen-1-ol and trans-3-hexen-1-ol and then further hydrogenated to 1-hexanol and hexane, respectively. However, the desired product for this reaction is cis-3-hexen-1-ol. The byproducts are trans-3-hexen-1-ol, other isomerization products, 1-hexanol and hexane.

2.5 Benzyl alcohol oxidation

Alcohol oxidation is an importance organic reaction to produce many intermediated organic compounds such as aldehyde, carboxylic acid, or ketone. Alcohol oxidation commonly involves the removal of the hydroxyl group (-OH group) and a hydrogen group from the alcohol and replaces it with oxygen by forming a carbon-oxygen double bond. Theoretically, only primary and secondary alcohol will undergo oxidation reaction. Tertiary alcohol cannot undergo any oxidation process. Primary alcohols are oxidized initially to form aldehydes and further oxidized to form carboxylic acids whereas secondary alcohols are oxidized to ketones. The end products of alcohol oxidation produce different functional groups depended on the type of alcohol used.

The selective oxidation of benzyl alcohol to benzaldehyde is one of the most importance and versatile reaction for transforming functional groups in organic synthesis of fine chemical industry [6, 40, 41]. Benzaldehyde is a valuable intermediate for many organic compounds, which widely used in the pharmaceutical, perfume, plastic, dyestuff, and agrochemical industries. Typically, commercial benzaldehyde is produced mainly through the hydrolysis of benzyl chloride and the oxidation of toluene [19]. The benzaldehyde that produced from these routes is suffered from the problem of chlorine contamination with poor selectivity. The solvent-free liquid phase selective oxidation of benzyl alcohol by using molecular oxygen is the preferable reaction route for the production of chlorine free benzaldehyde with high selectivity [24, 42]. Many heterogeneous catalyst systems such as Ru catalysts [43, 44], Co catalysts [45], Au catalysts [46-48], and Pd catalysts [6, 40, 49-51] have been reported to be active for the selective oxidation of benzyl

alcohol. Among of these, Pd catalysts appear to be very promising ones because high activity and high selectivity can be obtained simultaneously.

In this research, all 1%Pd/TiO₂ catalysts derived by different preparation methods were evaluated in the solvent free liquid phase selective oxidation of benzyl alcohol to benzaldehyde. The reaction pathways are shown in **Figure 2.3**.

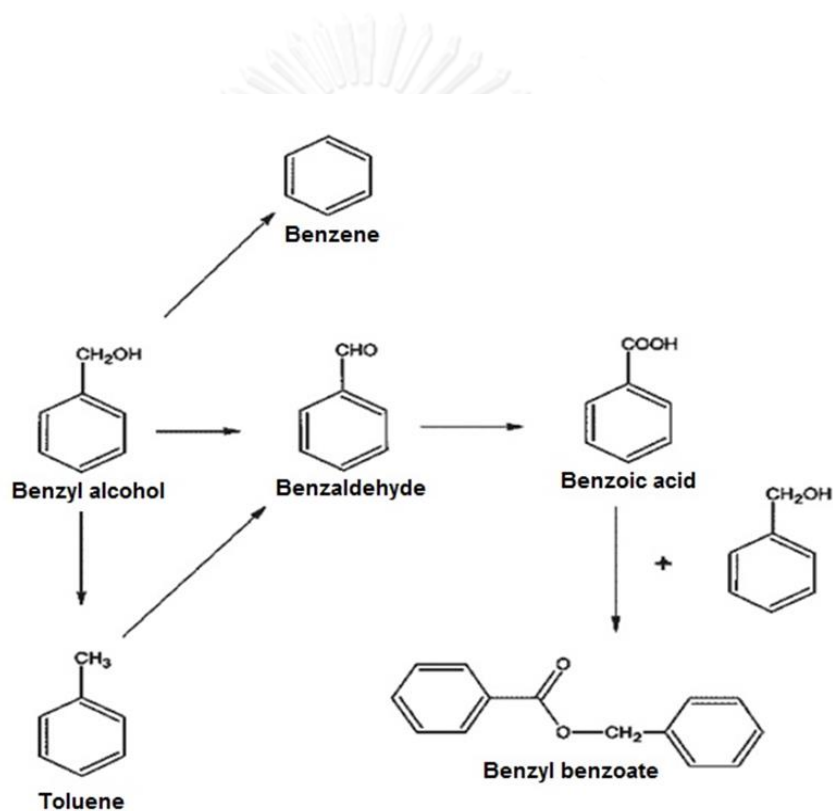


Figure 2.3 General reaction pathways of benzyl alcohol oxidation [52]

CHAPTER III

LISTERATURE REVIEWS

3.1 Supported Pd catalyst in liquid-phase hydrogenation

F. Arena et al. [53] investigated the catalytic behavior of palladium supported on oligomeric aramides in the liquid phase selective hydrogenation of phenylacetylene to styrene, by comparison with conventional Pd-supported systems, such as Pd/oligo-p-phenylenterephthalamide (OPTA), Pd/carbon, Pd/Al₂O₃ and Pd/SiO₂. The influences of the reduction temperature and metal loading on the activity/selectivity of the title reaction are explained in terms of different reducibility patterns of the catalysts, as well as in the light of a peculiar support effect of the organic matrix on Pd particles.

M.G. Musolino et al. [54] studied liquid phase hydrogenation and isomerization of some α,β -unsaturated primary and secondary alcohols have been investigated in tetrahydrofuran over a 2.5% TiO₂ supported palladium catalyst at 303 K and 0.01 MPa partial hydrogen pressure. The double bond isomerization reaction of these substrates leads also to formation of the corresponding saturated aldehydes or ketones. Catalytic activity and selectivity were found to depend strongly on the steric and electronic effects of the substituents on the double bond of the alcohol.

T.A. Nijhuis et al.[55] studied to optimized palladium catalyst systems for the selective liquid-phase hydrogenation of alkyne to alkene. As a model reaction the hydrogenation of 3-methyl-1-pentyn-3-ol was chosen. This paper discussed the preparation of palladium on silica catalysts and different manners to optimize the catalysts system: by preparing bimetallic copper-palladium catalysts and by adding reaction modifiers to the system. The results show that addition of a small amount

of copper to a palladium catalyst increased the catalyst selectivity while the activity is retained. The selectivity enhancing effect of copper can be explained by copper decreasing the relative adsorption strength of the alkene compared to that of the alkyne. Alternatively copper addition can increase the selectivity by reducing the size of the available ensembles of palladium sites, assuming for the alkene hydrogenation larger ensembles are required than for the alkyne hydrogenation. Moreover, the addition of a reaction modifier like quinoline can help to increase the yield of the desired product. The effect of quinoline seems to be partly by blocking the adsorption of adsorption sites on the catalyst resulting in a lower catalyst activity and changing mass-transfer influences. Secondly electronic effects of quinoline change the relative adsorption strength of the reactant and product molecules. However, using a PdCu catalyst is preferable to using a reaction modifier, since adding a reaction modifier makes an additional separation step in the process necessary.

J. Panpranot et al. [56] studied the differences between Pd/SiO₂ and Pd/MCM-41 catalysts in liquid-phase hydrogenation of 1-hexene. SiO₂-small pore, SiO₂-large pore, MCM-41-small pore and MCM-41-large pore were used as supports. The catalysts were prepared by incipient wetness impregnation. The reaction was carried out at 25°C and 1 atm in a stainless steel Parr autoclave. The results showed that the characteristics and catalytic properties of the silica supported Pd catalysts in liquid-phase hydrogenation of 1-hexene were affected by type of silica, pore size and pore structure. The catalyst activities were found to be merely dependent on the Pd dispersion, which as itself a function of the support pore structure. Among the four types of the supported Pd catalysts used in this study, Pd/MCM-41-large pore

showed the highest Pd dispersion and the highest hydrogenation rate with the lowest amount of metal loss.

M. G. Musolino et al. [57] studied the effect of metal particle size and supports of palladium catalysts in selective liquid phase conversion of cis-2-butene-1,4-diol affording also, when hydrogenated, 2-hydroxytetrahydrofuran. Palladium catalysts on different supports (SiO_2 , Al_2O_3 , TiO_2 , ZrO_2 , MgO and ZnO) have been tested. The metal particle size was determined by TEM. The acidic properties of the catalysts were studied by FT-IR spectroscopy using pyridine as probe molecule. The influence of some preparative variables, such as the particle size, the support, the partial hydrogen pressure, on the catalytic behavior of palladium catalysts has been investigated. TEM measurements indicated that Pd particles diameter observed was in the range 2.5–10 nm. No significant variation of TOF and selectivity values with the metal particle size was observed in this range. Moreover, the activity and the selectivity towards reaction products were found to be strongly dependent on the acid–base characteristics of the support. The acid systems have been found more active and selective to isomerisation and hydrogenolysis products than the basic ones. No hydrogenolysis reaction was observed on basic supports. Among the examined catalysts, Pd/TiO_2 resulted the most selective to 2-hydroxytetrahydrofuran. A maximum yield to this compound of about 74% was, in fact, obtained at 0.01 MPa of H_2 pressure.

B. C. Campo et al. [58] studied the selective hydrogenation of crotonaldehyde in liquid phase over different palladium- and platinum-based catalysts ($\text{Pd-Pb}/\alpha\text{-Al}_2\text{O}_3$, $\text{Pd-Zn}/\alpha\text{-Al}_2\text{O}_3$, Pd/ZnO , and two Pt/ZnO samples, prepared from $\text{Pt}(\text{NH}_3)_4(\text{NO}_3)_2$ and H_2PtCl_6 , respectively). It was found that the intrinsic selectivity of

palladium cannot be modified by alloying or following a promotion with a second metal, and the selectivity of crotyl alcohol measured over palladium-based samples is nil or extremely low. The selectivity corresponding to the Pt/ZnO catalysts increases with the time-on-stream reaching high levels. The formation of a Pt-Zn alloy is the origin of the enhanced selectivity toward crotyl alcohol; this effect is more pronounced for the sample that has been prepared from H_2PtCl_6 .

G. Alvez-Manoli et al. [59] studied the effect of mesostructured materials in the stereoselective hydrogenation of 3-hexyne at 298K and 40 psig pressure of H_2 over Pd-supported catalysts at different substrate:palladium (S:Pd) molar ratios. The catalysts were prepared by impregnation using a toluene solution of $\text{Pd}(\text{acac})_2$ to obtain a metal content close to 1 wt.% over SBA-15 with one-dimensional hexagonal structure, MCM-48 silica with cubic structure and three-dimensional pore system and MSU- γ -alumina with a lathlike particle morphology. The results show that, in general, the Pd supported on mesostructured solids are effective catalysts for the stereoselective hydrogenation of 3-hexyne to cis-3-hexene in toluene. The most active catalyst was 1% Pd/SBA-15 in comparison to 1% Pd/MSU- γ , 1% Pd/MCM-48 and commercial 1% Pd/ Al_2O_3 catalysts. This behaviour can be attributed to several factors such as (i) the mesoporous framework effect which mediates substrate access to active sites on the palladium particles and diffusion of the cis-olefin away from active sites, (ii) differences in the textural porosity observed for these catalysts which also mediates substrate and product diffusion to and from active sites and (iii) the size of the metal particles or the metal particle dispersion effect on the catalysts. The reactions were found to be zero with respect to 3-hexyne concentration. The starting 3-hexyne produces primarily cis-3-hexene, which subsequently is either

hydrogenated to hexane or isomerized to trans-3-hexene and 2-hexenes that are found in very small amounts depending on the nature of the support used.

3.2 Supported Pd catalyst in alcohol oxidation

L.F. Liotta et al. [60] studied the oxidation state of active metals and catalytic properties of Pd catalyst and Pd-Ag catalysts supported on pumice in the liquid phase selective oxidation of benzyl alcohol. Preliminary kinetic of benzyl alcohol oxidation was studied using an autoclave reactor at p_{O_2} 2 atm, 333 K. Under these conditions, small amounts of benzoic acid were detected with monometallic Pd pumice being the most active catalyst. In addition, the catalytic activity of the catalysts was measured after different oxidation and reduction treatment at high temperature. The structural data which was characterized by XRD, XPS, EXAFS indicated that Pd^0 and Ag^0 species are the active sites with certain synergism.

A. Villa et al. [61] prepared Pd catalysts supported on carbon nanotube which various surface properties (hydrophilic/hydrophobic) and then studied the catalytic activities in the liquid phase oxidation of alcohols (benzyl alcohol and glycerol). In addition, the effect of surface support properties, reactants and solvents were also investigated. The results indicated that the catalytic activities of catalysts depended on the match among reactant, solvent and support surface.

Z. Ma et al. [62] investigated the catalytic properties of Pd nanoparticles confined in the nanocages of the modified SBA-16 in the aerobic oxidation of alcohol. The catalyst showed high activity for the oxidation of benzylic alcohols, 1-phenylethanol and allylic alcohols under air or O_2 atmosphere in water even at room temperature. The selectivity for the corresponding aldehydes and ketones

were more than 99% in all the cases investigated. The developed catalyst could be facilely recovered and reused twelve times without significant decreases in activity and selectivity.

E. V. Johnston et al. [63] investigated the application of Pd nanoparticles supported on mesocellular foam catalyst in aerobic oxidation of alcohols under molecular oxygen and air. A variety of primary and secondary alcohols were used as alcohol substrates. The catalytic system demonstrated a greater reactivity for benzylic and allylic alcohols than for aliphatic ones. However, this Pd nanocatalyst was found to be a highly efficient heterogeneous catalyst for oxidation of alcohols. Primary and secondary benzylic alcohols were oxidized to their corresponding carbonyl compounds in high to excellent yield. In addition, the catalyst was found to be highly stable and was recycled several times without any leaching of the metal.

B. Wang et al. [19] investigated the effect of surface acido-basicity of Pd and Rh catalysts supported on N-doped mesoporous carbon (NMC), mesoporous carbon (MC), pristine and nitric acid treated activated carbons (AC and ACN) in the selective oxidation of benzyl alcohol. Surface acido-basicity property of catalyst support was found to be a key factor influencing the catalytic performance. Both Pd and Rh catalysts on the basic NMC support exhibited higher activity and selectivity toward benzaldehyde than those of MC supported catalysts. While acidic AC and CAN supported catalysts promote side reactions leading to formation of byproducts.

3.3 Role of TiO₂ in the selective hydrogenation and oxidation

A. Dandekar and M.A.Vannice [64] studied crotonaldehyde hydrogenation on Pt/TiO₂ and Ni/TiO₂ SMSI catalysts. A kinetic and DRIFTS (diffuse reflectance FTIR)

investigation of crotonaldehyde adsorption and hydrogenation was conducted over TiO_2 -supported Pt and Ni with the intent of gaining insight into the adsorption modes of molecules with carbonyl groups on these catalysts in the SMSI and non-SMSI states. Significant enhancement in selectivity toward crotyl alcohol was observed with each catalyst after reduction at 773 K. DRIFT spectra under reaction conditions identified crotonaldehyde species strongly adsorbed through the C=C bond and weakly coordinated through both the C=C and the C=O bonds on these catalysts after reduction at 573 K, which gave a peak at 1693 cm^{-1} . After reduction at 773 K, an additional adsorbed species with a strong band at 1660 cm^{-1} , indicating a significant interaction between the carbonyl group and the surface, was observed, which is presumed to be stabilized at interfacial Pt– TiO_x and Ni– TiO_x sites. A decrease in the surface coverage of this species paralleled a drop in selectivity to crotyl alcohol with time on stream. After reduction at 573 K, decarbonylation occurred during the initial few minutes on stream to create adsorbed CO on Pt/ TiO_2 in addition to carbon deposition, but these reactions were significantly suppressed after reduction at 773 K, presumably due to a TiO_x overlayer which covers part of the Pt surface and breaks up the ensembles of Pt atoms required for these reactions.

D.C. Lee et al. [65] studied the selective hydrogenation of 1,3-butadiene on TiO_2 -modified Pd/ SiO_2 catalysts. The properties of Pd/ SiO_2 catalysts modified with titanium oxide were examined by determining their activity with respect to the partial hydrogenation of 1,3-butadiene included in an excess amount of butenes and by characterizing their surfaces using infrared (IR) spectroscopy, X-ray photoelectron spectroscopy (XPS), H_2 chemisorption, and temperature-programmed desorption (TPD). The results indicated that TiO_2 -modified catalysts had an improved selectivity

for the conversion of 1,3-butadiene to 1-butene, particularly when the catalysts were reduced at high temperatures, e.g., 500°C. IR and chemisorption results suggest that, when the catalyst is reduced at 500°C, the Pd surface is decorated with partially-reduced TiO_x similar to the case of TiO_2 -supported catalysts, which show strong metal-support interaction (SMSI). XPS and TPD results indicate that Pd surface is also modified electronically, in that the charge is transferred from the Ti species to Pd and the adsorption of 1-butene to the Pd surface becomes weaker. It can be concluded that the strong interaction between the Pd surface and partially reduced TiO_2 is responsible for the improved selectivity of the catalyst for the conversion of 1,3-butadiene to 1-butene.

Y. Li et al. [28] investigated in situ EPR and IR by using CO as probe molecules show that even pre-reduced by H_2 at lower temperature results in SMSI for anatase titania supported palladium catalyst, but not for rutile titania supported palladium catalyst, which is attributed that the Ti^{3+} ions produced by reduction of Ti^{4+} are fixed in the surface lattice of TiO_2 , as rutile titania is more thermodynamically and structurally stable than anatase titania so that the Ti^{3+} ions fixed in the surface lattice of anatase TiO_2 is easier to diffuse to surface of palladium particle than one in the surface lattice of rutile TiO_2 . The reason why the pre-reduction of both anatase and rutile supported palladium catalyst at higher temperature results in SMSI between Ti^{3+} and Pd is attributed that the thermal diffusion of produced Ti^{3+} ion at higher temperature is much easier than at lower temperature so that it could overcome the binding of surface lattice of both anatase and rutile titania to move to the surface or surrounding of palladium particle.

J. Xu et al. [66] studied liquid phase selective hydrogenation of maleic anhydride (MA) to butyric acid (BA) used Pd/TiO₂ catalyst which prepared by difference method, sol-gel, impregnation and deposition-precipitation method. It was clearly seen that Pd/TiO₂ catalyst prepared by sol-gel is an excellent catalyst for selective hydrogenation of MA in liquid phase to BA. The high conversion (100%) of MA and high yield towards BA were attributed to the strong adsorption of MA or succinic anhydride (SAH) species via the C=O bond in di-σ mode on interfacial Pd-TiO_x site which was induced by the high temperature reduction step. Meanwhile, the reaction temperature and the interaction between metal and support has an obvious influence on the yield of BA.

J. Panpranot et.al. [22] studied the selective hydrogenation of acetylene in excess ethylene on micron-sized and nanocrystalline TiO₂ supported Pd catalysts. The Pd catalysts supported on commercial micron-sized and nanocrystalline TiO₂ synthesized by sol-gel and solvothermal method. The results show that acetylene conversions were found to be merely dependent on Pd dispersion; ethylene selectivity appeared to be strongly affected by the presence of Ti³⁺ in the TiO₂ samples. The use of pure anatase TiO₂ (either micron- or nano-sized) that contained significant amount of Ti³⁺ as supports for Pd catalysts gave high ethylene selectivities, while the use of pure rutile TiO₂ (without Ti³⁺ present) resulted in ethylene loss. The results suggest that the effect of Ti³⁺ on the TiO₂ supports was more important for high ethylene selectivity than the effect of TiO₂ crystallite size for selective acetylene hydrogenation over Pd/TiO₂ catalysts.

D. I. Enache et al. [67] investigated the catalytic activity of TiO₂-supported Au-Pd alloy catalysts compared with Pd/TiO₂ and Au/TiO₂ catalysts in the solvent-free

oxidation of benzyl alcohol with molecular oxygen at high reaction temperatures (160°C, and 100°C). Under these conditions the 2.5 wt. % Au-2.5 wt. % Pd/TiO₂ was found to be the most active catalyst, whereas the Au/TiO₂ catalyst shows the highest selectivity to benzaldehyde.

P. J. Miedziak et al. [68] studied the catalytic activity of Au-Pd/TiO₂ catalysts which prepared by different preparation methods, impregnation and deposition-precipitation methods. The catalytic efficiency was enhanced further by the alloying of gold with palladium. Furthermore, the most active catalysts were Au-Pd/TiO₂ catalysts prepared by the deposition-precipitation method.

M. Sankar et al. [69] studied the controlling of mechanism in solvent-free liquid-phase oxidation of benzyl alcohol using Au-Pd catalysts supported on different metal oxide supports (activated-carbon, TiO₂, Nb₂O₅, MgO, and ZnO). The results demonstrated that a disproportionation reaction is the source of the major byproduct, toluene (together with an equimolar amount of benzaldehyde), and oxidation by O₂ is the other source of benzaldehyde. All five catalysts exhibited very similar activity in the oxidation reaction alone. The higher overall activity was found in the cases of activated-carbon, Nb₂O₅ and TiO₂ supported catalysts because the additional disproportionation reaction occurred alongside the oxidation reaction. However, it can be concluded that the MgO and ZnO supported Au-Pd catalysts are superior to TiO₂, Nb₂O₅ and activated-carbon- supported catalysts because they catalyzed exclusively the oxidation reaction, yielding more than 99% selectivity to benzaldehyde. The switching off the disproportionation reaction for MgO and ZnO supported catalysts occurred because they do not promote the formation of the required adsorbed species.

X. Wang et al. [24] studied the effect of calcination pretreatments and reconstruction of Pd sites by using Pd/TiO₂ and Pd/Al₂O₃ catalysts in the solvent-free selective oxidation of benzyl alcohol with molecular oxygen. The calcination pretreatments of supported Pd catalysts show great effects on catalytic activity. The pretreating supported Pd catalysts in oxidizing or inert atmosphere and subsequent reducing of Pd species in situ by benzyl alcohol reactant can create a higher amount of defective sites than pretreating Pd catalysts in reducing atmosphere. The activity of supported Pd catalysts in selective oxidation of alcohols can be enhanced via the in situ reduction pathway.

N. Dimitratos et al. [70] studied the catalytic activities of Au/TiO₂ and Au/C catalysts prepared by sol immobilization method in the solvent free oxidation of benzyl alcohol. The sol immobilization method can be produced gold catalysts with narrow metal particle size distribution around 3 nm, which exhibited very high activity compared with that one prepared by impregnation method. Additional, comparison between the Au supported catalysts demonstrated that activity and distribution of products was dependent on the nature of support and heat treatment. Furthermore, when TiO₂ was used as support, substantial differences in terms of activity and distribution of products were observed between the two supports.

3.4 Modification of TiO₂ with 3-(aminopropyl)triethoxysilane (APTES)

E. Ukaji et al. [71] investigated the effect of surface modification with 3-aminopropyltriethoxysilane (APTES) and n-propyltriethoxysilane (PTES) on photocatalytic activity and UV-shielding ability of fine TiO₂ particles. The number of surface

functional groups (N_R), which is the density of silane coupling agents modified on TiO_2 surface, was calculated by carbon contents [wt. %] and specific surface area [m^2/g]. N_R increased with an increase in the concentration of modifier, and affected the photo-catalytic ability and UV shielding ability of modified TiO_2 . When the photo-catalytic activity and UV-shielding ability of modified samples were evaluated, it was found that APTES was more effective modifier than PTES to obtained samples with low photo-catalytic activity and high UV shielding ability. This is probably because the adsorption mechanisms on TiO_2 surface between modifiers were different and N_R is a key factor to control the performances of fine TiO_2 particles. Surface modification with APTES in $N_R = 6.2$ leads to suppress the photo-catalytic activity equal to 25% and to keep 80% of UV-shielding ability of original TiO_2 . From the zeta-potential measurements, the surface character of samples changed drastically until N_R is 6.2. When N_R is higher than 6.2, the surface character of samples is similar to that of sample with $N_R = 6.2$. These results indicated that the character of surface layer formed by modifier differs in N_R . Consequently, N_R affected the photo-catalytic activity and UV-shielding ability of modified samples.

A. R. Morrill et al. [72] synthesized the self-assembled monolayers (SAM) of 3-aminopropyltriethoxysilane (APTES) on nanostructured titania (NST) and tin oxide nanowires (SnO_2 NW). The functionalized metal oxide surfaces were decorated with borohydride-reduced silver nanoparticles (AgNPs) and imaged. Furthermore, comparative studies with the mono- and di-ethoxysilanes were also carried out. The APTES is found to form the densest SAM, which shows the largest density of exposed amino groups, an APDES-SAM had a lower density of exposed amines, and APMES the lowest density. The nanoparticle-modified silane films are found to be greatly

stabilized against oxidation. Because colloidal AgNP bind preferentially to the amino functionality of the silane molecules, they serve as an assay for the surface's utility towards species that bind to that group. The particle density also reflects the relative number of natively bound APTES in the SAM.

Y.-Y. Song et.al. [73] investigated the optimum conditions for grafting of 3-aminopropyltriethoxysilane (APTES) onto amorphous, anatase and rutile titanium dioxide (TiO_2) surfaces. The attachment process and extent was characterized using X-ray photoelectron spectroscopy (XPS). In particular, the effect of attachment time, silane concentration, reaction temperature and the TiO_2 crystalline structure on the growth kinetics of the silane layers was studied. The results show that critical experimental conditions exist where APTES attachment to the TiO_2 surface changes from a monolayer to a multilayer growth mode. Furthermore, the results confirm that APTES attachment on TiO_2 occurs far from an ideally oriented monolayer. About 50% of all molecules show reverse attachment (i.e. coordination with the amino group on the TiO_2). Amount and APTES molecule orientation depend on the crystal structure of the substrate. Reverse attachment is more pronounced on rutile than on anatase or amorphous substrates. Obtained results are expected to be most valuable in synthesis approaches that aim at controlled organic modification of TiO_2 where APTES still is the key linker molecule.

G. Tan et al. [74] studied the microstructure and component of the modification titanium substrate. 3-Aminopropyltriethoxysilane (APTES) films were successfully grafted onto the surface of the NaOH-heat-treated titanium by chemically bound via SAMs, which can become a "molecular bridge" between the interface of organic materials and inorganic materials. The surfaces of titanium before

and after modification were characterized by scanning electronic microscopy (SEM), X-ray photoelectron spectroscopy (XPS) and attenuated total reflection–Fourier transform infrared spectroscopy (ATR–FTIR). After bonding the APTES films on the modification titanium, the new peaks located around 1095 cm^{-1} attributes to siloxane groups indicating that silane agent had been grafted onto the surface of the modification titanium substrate by SAMs. Following the deposition of APTES films on titanium, significant change were seen in the amounts of oxygen, silicon and carbon present on the titanium surface, which were consistent with the anticipated reaction steps. Both the surface chemistry and topography are important factors known to influence the biological response to biomaterials. Bioactive coating of silane agent may have the ability to create a strong interface between bone tissue and implant.

From the literature reviews, Pd is one of the most useful catalysts that can be used in both hydrogenation and oxidation. Furthermore, TiO_2 is one of the most interesting supports in both reactions. However, the surface modification of TiO_2 to develop the catalyst support in the liquid-phase hydrogenation and oxidation has not been well studied so far. Thus it is the aim of this research to investigate the catalytic behaviors of Pd catalysts supported on APTES modified TiO_2 in the liquid-phase selective hydrogenation of 3-hexyn-1-ol to cis-3-hexen-1-ol and liquid-phase selective oxidation of benzyl alcohol to benzaldehyde.

CHAPTER IV

EXPERIMENTAL

This chapter describes all of experimental procedures which used in this research. The details of surface modification of TiO_2 support with 3-(aminopropyl)triethoxysilane or APTES are explained in section 4.1. The different preparation methods for Pd supported on TiO_2 catalysts such as electroless deposition (ED), sonochemical (SN), sol immobilization (IM), and incipient wetness impregnation (I) method are demonstrated in section 4.2. The details of reaction study in the liquid-phase selective hydrogenation of 3-hexyn-1-ol to cis-3-hexen-1-ol and phenylacetylene to styrene, including to the solvent-free selective oxidation of benzyl alcohol to benzaldehyde are given in section 4.3. Finally, the characterization techniques for the APTES modified TiO_2 supports and all of Pd supported on TiO_2 catalysts are illustrated in section 4.4.

4.1 Surface modification of TiO_2 support with APTES

Surface modification of TiO_2 support with APTES was prepared via a post synthesis grafting method. The commercial anatase TiO_2 support available from Sigma-Aldrich was used in this experiment. Various concentrations of APTES in anhydrous toluene at 0.1, 1.0, and 10 mM were prepared in 25 cm³ volumetric flask. Typically, 1.5 g of TiO_2 was dispersed in 25 cm³ of APTES solution using Teflon reactor with magnetic stirrer bar and then left it to gently stir at room temperature for 15 min. After that, the Teflon bottom was heated and held at 100°C for 8h in the furnace. Upon completion, the Teflon bottom was cooled down to room temperature and the resulting powders were filtered, washed with anhydrous toluene once and followed by dichloromethane twice. The weakly adsorbed

materials were removed during the washing steps. Then they were dried in the oven at 110°C for 12 h. The TiO₂ samples were denoted as TiO₂-0.1APTES, TiO₂-1APTES, and TiO₂-10APTES, respectively.

Table 4.1 Chemicals used in modification of TiO₂ supports

| Chemicals | Formula |
|--|---|
| Titanium dioxide (Aldrich) | TiO ₂ (pure anatase) |
| (3-aminopropyl)triethoxysilane (Aldrich) | H ₂ N(CH ₂) ₃ Si(OC ₂ H ₅) ₃ , (≥98%) |
| Toluene anhydrous (Aldrich) | C ₆ H ₅ CH ₃ , (99.8%) |
| Dichloromethane (Aldrich) | CH ₂ Cl ₂ |

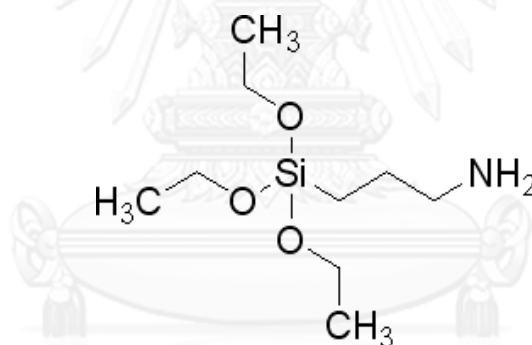


Figure 4.1 Structure of 3-(aminopropyl)triethoxysilane (APTES)

4.2 Preparation of Pd supported on TiO₂ catalysts

1 wt. % of Pd was deposited on pristine TiO₂ and APTES modified TiO₂ supports by three different preparation methods which were the chemical reduction techniques such as electroless deposition (ED), sonochemical (SN), and sol immobilization (IM). All 1%Pd/TiO₂ catalysts were studied in the liquid-phase

selective hydrogenation of 3-hexyn-1-ol to cis-3-hexen-1-ol and solvent-free liquid-phase selective oxidation of benzyl alcohol to benzaldehyde. In addition, 1 wt. % of Pd was also deposited on non-modified TiO₂ support by non-chemical reduction techniques such as sonochemical with H₂ reduction (S) and incipient wetness impregnation (I) methods. These 1%Pd/TiO₂ catalysts were studied in the liquid-phase selective hydrogenation of phenylacetylene to styrene. The details for each catalyst preparation methods are demonstrated as following:

4.2.1 Electroless deposition (ED)

For preparation of 1 wt. % Pd/TiO₂ catalysts by electroless deposition method with conventional SnCl₂ sensitization process, this consists of three main processes, pretreating (etching and cleaning), sensitization, and Pd deposition processes. For pretreating process, 1 g of TiO₂ support was dispersed in 100 cm³ of 14%HCl for 15 min and then washed with distilled water. Following by sensitization process, the TiO₂ sample was re-dispersed in a 50 cm³ aqueous solution containing 0.001 g/cm³ of PdCl₂, 0.05 g/cm³ of SnCl₂, and 4.6 cm³ of 37%HCl for 20 minutes under ultrasonic vibration at room temperature, washed with distilled water and then dried in the oven at 110°C for 12 h. After sensitization process, Pd (1 wt. %) was deposited on the activated TiO₂ support by ultrasonic dispersion, the activated TiO₂ support was continuously dispersed for 1 h in the 50 cm³ of Pd electroless plating bath which containing the chemical compositions as show in **Table 4.3**. During Pd deposition process, the electroless plating bath was maintained at 50°C with the pH of 9.8±0.2 by using 0.1M NaOH to ensure a high cations exchange. Finally, the 1%Pd/TiO₂ catalyst was washed with deionized water and then dried overnight in the oven at 110°C. The Pd supported on non-modified TiO₂ and APTES modified TiO₂ catalysts

were denoted as 1%Pd/TiO₂-ED, 1%Pd/TiO₂-0.1APTES-ED, 1%Pd/TiO₂-1APTES-ED, and 1%Pd/TiO₂-10APTES-ED, respectively.

Table 4.2 Chemicals used in sensitization process for electroless deposition

| Chemicals | Formula |
|-----------------------------------|-----------------------------|
| Palladium (II) chloride (Aldrich) | PdCl ₂ (99.99%) |
| Tin (II) chloride (Aldrich) | SnCl ₂ (≥99.99%) |
| Hydrochloric acid (ACS) | HCl (37%) |

Table 4.3 The chemical compositions of Pd electroless plating bath

| Chemicals | Formula | Quantity per 50 cm ³ bath |
|-----------------------------------|--|--------------------------------------|
| Palladium chloride (Aldrich) | PdCl ₂ | 0.0168 g |
| Hydrochloric acid (Aldrich) | HCl (37%) | 0.2 cm ³ |
| Ammonia hydroxide (Aldrich) | NH ₄ OH (28%) | 8.0 cm ³ |
| Ammonium chloride (Carlo Erba) | NH ₄ Cl | 1.3500 g |
| Sodium hypophosphite (Carlo Erba) | NaH ₂ PO ₂ .H ₂ O | 0.1004 g |

4.2.2 Sonochemical (SN, S)

The principle of sonochemical technique is an application of ultrasonic irradiation in the catalysts preparation method. In this experimental, we separated the sonochemical method into two different types depending on the reduction step. The first one, Pd was reduced by using a chemical reducing agent and then deposited on TiO₂ support using ultrasonic vibration. The second one, Pd was deposited on TiO₂ support during ultrasonic vibration without chemical reduction

and then calcined in air following to reduce by H_2 gas. Two procedures are demonstrated as following:

▪ **Sonochemical reduction by chemical reducing agent (SN)**

For the synthesis of 1 wt. % Pd/TiO₂ catalyst by sonochemical method using chemical reducing agent, Pd(NO₃)₂·6H₂O and hydrazine hydrate solution were used as the Pd precursor and reducing agent, respectively. A desired amount of Pd precursor was dissolved in 25 cm³ of deionized water and then the hydrazine hydrate solution was slowly added drop wise in order to reduce PdO to metallic Pd⁰ specie (mole of Pd metal: mole of hydrazine = 1:10). The Pd solution was continuously stirred for 1 h. Then, TiO₂ support was dispersed in Pd solution and it was gently stirred at room temperature for 12 h. The resulting slurry was re-dispersed by using the ultrasonic vibration bath (TRU-sweep ultrasonic cleaner, 40 kHz) under temperature controlled 50°C for 6 h. Finally, the slurry was filtered and washed several times with deionized water and then dried overnight in the oven at 110°C. The Pd supported on non-modified TiO₂ and x-APTES modified TiO₂ catalysts were denoted as 1%Pd/TiO₂-SN, 1%Pd/TiO₂-0.1APTES-SN, 1%Pd/TiO₂-1APTES-SN, and 1%Pd/TiO₂-10APTES-SN, respectively.

▪ **Sonochemical reduction by H₂ gas (S)**

For the synthesis of 1 wt. % Pd/TiO₂ catalyst by sonochemical reduction by H₂ atmosphere, Pd(NO₃)₂·6H₂O was used as the Pd precursor. A desired amount of Pd precursor was dissolved in 25 cm³ of deionized water. The 1 g of TiO₂ support was dispersed in Pd solution and then gently stirred at room temperature for 12 h. After that, the slurry was re-dispersed using the ultrasonic vibration bath (TRU-sweep ultrasonic cleaner, 40 kHz) for 6 h under temperature controlled 50°C. The slurry was

filtered and washed several times with deionized water and then dried overnight in the oven at 110°C. Finally, the 1%Pd/TiO₂ catalyst was calcined in air at 450°C for 3 h with a heating rate 10°C/min. Before reaction study, the catalyst was reduced in H₂ atmosphere with the H₂ flow rate 50 cm³/min. at desired temperature (40°C or 500°C). They were denoted as 1%Pd/TiO₂(S), 1%Pd/TiO₂(S)-R40, and 1%Pd/TiO₂(S)-R500.

Table 4.4 Chemicals used for 1%Pd/TiO₂ catalysts prepared by sonochemical

| Chemicals | Formula |
|--------------------------------------|--|
| Palladium nitrate (Aldrich) | Pd(NO ₃) ₂ ·6H ₂ O |
| Hydrazine hydrate solution (Aldrich) | NH ₂ NH ₂ ·H ₂ O (78-82%) |
| Hydrogen gas (Linde) | H ₂ (UHP) |

4.2.3 Sol immobilization (IM)

For the synthesis of 1 wt. % Pd/TiO₂ catalysts by sol-immobilization method, an aqueous solution of PdCl₂ (6.25 g/dm³), poly (vinyl alcohol) (PVA) (1 wt. % aqueous solution, Aldrich, Mw = 10,000, 80% hydrolyzed) and 0.1M aqueous solution of NaBH₄ were prepared. The desired amount of aqueous PdCl₂ solution (1 wt.% Pd loading) was added in 400 cm³ deionized water and left it to stir for 15 min. The PVA solution (1 wt. %; PVA/Pd (wt./wt.)=1.2) and a freshly prepared solution of 0.1M NaBH₄ (NaBH₄/Pd (mol/mol) = 5) were added and then left it to stir for 30 min to generate a dark-brown Pd colloid solution. Afterword, the Pd colloid was immobilized by adding the TiO₂ support (adjust at pH = 1 by conc. H₂SO₄) under vigorous stirred for 2 h. Then, the slurry was filtrated and was washed thoroughly

with distilled water until the liquors was neutral. Finally, the catalyst was dried in the oven at 110°C for 16h. They were denoted as 1%Pd/TiO₂-IM, 1%Pd/TiO₂-0.1APTES-IM, 1%Pd/TiO₂-1APTES-IM, and 1%Pd/TiO₂-10APTES-IM, respectively.

Table 4.5 Chemicals used for 1%Pd/TiO₂ catalysts prepared by sol immobilization

| Chemicals | Formula |
|---|--|
| Palladium chloride (Aldrich) | PdCl ₂ |
| Sodium borohydride (Aldrich) | NaBH ₄ (98%) |
| Poly(vinyl alcohol) (Mw 10,000) (Aldrich) | [-CH ₂ CHOH-] _n (80% hydrolyzed) |
| Hydrochloric acid (Aldrich) | HCl (37%) |
| Sulfuric acid (Aldrich) | H ₂ SO ₄ (98%) |

4.2.4 Incipient wetness impregnation (I)

For synthesis of 1%Pd/TiO₂ catalyst by incipient wetness impregnation method, Pd(NO₃)₂·6H₂O was used as the Pd precursor. A desired amount of palladium nitrate hydrate (1 wt. % Pd) was dissolved in deionized water which the volume equaled to pore volume of TiO₂ support. After that, Pd solution was added dropwise to TiO₂ support (1 g) and the resulting catalyst was left to stand at room temperature for 6 h. Then, it was dried overnight in the oven at 110°C and then calcined in air at 450°C for 3 h with a heating rate 10°C/min. Before reaction study, the catalyst was reduced in H₂ atmosphere with the H₂ flow rate 50 cm³/min at desired temperature (40°C or 500°C). They were denoted as 1%Pd/TiO₂(I), 1%Pd/TiO₂(I)-R40, and 1%Pd/TiO₂(I)-R500, respectively.

Table 4.6 Chemicals used for 1%Pd/TiO₂ catalysts prepared by incipient wetness impregnation

| Chemicals | Formula |
|-----------------------------|---|
| Palladium nitrate (Aldrich) | Pd(NO ₃) ₂ ·6H ₂ O (99.99%) |
| Hydrogen gas (Linde) | H ₂ (UHP; 99.99 vol.%) |

4.3 Reaction study

The liquid-phase selective hydrogenation of 3-hexyn-1-ol to cis-3-hexen-1-ol and the solvent-free liquid-phase selective oxidation of benzyl alcohol to benzaldehyde were performed to investigate the catalytic performances of 1%Pd/TiO₂ catalysts prepared by electroless deposition (ED), sonochemical (SN) and sol immobilization (IM) methods. Whereas the liquid-phase selective hydrogenation of phenylacetylene to styrene was carried out to investigate the catalytic performances of 1%Pd/TiO₂ catalysts prepared by sonochemical with H₂ reduction (S) and incipient wetness impregnation (I) methods.

4.3.1 The liquid-phase selective hydrogenation of 3-hexyn-1-ol to cis-3-hexen-1-ol procedure.

The liquid-phase selective hydrogenation of 3-hexyn-1-ol to cis-3-hexen-1-ol was carried out in the 100 cm³ stainless steel autoclave reactor with a Teflon line inside. Prior to reaction, the catalysts were pretreated with H₂ gas (flow rate 50 cm³/min) at 40⁰C for 2 h. Approximately 5 mg of reduced catalyst was placed into the autoclave reactor. The reactant consisting of 0.2 cm³ of 3-hexyn-1-ol and 9.8 cm³ of ethanol (solvent) were mixed in a 10 cm³ volumetric flask before being introduced into the autoclave reactor. The reactor was purged with H₂ gas three times and then

heated up to 40°C, followed by filling with 2 bar of H₂. The H₂ pressure was controlled at 2 bar, the liquid phase hydrogenation was started immediately by continuously stirring with a stirring speed 1000 rpm. The reaction time was varied from 5–90 min. After reaction, the reactor was cooled down to lower 10°C in ice bath and then the vent valve was slowly opened to prevent the loss of products. The product mixtures were filtered by centrifugation in order to separate the catalyst from the liquid mixtures. Then products were analyzed by gas chromatography (Shimadzu GC2014) with flame ionization detector (FID) using Rtx®-5 capillary column. The operating conditions of GC are shown in **Table 4.7**. The products were identified by comparison with known standards.

Table 4.7 The operating conditions of gas chromatography (GC2014)

| Gas chromatograph | Shimadzu GC2014 |
|----------------------|----------------------|
| Detector | FID |
| Capillary column | Rtx®-5 |
| Carrier gas | Helium (99.99 vol.%) |
| Make-up gas | Air (99.9 vol.%) |
| Column temperature | 70°C |
| Injector temperature | 250°C |
| Detector temperature | 310°C |

Table 4.8 Chemicals used in the liquid-phase hydrogenation of 3-hexyn-1-ol

| Chemicals | Formula |
|------------------------|--|
| 3-hexyn-1-ol (Aldrich) | C ₂ H ₅ CCCH ₂ CH ₂ OH (98%) |
| Hydrogen gas (Linde) | H ₂ (UHP; 99.99vol. %) |
| Ethanol (Aldrich) | C ₂ H ₅ OH (99.5%) |

4.3.2 The liquid-phase selective hydrogenation of phenylacetylene to styrene procedure.

The liquid-phase selective hydrogenation of phenylacetylene to styrene was carried out in 50 cm³ autoclave stainless steel reactor with Teflon line inside. Prior to reaction, catalyst was reduced in H₂ gas (flow rate 50 cm³/min) at 40°C and 500°C for 2 h. Approximately 5 mg of reduced catalyst was placed into the autoclave reactor. The reactant consisting of 0.5 cm³ of phenylacetylene and 4.5 cm³ of ethanol (solvent) were mixed in a volumetric flask before being introduced into the autoclave reactor. The reactor was purged with H₂ gas three times and then heated up to 40°C, followed by filling with H₂. When H₂ pressure reached to 3 bar, the liquid-phase hydrogenation was started immediately by vigorous stirring with a stirring rate 1000 rpm. The reaction time was varied from 10-40 min. After reaction, the vent valve was slowly opened to prevent the loss of products. The products mixture was filtrated by centrifugation in order to separate the catalyst out. Finally, the liquid products were analyzed by gas chromatography (Shimadzu GC14B) with flam ionization detector using GS-alumina capillary column. The operating conditions of GC are shown in **Table 4.9**. The products were identified by comparison with known standards.

Table 4.9 The operating conditions of gas chromatography (GC14B)

| Gas Chromatograph | Shimadzu GC14B |
|----------------------|------------------------|
| Detector | FID |
| Capillary column | GS-alumina |
| Carrier gas | Helium (99.99vol. %) |
| Make-up Gas | Nitrogen (99.99vol. %) |
| Column temperature | 200°C |
| Injector temperature | 250°C |
| Detector temperature | 280°C |

Table 4.10 Chemicals used in the liquid-phase hydrogenation of phenylacetylene

| Chemicals | Formula |
|---------------------------|--|
| Phenylacetylene (Aldrich) | C ₆ H ₅ CCH (98%) |
| Hydrogen gas (Linde) | H ₂ (UHP; 99.99vol. %) |
| Ethanol (Aldrich) | C ₂ H ₅ OH (99.5%) |

The schematic diagram of liquid-phase hydrogenation of 3-hexyn-1-ol and phenylacetylene are demonstrated in **Figure 4.2**.

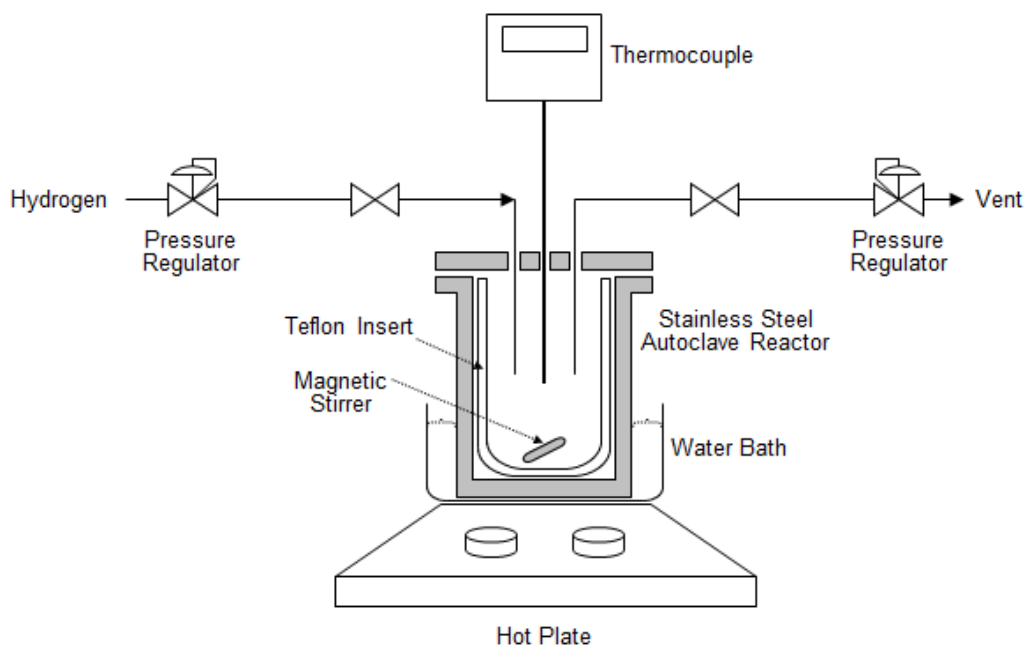


Figure 4.2 The schematic diagram of the liquid-phase hydrogenation system

4.3.3 The solvent-free selective oxidation of benzyl alcohol to benzaldehyde procedure.

The solvent-free liquid-phase selective oxidation of benzyl alcohol to benzaldehyde was carried out in a 50 cm³ glass stirred reactor. Approximately, 25 mg of catalyst and 10 cm³ of benzyl alcohol were charged into the reactor and then purged with O₂ gas three times before closing. The O₂ pressure was maintained at 1 bar. The reactor was put in a heating block, which was preheated to the reaction temperature at 120°C. The reaction was performed for 0.5-7 h using a magnetic bar inside the reactor with a stirring rate at 1000 rpm. After reaction, the reactor was cooled down to room temperature in an ice bath. The products mixture was centrifuged to separate catalyst out. The liquid products were mixed with mesitylene

(internal standard) in the ratio of 1:1 (vol/vol) and then they were analyzed by gas chromatography (GC Varian star 3800 cx) with flame ionization detector using a CP-Wax 52 CB column. The operating conditions for GC Varian star 3800 cx are shown in **Table 4.11**. The products were identified by comparison with known standards.

Table 4.11 The operating conditions for gas chromatography (GC Varian star 3800 cx)

| Gas Chromatograph | GC Varian star 3800 cx |
|----------------------|--|
| Detector | FID |
| Capillary column | CP-Wax 52 CB column |
| Carrier gas | Helium (99.99vol. %) |
| Make-up Gas | Helium (99.99vol. %) |
| Column temperature | Temp. program 60-250°C , rate 20°C/min |
| Injector temperature | 250°C |
| Detector temperature | 260°C |

Table 4.12 Chemicals used in solvent-free liquid-phase selective oxidation of benzyl alcohol

| Chemicals | Formula |
|--------------------------|------------------------------------|
| Benzyl alcohol (Aldrich) | $C_6H_5CH_2OH$ ($\geq 99.0\%$) |
| Oxygen gas | O_2 (UHP; 99.99vol. %) |
| Mesitylene (Aldrich) | $C_6H_3(CH_3)_3$ ($\geq 99.0\%$) |

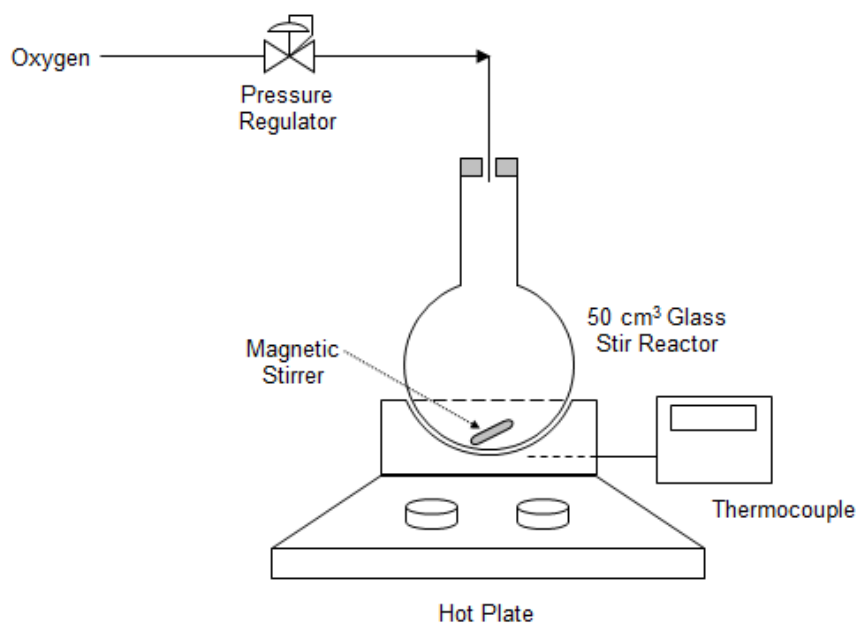


Figure 4.3 The schematic diagram of the liquid-phase oxidation system

4.4 Characterization techniques

All modification of TiO_2 supports and 1%Pd/ TiO_2 catalysts were characterized by several techniques such as:

4.4.1 X-ray Diffraction (XRD)

The bulk crystal structure and chemical phase composition were determined by diffraction of an X-ray beam as a function of the long fine focus. The XRD spectrum of the TiO_2 supports and 1%Pd/ TiO_2 catalyst were measured by using a D8 Advance Bruker AXS X-ray diffractometer and $\text{CuK}\alpha$ radiation with Ni filter in the 2θ range of 10-80 degrees with resolution 0.02. The crystallite size was calculated from Scherrer's equation.

4.4.2 N_2 Physisorption

The BET surface area, pore volume, and average pore size diameter of

pristine TiO₂ support was measured through nitrogen gas adsorption at liquid nitrogen temperature (-196 °C) using Micromeritics ASAP 2020 instrument. Prior to physisorbed nitrogen, the sample was degased at 150 °C for 2 h.

4.4.3 X-ray Photoelectron Spectroscopy (XPS)

The XPS spectra, the binding energy and the composition on the surface layer of the modification of TiO₂ supports and 1%Pd/TiO₂ catalysts were determined by using a Kratos Axis Ultra DLD spectrometer with a monochromatic Al K α X-ray source (75-150 W) and analyzer pass energies of 160 eV (for survey scans) or 40 eV (for detailed scans). The C 1s line was taken as an internal standard at 284.8 eV.

4.4.4 Scanning Electron Microscope (SEM)

The SEM quantitative line scan analysis was performed to determine the amount of elements on APTES-modified TiO₂ supports along the horizontal line by using JEOL scanning electron microscope JSM-5410LV. The catalysts are prepared with gold coating prior to analysis.

4.4.5 Transmission Electron Microscopy (TEM)

The morphologies of TiO₂ supports and 1%Pd/TiO₂ catalysts were investigated using JEOL-JEM 2010 transmission electron microscope using energy-dispersive X-ray detector operated at 80-200 kV. Prior to analysis, the sample was dispersed in 2 ml of ethanol using ultrasonic vibration until the solution look like the colloidal. The solution was dropped on the copper-grid that coated with polymer, following to dry in atmospheric air for 1 h and then kept in the desiccator before analysis. Besides the morphologies of catalysts, the average Pd particle size and distribution of Pd on the TiO₂ supports were also investigated.

4.4.6 Fourier Transform Infrared Spectroscopy (FTIR)

The functional groups of APTES modified TiO₂ supports and 1%Pd/TiO₂ catalysts were determined by using JASCO FTIR-660 Plus on transmittance mode at spectral resolution of 1 cm⁻¹ accumulating 64 scans. The sample pellets were made from grinded sample with KBr. The KBr pellet was used as a background standard for analysis.

4.4.7 CO-Pulse Chemisorption

The Pd active sites and the relative percentages dispersion of Pd supported catalysts were determined by CO-pulse chemisorption technique using Micromeritics ChemiSorb 2750 (pulse chemisorption system).

Approximately 0.2 g of catalyst was filled in a u-tube, incorporated in a temperature-controlled oven and connects to a thermal conductivity detector (TCD). Then, helium (He) was purged into the reactor with a flow rate 30 cm³/min in order to remove remaining air. Prior to chemisorption, the catalyst was reduced in H₂ (flow rate 50 cm³/min) at 40°C or 500°C for 2 h. After that cooled down to room temperature under Helium flow, then CO is plus into the catalyst bed at 30°C. The non-adsorbed CO was measured using thermal conductivity detector. Pulsing was continued until no further CO adsorption is observed. The amount of Pd metal active sites and the relative percentage dispersions of Pd were calculated from CO adsorbed based on CO:Pd ratio of 1:1.

4.4.8 Inductive Coupled Plasma Optical Emission Spectrometer (ICP-OES)

The actual amount of the Pd loading was determined by a Perkin Elmer Optima 2100DV AS93 PLUS inductive coupled plasma optical emission spectrometer.

The catalysts were prepared in a solution containing 49% HF and 37% HCl with volume ratio 5:1 and were heated for increasing of dissolve it.



CHAPTER V

RESULTS AND DISCUSSION

The results and discussion in this chapter are divided into three parts. In the first part the characteristics and properties of pristine TiO₂ and APTES modified TiO₂ supports were investigated by several techniques such as N₂-physisorption, XRD, XPS, FTIR, and SEM analysis. Furthermore, the optimum concentration for APTES modified TiO₂ supports to obtain the monolayer instead of multilayer is also investigated. In the second part, the characteristics and catalytic properties of Pd supported on TiO₂ and APTES modified TiO₂ catalysts with different preparation methods; electroless deposition (ED), sonochemical (SN) and sol immobilization (IM) have been evaluated in the liquid-phase selective hydrogenation of 3-hexyn-1-ol to cis-3-hexen-1-ol and the solvent-free liquid-phase selective oxidation of benzyl alcohol to benzaldehyde. Several techniques were used for characterization of the 1%Pd/TiO₂ catalysts such as, XRD, FTIR, TEM, and XPS. The specific characteristic of each catalyst prepared by different methods has been demonstrated. Including to catalytic performances of all catalysts were compared in the liquid-phase hydrogenation and oxidation. In the third part, the characteristics and catalytic activities of 1%Pd/TiO₂ catalysts prepared by sonochemical with H₂ reduction (S) have been investigated in the liquid-phase selective hydrogenation of phenylacetylene to styrene under mild conditions compared with catalysts prepared by conventional incipient wetness impregnation (I) method. Moreover, the effect of Pd particle size to the strong metal-support interaction (SMSI) has been evaluated.

Part I

Surface modification of TiO₂ supports with 3-(aminopropyl)triethoxysilane (APTES)

5.1 The characteristics and properties of TiO₂ and APTES modified TiO₂ supports

5.1.1 N₂-physisorption

BET surface area, pore volume and pore diameter of the pristine TiO₂ available from Sigma-Aldrich were determined by N₂ physisorption technique. The N₂ adsorption-desorption isotherm of pristine TiO₂ is shown in **Figure 5.1**. According to the Brunauer, Emmett, and Teller (BET) theory for classification of sorption isotherms, TiO₂ support shows type IV isotherm with hysteresis loop at high relative pressure range (P/P_0) 0.8-1.0, indicating to the characteristic of mesoporous material which pore diameter was in the range of 2 to 50 nm. The BET surface area of TiO₂ was 10m²/g. The pore volume and average pore diameter were 0.02cm³/g and 7.6 nm, respectively. The BET surface area of TiO₂ in this research was lower than many commercially available TiO₂ supports such as P25 (Degussa), PC-500 and AT-1 (Millennium Chemicals), and Hombikat UV-100 (Sachtleben Chemie).

5.1.2 X-Ray Diffraction (XRD)

The crystal structure and chemical phase composition of pristine TiO₂ and APTES modified TiO₂ supports were characterized by X-ray diffraction technique. The measurements were carried out at the diffraction angles (2θ) between 20° and 80°. Broadening of the diffraction peaks were used to estimate crystallite diameter from Scherrer Equation.

The XRD patterns of TiO₂ and APTES modified TiO₂ supports are illustrated in **Figure 5.2**. All TiO₂ supports were exhibited the characteristic peaks of pure anatase

TiO₂ at $2\theta=25^\circ$ (major), 37° , 48° , 55° , 56° , 62° , and 69° with no contamination of other crystalline phases. The peak position of anatase (101) TiO₂, d-spacing, and the lattice parameters for TiO₂ and APTES modified TiO₂ supports are given in **Table 5.1**. All APTES modified TiO₂ supports show the same position peaks of anatase (101) TiO₂ at $2\theta=25.32^\circ$ compared with pristine TiO₂, indicating that the distance between crystal planes (d spacing), which related to the lattice parameters were not changed. It was suggested that APTES did not inserted in the TiO₂ lattice and it was only grafted on the TiO₂ surface. Furthermore, the average crystallite size of TiO₂ and APTES modified TiO₂ supports calculated from the full width at half maximum of the XRD peak at $2\theta=25^\circ$ using Scherrer equations were around 66-67 nm. From the XRD results, it can be confirmed that modification of APTES occurred only on the TiO₂ surface.

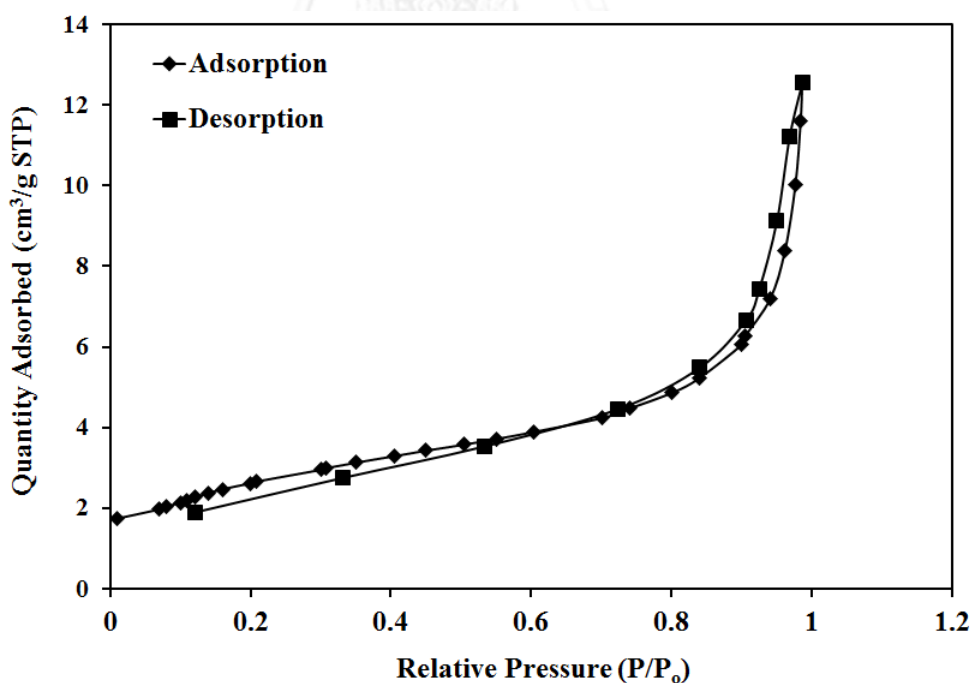


Figure 5.1 N₂ adsorption-desorption isotherm of pristine TiO₂ support

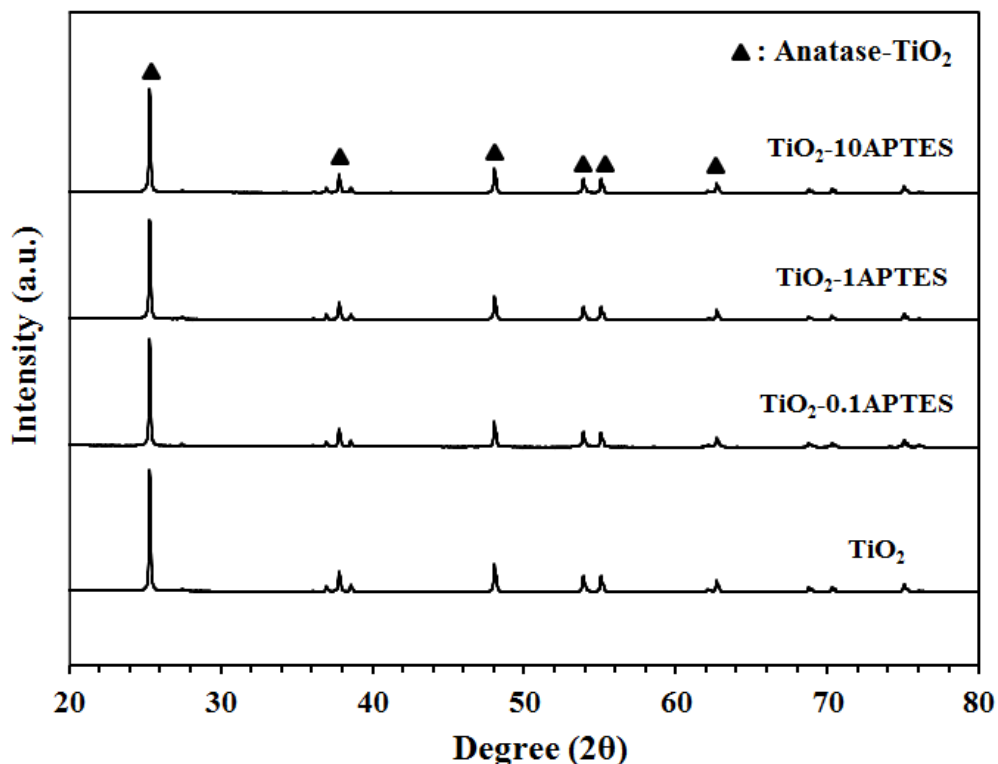


Figure 5.2 The XRD patterns of pristine TiO_2 and APTES modified TiO_2 supports

Table 5.1 The peak position of anatase (101) TiO_2 , d-spacing, lattice parameters and average crystallite size of TiO_2 and APTES modified TiO_2 supports

| Sample | Peak position of anatase (101) TiO_2 (2θ , degree) | d-spacing (nm) | Lattice parameters ^a (Å) | | | Crystallite size of TiO_2 (nm) |
|--------------------------|--|-------------------|-------------------------------------|--------|-------|---|
| | | | $a (=b)$ | c | c/a | |
| TiO_2 | 25.32 | 0.3515 | 3.7830 | 9.5019 | 2.51 | 65.8 |
| TiO_2 -0.1APTES | 25.32 | 0.3515 | 3.7845 | 9.4778 | 2.50 | 66.8 |
| TiO_2 -1APTES | 25.32 | 0.3515 | 3.7830 | 9.5019 | 2.51 | 66.5 |
| TiO_2 -10APTES | 25.32 | 0.3515 | 3.7830 | 9.5019 | 2.51 | 66.4 |

^a calculated from Bragg's law using the diffraction peaks of anatase (101) and (200) TiO_2 .

5.1.3 Fourier Transform Infrared Spectroscopy (FTIR)

The functional groups of pristine TiO₂ and APTES modified TiO₂ supports were investigated by Fourier Transform Infrared Spectroscopy with a transmittance mode. **Figure 5.3** illustrates the FTIR spectra of pristine TiO₂ and APTES modified TiO₂ supports with various concentrations of APTES. All TiO₂ samples show the typical IR band at 680 cm⁻¹, which was assigned to the symmetric stretching vibration of Ti-O-Ti bonds in the TiO₂ lattice [75, 76]. The IR bands at ca. 1630 cm⁻¹ and 3450 cm⁻¹ were attributed to H-OH stretching vibration of physisorbed water and the stretching vibration of hydroxyl group of Ti-OH bonds, respectively [75]. After APTES modification, all the APTES modified TiO₂ supports show the IR band at 1080 cm⁻¹, which can be attributed to the asymmetric stretching vibration of Si-O-Si bridge [77, 78]. The intensity of Si-O-Si band increased as the concentrations of APTES increased suggesting that APTES was successfully grafted on the TiO₂ surface. The presence of small IR band at around 910 cm⁻¹ was assigned to the stretching vibration of Ti-O-Si [71, 79], indicating the successful replacement of hydroxyl groups on the TiO₂ surface with APTES modifier. In addition, the peaks at 1460 cm⁻¹ and 1390 cm⁻¹ were detected and assigned to the characteristic of C-H and C-N stretching vibration of APTES, respectively [19, 77].

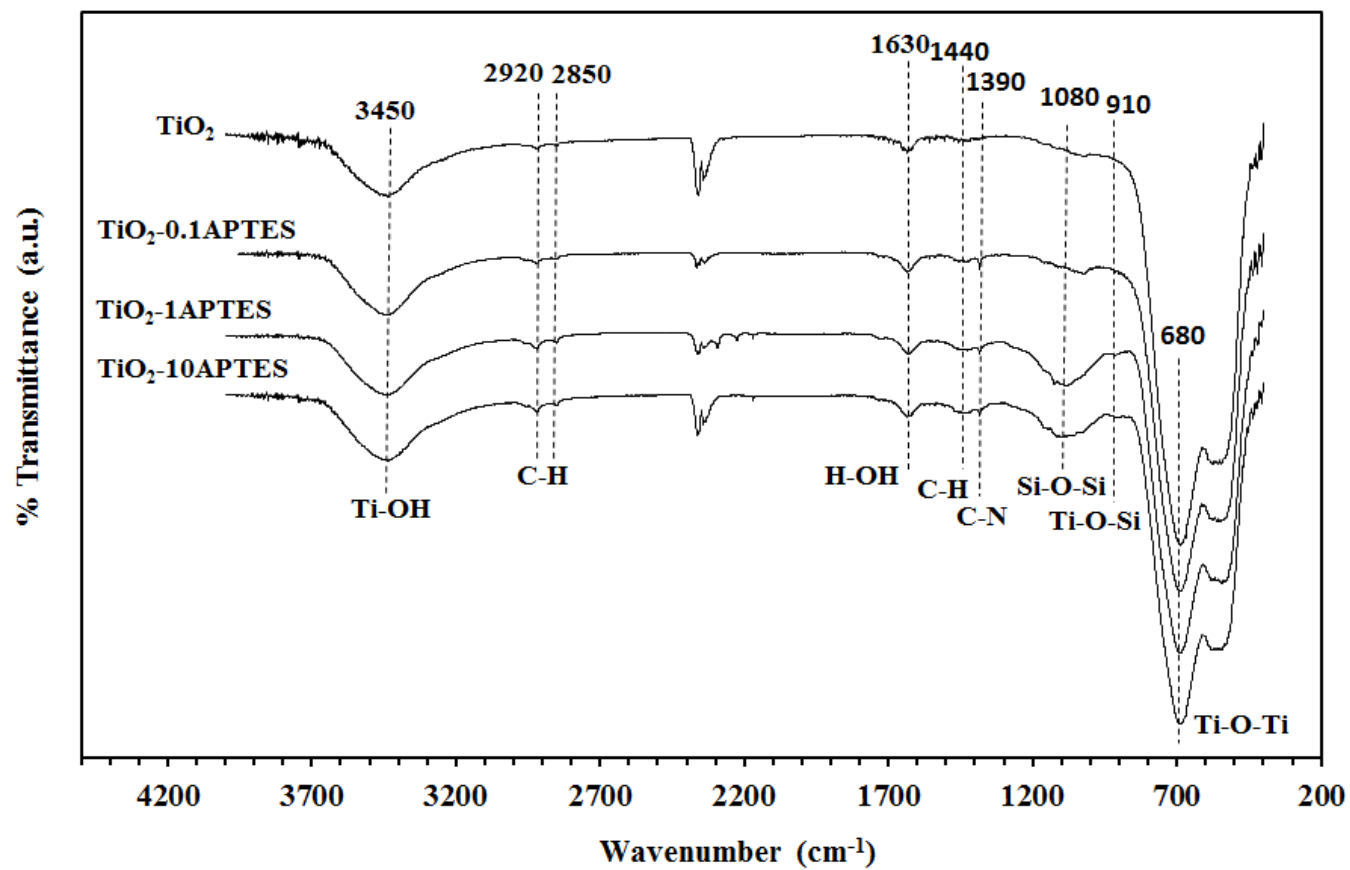


Figure 5.3 FTIR spectra of pristine TiO_2 and APTES modified TiO_2 supports with various concentrations of APTES

5.1.4 X-ray photoelectron spectroscopy (XPS)

The electronic states and surface compositions of TiO₂ and APTES modified TiO₂ supports were investigated by XPS analysis in order to understand the characteristic attachment between TiO₂ surface and APTES molecules. Generally, the APTES molecule (NH₂-(CH₂)₃-Si-(OC₂H₅)₃) consists of one head of amine group (NH₂-(CH₂)₃-Si-) and three arms of ethoxy groups (-Si-(OC₂H₅)₃). The attachment of APTES on the metal oxide surface performed via the nucleophilic substitution reaction [72, 80]. The lone pair oxygen electrons of hydroxyls group on metal oxide surface act as the nucleophilic attached toward the electron deficient silicon of APTES molecules occurring an oxide linkage, anchoring silane molecule. Modification of APTES is expected to form self-assembled monolayer and given free amine terminating groups. **Figure 5.4** and **Figure 5.5** illustrate the XPS spectra of (a) Ti 2p, (b) O 1s, (c) N 1s, and (d) Si 2p for TiO₂ and APTES modified TiO₂ supports. The doublet peaks of Ti 2p_{3/2} and Ti 2p_{1/2} at B.E. around 458.4 and 464 eV, which were assigned to Ti⁴⁺ species in anatase TiO₂, were observed for both unmodified TiO₂ and APTES modified TiO₂ supports. The intensity of Ti 2p was significantly decreased when the concentration of APTES increased from 0.1 to 10 mM, compared to unmodified one suggesting that APTES was successfully grafted on TiO₂ surface. From the O 1s spectra after APTES grafted, the O 1s peak at B.E. 529.7 eV, which was assigned to oxygen in the TiO₂ lattice [81, 82], was significantly decreased while the O1s peak at B.E. 531.9 eV, which was attributed to surface oxygen of O-Si-R [80], became more intense. For the N 1s signal, a small broad peak at B.E. 398.0-402.0 eV, which originated from N₂ adsorbed on TiO₂ surface, can be detected for APTES modified TiO₂ supports. The broad N 1s peak consisted of two different types of N₂ attachment mode, silane coupling or

reversed (amino) coupling. If silane coupling agent occurs, the free NH_2 termination is observed at B.E. 399.4 eV. If NH_2 attaches to the TiO_2 surface or reverse attachment, N 1s peak at B.E. 400.8 eV can be observed, which is assigned to the protonated amines $-\text{NH}_3^+$ [80, 83]. From the XPS results, it can be observed that the intensity of N 1S peaks corresponding to silane coupling and reversed (amino) coupling were both increased with increasing amount of APTES. It is likely that the multilayers present the NH_2 and Si termination and with equal probability. Moreover, the most clarify of APTES successfully grafted on the TiO_2 surface; the Si 2p peaks at B.E. 101.9 eV were detected for all APTES modified TiO_2 supports.

The binding energies and atomic concentrations of Ti 2p, O 1s, N 1s, and Si 2p of the TiO_2 and APTES modified TiO_2 supports are summarized in **Table 5.2**. In the present work, APTES attachment was studied for three levels of APTES concentrations; 0.1, 1, 10 mM at 100°C . The decreasing of surface atomic concentration ratios of Ti/O with increasing of APTES concentrations as well as the increasing of Si/Ti ratios indicated that the TiO_2 surface was successfully grafted with APTES. However, increasing of APTES concentrations may lead to different attachment kinetics. For an ideal attachment, Si exclusively attaches to TiO_2 surface while N presents as the terminal NH_2 group. The N/Si ratio should be larger than 1.0. For the samples with surface atomic concentration ratios of N/Si were less than 1.0, non-ideal attachment occurred, in which some of APTES gave the termination NH_2 and some of them became reversed attachment on the TiO_2 surface. The characteristics of APTES arrangement on the TiO_2 surface can also be indicated by the ratios between surface oxygen (O_S) and lattice oxygen (O_L) in term of $\text{O}_\text{S}/\text{O}_\text{L}$. It is generally known that APTES modified on TiO_2 surface occurs via condensation

between Ti-OH and Si-OR to form the Ti-O-Si bond. The amount of surface oxygen on pristine TiO₂ suggests the possible APTES attachment sites. Therefore if O_S/O_L ratio of the APTES modified TiO₂ sample is higher than O_S/O_L ratio of the non-modified TiO₂, APTES tends to form multilayer coverage on the TiO₂ surface. It is likely that when the concentration of APTES was excess, polymerization of APTES molecules to form multilayers arrangement occurred. The formation of a thick APTES, possibly by polymerization of APTES molecules, has been suggested by Song et al. [80]. Moreover, Kallury et al. also reported that electrostatic interactions may be negligible at high temperature and it is certainly possible for APTES to polymerize in solution [84]. In our case, the O_S/O_L ratio of the TiO₂-0.1APTES was lower than O_S/O_L ratio of pristine TiO₂ by ca. 10%, indicating the formation of APTES monolayer on the TiO₂ surface. On the contrary, the O_S/O_L ratios for the TiO₂-1APTES and TiO₂-10APTES samples were higher than the non-modified TiO₂ 19% and 61%, respectively, suggesting that APTES formed multilayers on the TiO₂ surface. The optimum monolayer of APTES without further tendency to form 3D networks can be expected when the concentration of APTES did not exceed 0.1 mM.

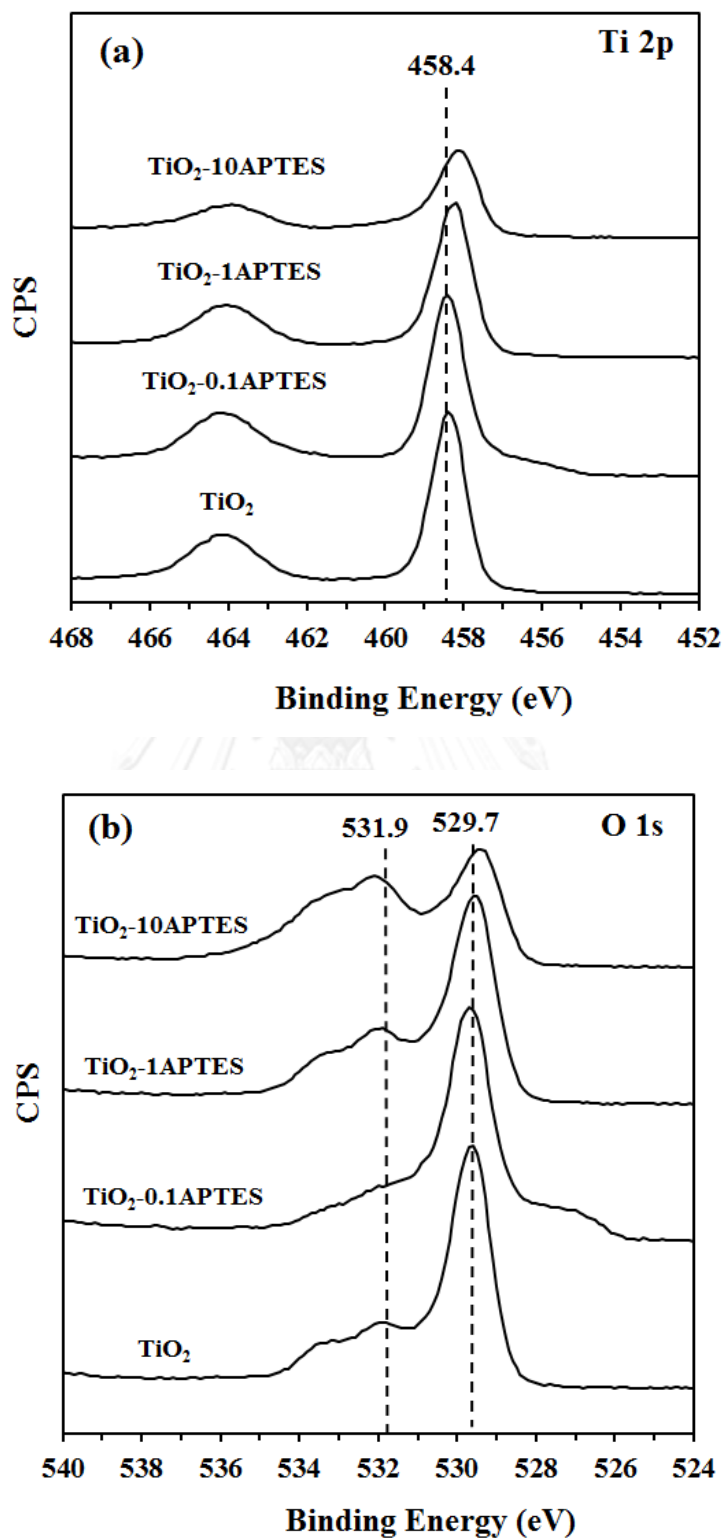


Figure 5.4 The XPS spectra of (a) Ti 2p, (b) O 1s for TiO₂ and APTES modified TiO₂ supports.

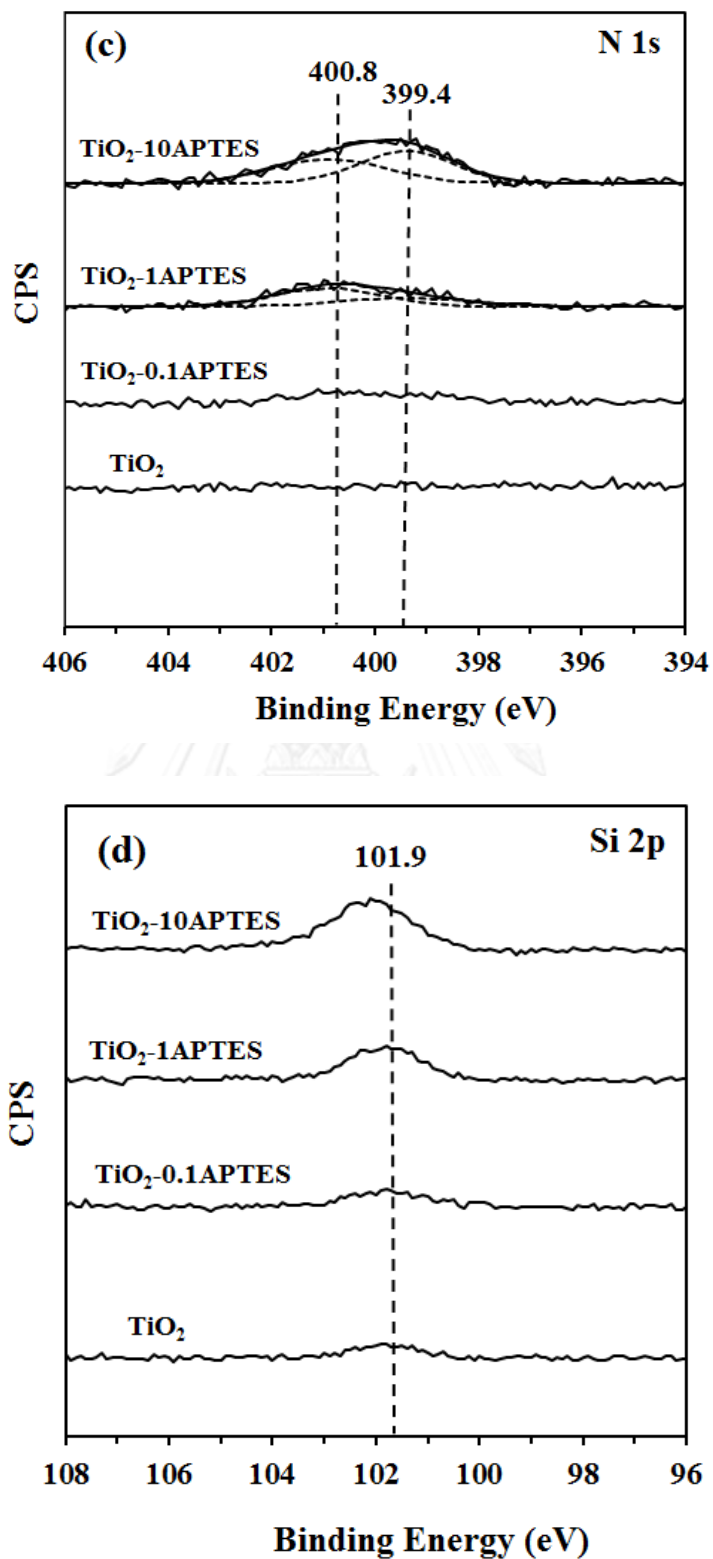


Figure 5.5 The XPS spectra of (c) N 1s, and (d) Si 2p for TiO₂ and APTES modified TiO₂ supports.

Table 5.2 The binding energy and surface compositions of TiO₂ and APTES modified TiO₂ supports.

| Samples | Binding Energy (eV) | | | | Surface atomic concentration ratio | | | |
|----------------------------|---------------------|-------|-------|-------|------------------------------------|-------|------|---|
| | Ti 2p | O 1s | N 1s | Si 2p | Ti/O | Si/Ti | N/Si | O _S /O _L ^a |
| TiO ₂ | 458.4 | 529.6 | - | - | 0.28 | 0.00 | 0.00 | 0.46 |
| TiO ₂ -0.1APTES | 458.4 | 529.7 | 400.8 | 101.8 | 0.30 | 0.01 | 0.00 | 0.42 |
| TiO ₂ -1APTES | 458.2 | 529.6 | 400.8 | 101.8 | 0.27 | 0.08 | 0.59 | 0.57 |
| TiO ₂ -10APTES | 458.1 | 529.4 | 400.8 | 102.1 | 0.18 | 0.28 | 0.64 | 1.20 |

^a O_S/O_L calculated from surface oxygen (O_S) and lattice oxygen (O_L)

5.1.5 Scanning Electron Microscopy (SEM)

To clarify the characteristic of APTES attachment orientations (monolayer or multilayer), the scanning electron microscopy connect with the quantitative line scan analysis equipment was performed to determine the percentage amount of elements along the horizontal line from left to right. The SEM micrographs and the quantitative line scan analysis results for TiO₂-0.1APTES and TiO₂-10APTES are shown in **Figure 5.6**. The morphologies of both TiO₂ samples were consisted of irregular shape of fine particles agglomerated. However, the surface of TiO₂-10APTES was obviously thicker than TiO₂-0.1APTES, indicating to the amount of APTES had an influence to the characteristic of APTES attachment on the TiO₂ surface. For the TiO₂-0.1APTES, the amount of Si content along the line was not significantly different with the maximum content at 0.5% while the Ti and O contents were 88.2% and 67.0%, respectively. It is suggested that Si was well dispersed on the TiO₂ surface. Higher amounts of Si and O along the line were observed on the TiO₂-10APTES at

1.1% and 69.9%, respectively. The Ti content was also decreased to 76.5%. Such results suggested the formation of multilayers APTES on the TiO₂-10APTES support, which are in line with the XPS results. The percentage amounts of Si along the line for both TiO₂ samples are shown in **Figure 5.7**.

Besides the quantitative line scan, the SEM microtome cross section technique was performed to investigate the thickness of APTES layer and the compositions of TiO₂ surface. Unfortunately, it cannot see the cross section area of TiO₂ particles because TiO₂ particle size, which used in this research, was too small. Hence it cannot determine the thickness of APTES layer and the compositions of TiO₂ surface by this technique. So it should be noted that the SEM microtome cross section technique is not suitable to analyse the material which is in the nanometer range.

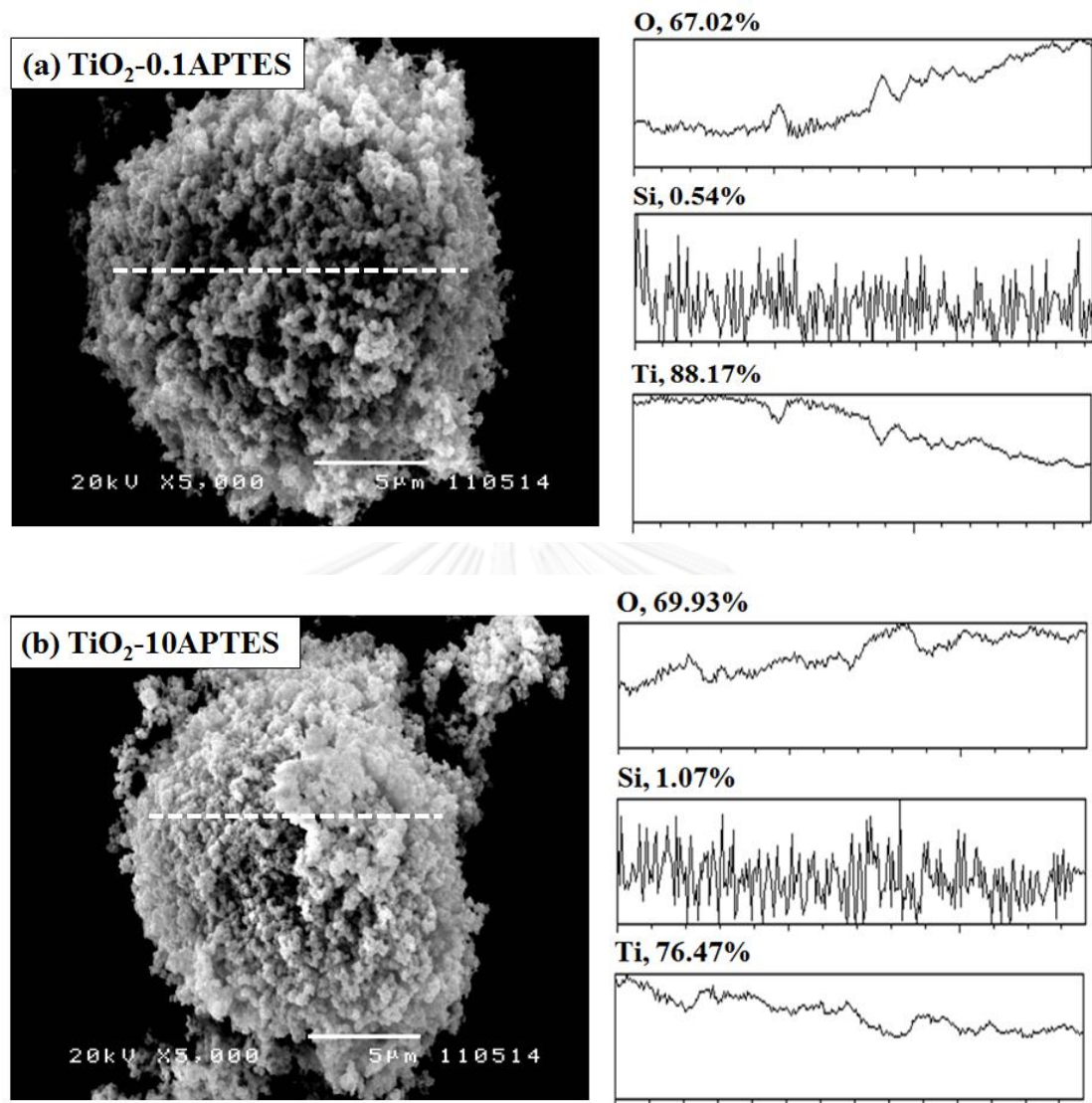


Figure 5.6 SEM micrographs with the quantitative line scan analysis of (a) $\text{TiO}_2\text{-0.1APTES}$ and (b) $\text{TiO}_2\text{-10APTES}$

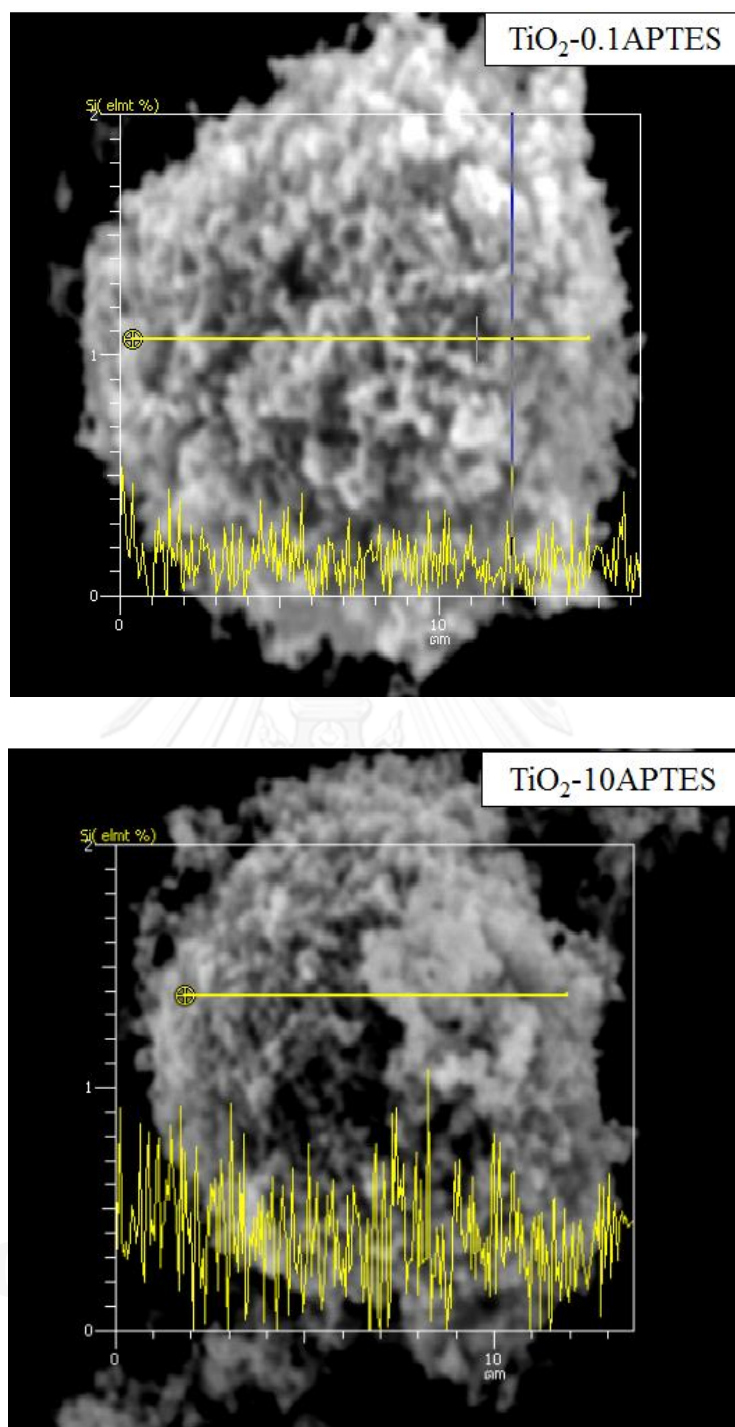


Figure 5.7 SEM quantitative line scan of Si contents on $\text{TiO}_2\text{-0.1APTES}$ and $\text{TiO}_2\text{-10APTES}$.

As revealed by several characterization techniques, surface modification of TiO_2 supports with various concentrations of APTES were successfully prepared by post synthesis grafting method. Various concentrations of APTES (0.1, 1.0, and 10 mM) was found to be an influence to the attachment orientations (monolayer or multilayer). The formation of monolayer APTES was found on TiO_2 -0.1APTES whereas multilayer APTES and reversed attachment of APTES were found on TiO_2 -1APTES and TiO_2 -10APTES. These results indicated that increasing of APTES concentrations effect to the different kinetic mechanism of APTES attached on TiO_2 surface. The features of APTES monolayer and multilayer are demonstrated in Figure 5.8.

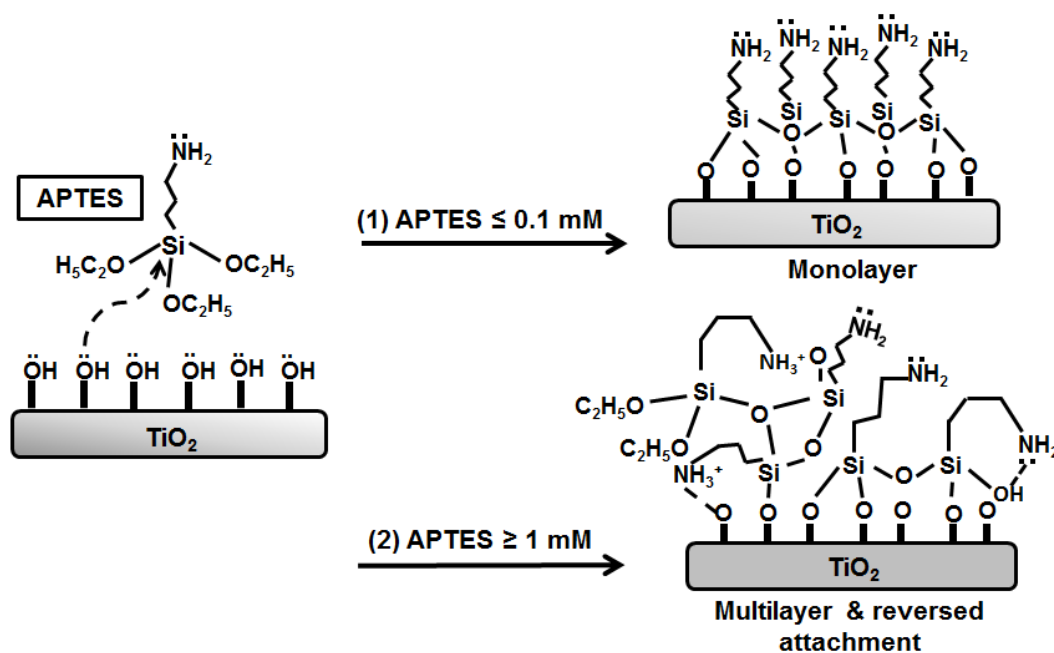


Figure 5.8 The features of APTES attachment modes with various APTES concentrations.

Part II

Comparative study the effect of catalysts preparation methods

In this part, 1 wt.% of Pd was deposited on pristine TiO₂ and APTES modified TiO₂ supports by different preparation methods, electroless deposition (ED), sonochemical (SN), and sol immobilization (IM) methods. The effect of different Pd deposition methods on the characteristics and catalytic properties of all 1%Pd/TiO₂ catalysts were investigated by several characterization techniques such as XRD, TEM, XPS, and FTIR. The catalytic behaviors of all 1%Pd/TiO₂ catalysts were evaluated in the solvent-free liquid phase selective oxidation of benzyl alcohol and the liquid-phase selective hydrogenation of 3-hexyn-1-ol. Furthermore, the effect of various preparation methods on the catalytic behavior of Pd catalysts supported on TiO₂ and APTES modified TiO₂ supports were studied and compared.

5.2 The characteristics and catalytic properties of 1%Pd/TiO₂ catalysts prepared by electroless deposition method

In this section, the characteristics and catalytic properties of all 1%Pd/TiO₂ catalysts prepared by electroless deposition with conventional SnCl₂ sensitization process were investigated as following:

5.2.1 Catalyst characterizations

5.2.1.1 X-ray diffraction (XRD)

The XRD patterns of the 1%Pd/TiO₂ catalysts prepared by electroless deposition method are shown in **Figure 5.9**. The XRD characteristic peaks of pure anatase TiO₂ were observed at $2\theta=25^\circ$ (major), 37° , 48° , 55° , 56° , 62° , and 69° without contamination of other phases such as rutile or brookite TiO₂. The XRD characteristic

peaks corresponding to Pd species were not detected due probably to the low amount of Pd loading and/or very small Pd/PdO crystallite size. The lattice parameters of anatase (101) TiO_2 for all 1%Pd/ TiO_2 catalysts (results shown in **Table 5.3**) calculated from Bragg's law were not significant difference from the original TiO_2 supports suggesting that Pd were deposited on the TiO_2 surface not in the lattice. However for the 1%Pd/ TiO_2 -xAPTES catalysts ($x = 0.1, 1, 10 \text{ mM}$) the diffraction peaks associated with the SnO_2 were observed at $2\theta=26.8^\circ, 33.8^\circ,$ and 51.5° . The appearance of SnO_2 or Sn^{4+} species resulted from oxidation of SnCl_2 (Sn^{2+}), which acted as the reducing agent of PdCl_2 to form Pd seed for subsequent particle growth in the electroless deposition process.

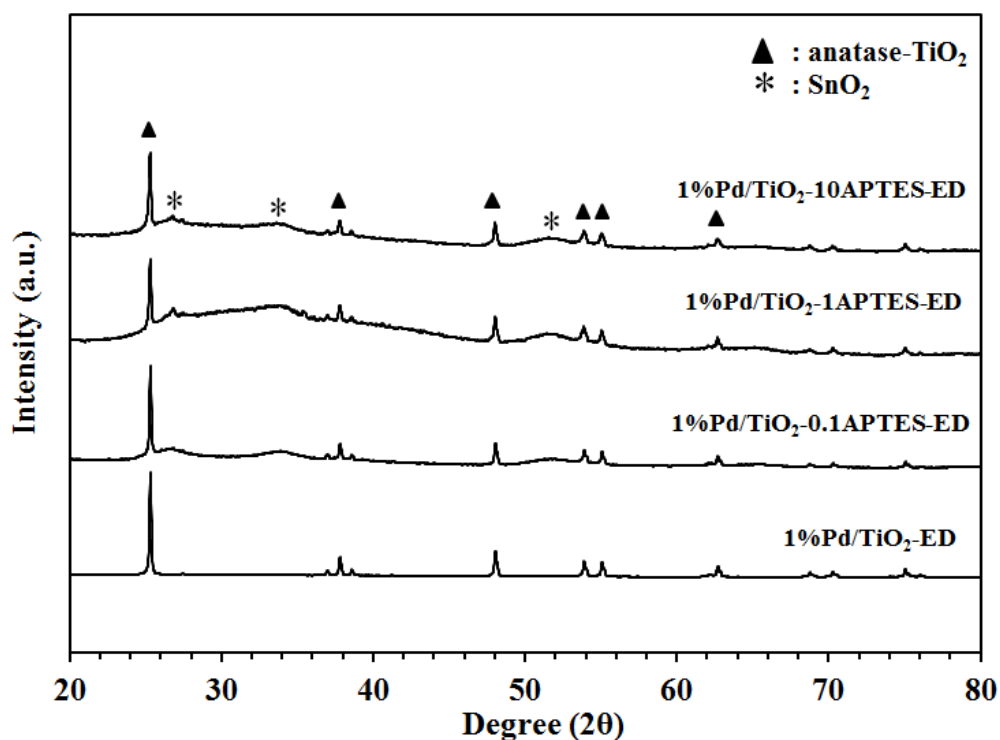


Figure 5.9 The XRD patterns of 1%Pd/ TiO_2 catalysts prepared by electroless deposition method

Table 5.3 The peak position of anatase (101) TiO₂, d-spacing and the lattice parameters of TiO₂ for 1%Pd/TiO₂ catalysts prepared by electroless deposition method.

| Catalysts | Peak position of anatase (101) TiO ₂ (2θ, degree) | d-spacing (nm) | Lattice parameters ^a (Å) | | |
|------------------------------------|--|----------------|-------------------------------------|--------|------|
| | | | a (=b) | c | c/a |
| 1%Pd/TiO ₂ -ED | 25.32 | 0.3515 | 3.7845 | 9.4778 | 2.50 |
| 1%Pd/TiO ₂ -0.1APTES-ED | 25.32 | 0.3515 | 3.7845 | 9.4778 | 2.50 |
| 1%Pd/TiO ₂ -1APTES-ED | 25.32 | 0.3515 | 3.7845 | 9.4778 | 2.50 |
| 1%Pd/TiO ₂ -10APTES-ED | 25.30 | 0.3517 | 3.7860 | 9.5091 | 2.51 |

^a calculated from Bragg's law using the diffraction peaks of anatase (101) and (200) TiO₂.

5.2.1.2 Transmission electron microscopy (TEM)

The TEM micrographs illustrating the morphology of 1%Pd/TiO₂-ED, 1%Pd/TiO₂-0.1APTES-ED, 1%Pd/TiO₂-1APTES-ED and 1%Pd/TiO₂-10APTES-ED catalysts and corresponding particle size distributions are shown in **Figure 5.10**. All the 1%Pd/TiO₂ catalysts show similar morphology of well dispersed Pd nanoclusters with narrow particle size distribution on the TiO₂ supports. The average particle size of Pd nanoclusters was slightly reduced from 4.1 to 3.5 nm upon APTES surface modification. More uniform and narrow particle sizes distribution of Pd nanoclusters in the range of 2-6 nm with average particle sizes 3.4 nm were found on the 1%Pd/TiO₂-0.1APTES-ED catalyst whereas larger Pd nanoclusters with broader particle size distribution in the range of 2-8 nm were formed on those one prepared with higher concentrations of APTES (1%Pd/TiO₂-1APTES-ED and 1%Pd/TiO₂-10APTES-ED). Such results suggested that suitable amount of APTES attachment (in this case,

APTES = 0.1 mM) plays an important role in controlling the size of Pd nanoparticles. The monolayer APTES grafting provided terminating amino functional groups (-NH₂) which acted as anchoring sites to stabilize the Pd nanoparticles via the covalent interactions, resulting in highly dispersed and uniform Pd particle size distribution.

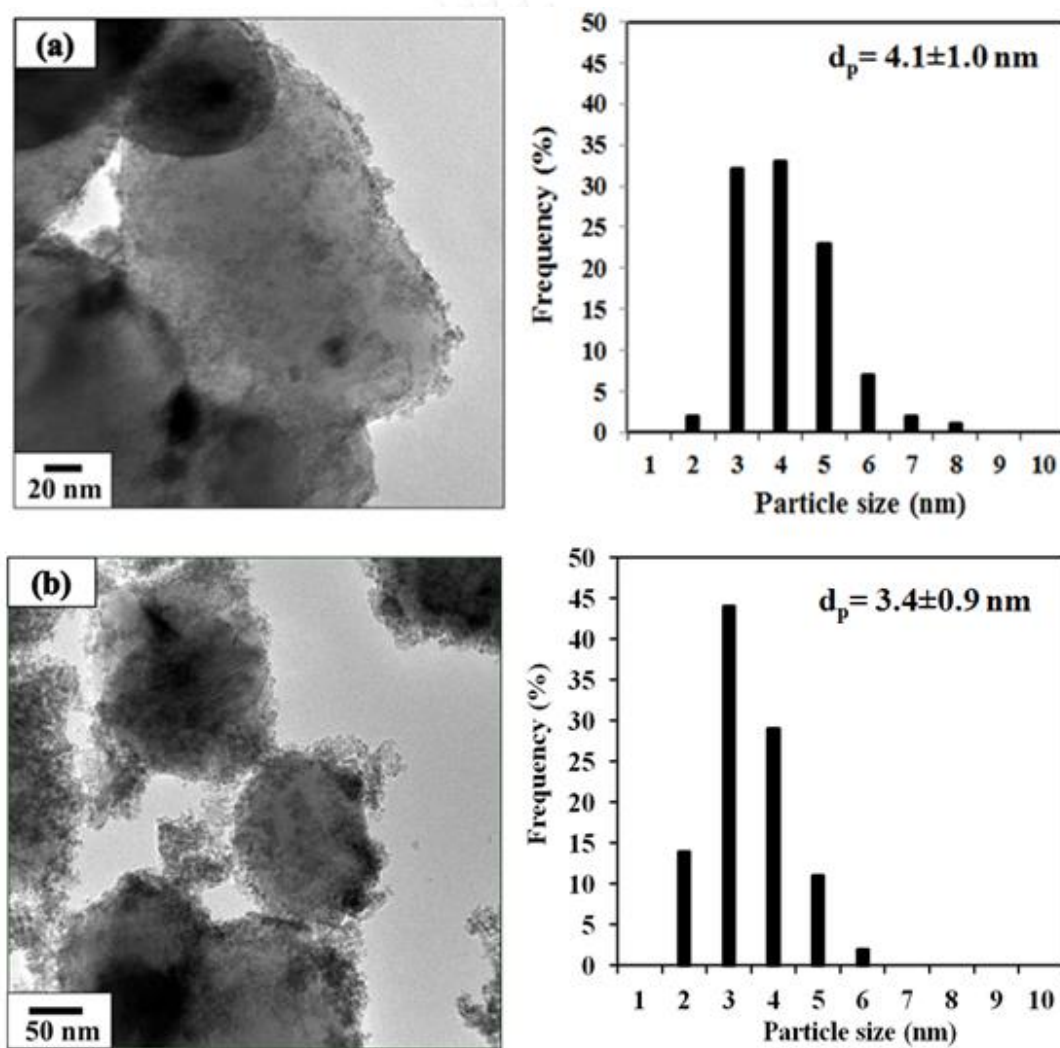


Figure 5.10 TEM micrographs and Pd particles size distributions of 1%Pd/TiO₂ catalysts prepared by electroless deposition method (a) 1%Pd/TiO₂-ED, (b) 1%Pd/TiO₂-0.1APTES-ED, (c) 1%Pd/TiO₂-1APTES-ED, and (d) 1%Pd/TiO₂-10APTES-ED

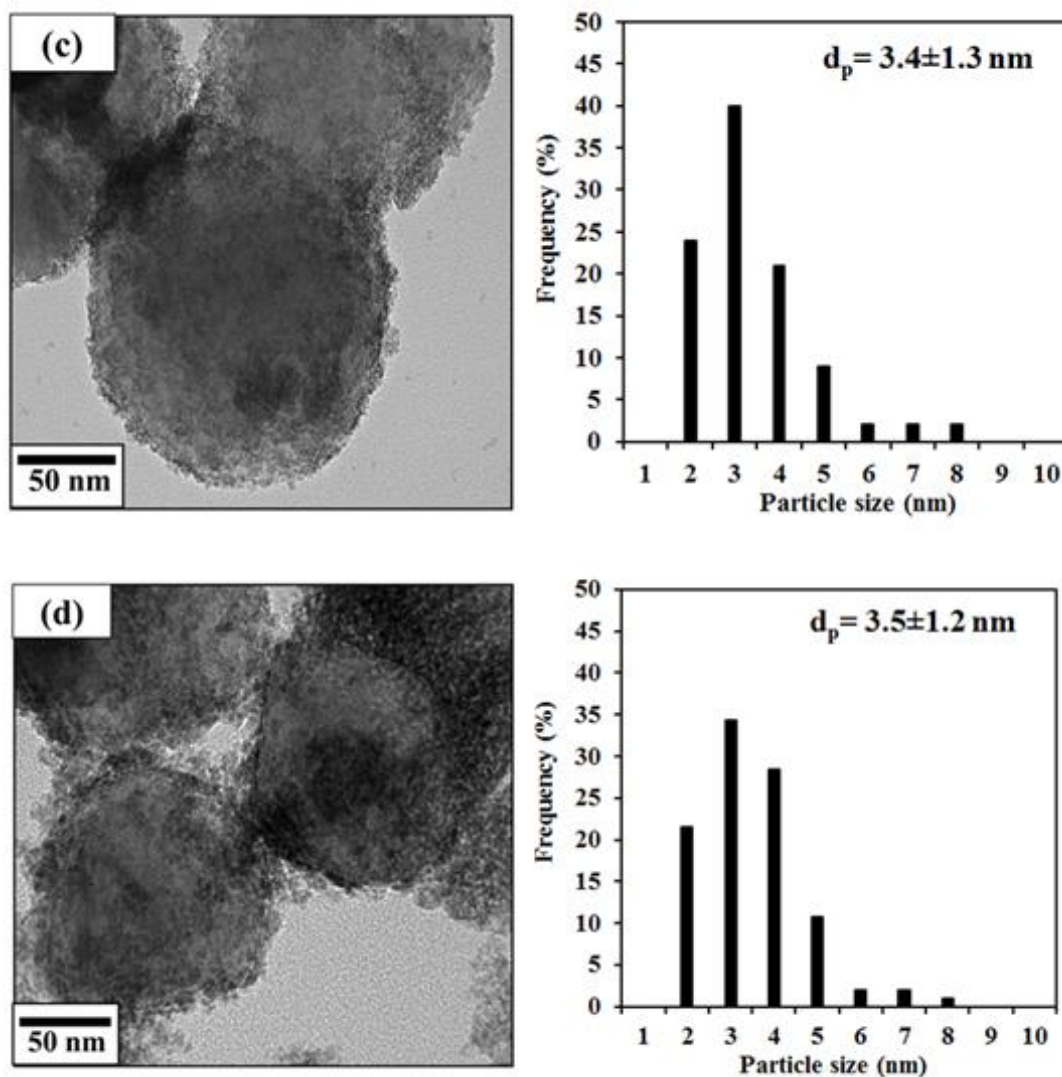


Figure 5.10 (cont.) TEM micrographs and Pd particles size distributions of 1%Pd/TiO₂ catalysts prepared by electroless deposition method (a) 1%Pd/TiO₂-ED, (b) 1%Pd/TiO₂-0.1APTES-ED, (c) 1%Pd/TiO₂-1APTES-ED, and (d) 1%Pd/TiO₂-10APTES-ED

5.2.1.3 X-ray photoelectron spectroscopy (XPS)

The elemental distribution and their electronic properties on the surface of 1%Pd/TiO₂ catalysts prepared by electroless deposition were analyzed by XPS. **Figure 5.11** shows the XPS spectra of Pd 3d for the 1%Pd/TiO₂ catalysts prepared by electroless deposition with various concentrations of APTES attachment. All the samples displayed a typical doublet peak of 3d core level, which was assigned to Pd 3d_{5/2} and Pd 3d_{3/2}. The Pd 3d core level could be fitted with three main doublets of the Pd 3d_{5/2} peaks at 335.3, 337.1 and 338.4 eV [81, 85, 86], which can be assigned to metallic Pd⁰ (Pd⁰), PdO (Pd²⁺) and PdO₂ (Pd⁴⁺), respectively. Surprisingly, PdO₂ (B.E. 338.4 eV) was observed as the major species on the catalysts surface, especially for the 1%Pd/TiO₂-0.1APTES catalyst. Generally, highly oxidizing Pd species (Pd⁴⁺) is known to be unstable in its anhydrous form, however, PdO₂ particles can be stabilized by the matrix of other oxides, such as Al₂O₃, SnO₂, and PdO [81, 86-88]. In the present work, stabilization of PdO₂ particles is possible due to the presence of PdO or SnO₂ obtained from electroless deposition process. The relative abundance of Pd species (Pd⁰, PdO, and PdO₂) on the catalysts is summarized in **Table 5.4**. The percentages of atomic concentration of the total Pd species were found to be in the order 1%Pd/TiO₂-0.1APTES-ED > 1%Pd/TiO₂-ED > 1%Pd/TiO₂-1APTES-ED > 1%Pd/TiO₂-10APTES-ED, respectively. It is noted that increasing the concentrations of APTES resulted in lower amount of Pd being deposited on the TiO₂ surface, due to the formation of multilayers and/or reversed attachment of APTES. The ratios of surface atomic concentration of Pd⁰/PdO_x (1 ≤ x ≤ 2) were determined to be 0.36, 0.18, 0.05, and 0.22 for 1%Pd/TiO₂-ED, 1%Pd/TiO₂-0.1APTES-ED, 1%Pd/TiO₂-1APTES-ED, and 1%Pd/TiO₂-10APTES-ED, respectively.

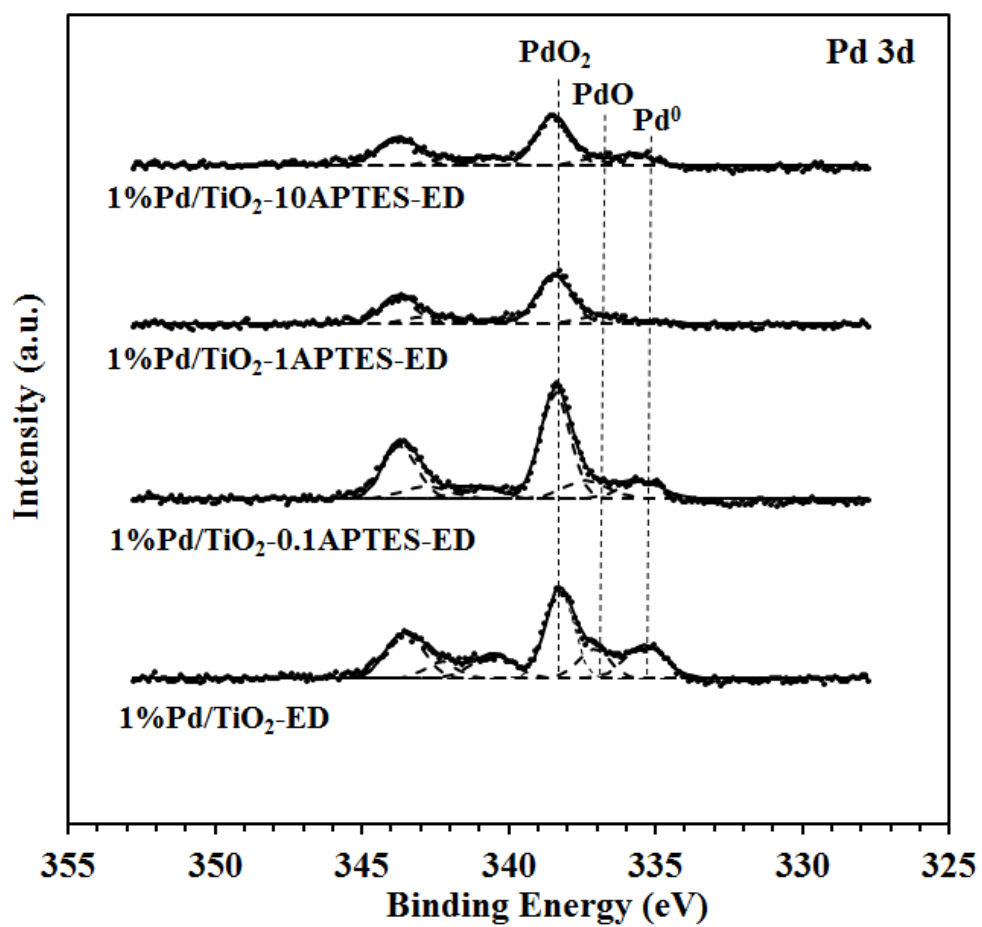


Figure 5.11 The XPS spectra of Pd 3d for 1%Pd/TiO₂ catalysts prepared by electroless deposition method

Table 5.4 Surface compositions and the relative abundance of Pd species of 1%Pd/TiO₂ catalysts prepared by electroless deposition

| Catalysts | Binding Energy (eV) | | | | | At. (%) Pd | Relative abundance of Pd ⁰ , PdO, and PdO ₂ (%) ^a | | | Surface atomic ratio | | |
|------------------------------------|---------------------|-------|-------|-------|-------|---------------|---|-------|------------------|----------------------|-------|--|
| | Ti 2p | O 1s | Pd 3d | N 1s | Sn 3d | | Pd ⁰ | PdO | PdO ₂ | Ti/O | Pd/Ti | Pd ⁰ /PdO _x ^b |
| 1%Pd/TiO ₂ -ED | 458.7 | 530.6 | 338.2 | - | 486.8 | 0.96 | 26.58 | 21.09 | 52.33 | 0.12 | 0.12 | 0.36 |
| 1%Pd/TiO ₂ -0.1APTES-ED | 458.8 | 530.9 | 338.3 | 400.1 | 486.9 | 0.98 | 15.45 | 17.25 | 67.30 | 0.05 | 0.32 | 0.18 |
| 1%Pd/TiO ₂ -1APTES-ED | 458.9 | 530.9 | 338.2 | 400.5 | 487.0 | 0.57 | 4.85 | 14.53 | 80.62 | 0.05 | 0.16 | 0.05 |
| 1%Pd/TiO ₂ -10APTES-ED | 458.8 | 531.0 | 338.4 | 400.4 | 487.0 | 0.51 | 17.75 | 9.29 | 72.96 | 0.06 | 0.13 | 0.22 |

^a Obtained from the deconvoluted area of XPS spectra of Pd 3d using Origin program.

^b Determined from ratio between metallic Pd⁰ and total of PdO_x (1 ≤ x ≤ 2)

5.2.1.4 Fourier transforms infrared spectroscopy (FTIR)

The functional groups of 1%Pd/TiO₂ catalysts prepared by electroless deposition method compared with pristine TiO₂ were investigated by Fourier Transform Infrared Spectroscopy with a transmittance mode. **Figure 5.12** illustrates the FTIR spectra of pristine TiO₂ and 1%Pd/TiO₂ catalysts prepared by electroless deposition. All Pd/TiO₂ catalysts show the typical IR band at 680 cm⁻¹, which was assigned to the symmetric stretching vibration of Ti-O-Ti bonds in the TiO₂ lattice [75, 76]. However, the intensity of IR-peaks decreased compared with pristine TiO₂ support indicating to the surface of TiO₂ was covered by some materials. It was possible due to SnCl₂ sensitization process in electroless deposition facilitated the SnO₂ stabilized Pd metal and then metallic Pd⁰ was deposited on the TiO₂. Moreover, the IR band at 1080 cm⁻¹, which can be attributed to the asymmetric stretching vibration of Si-O-Si bridge [77, 78] and the IR bands at ca. 1600 cm⁻¹ and 3450 cm⁻¹, which were attributed to H-OH stretching vibration of physisorbed water and the stretching vibration of hydroxyl group of Ti-OH bonds [75], were observed on all 1%Pd/TiO₂ catalysts. However, the IR band at around 900 cm⁻¹, which was assigned to the stretching vibration of Ti-O-Si, and the IR peaks at 1460 cm⁻¹ and 1390 cm⁻¹, which assigned to the characteristic of C-H and C-N stretching vibration of APTES [19, 77], became smaller.

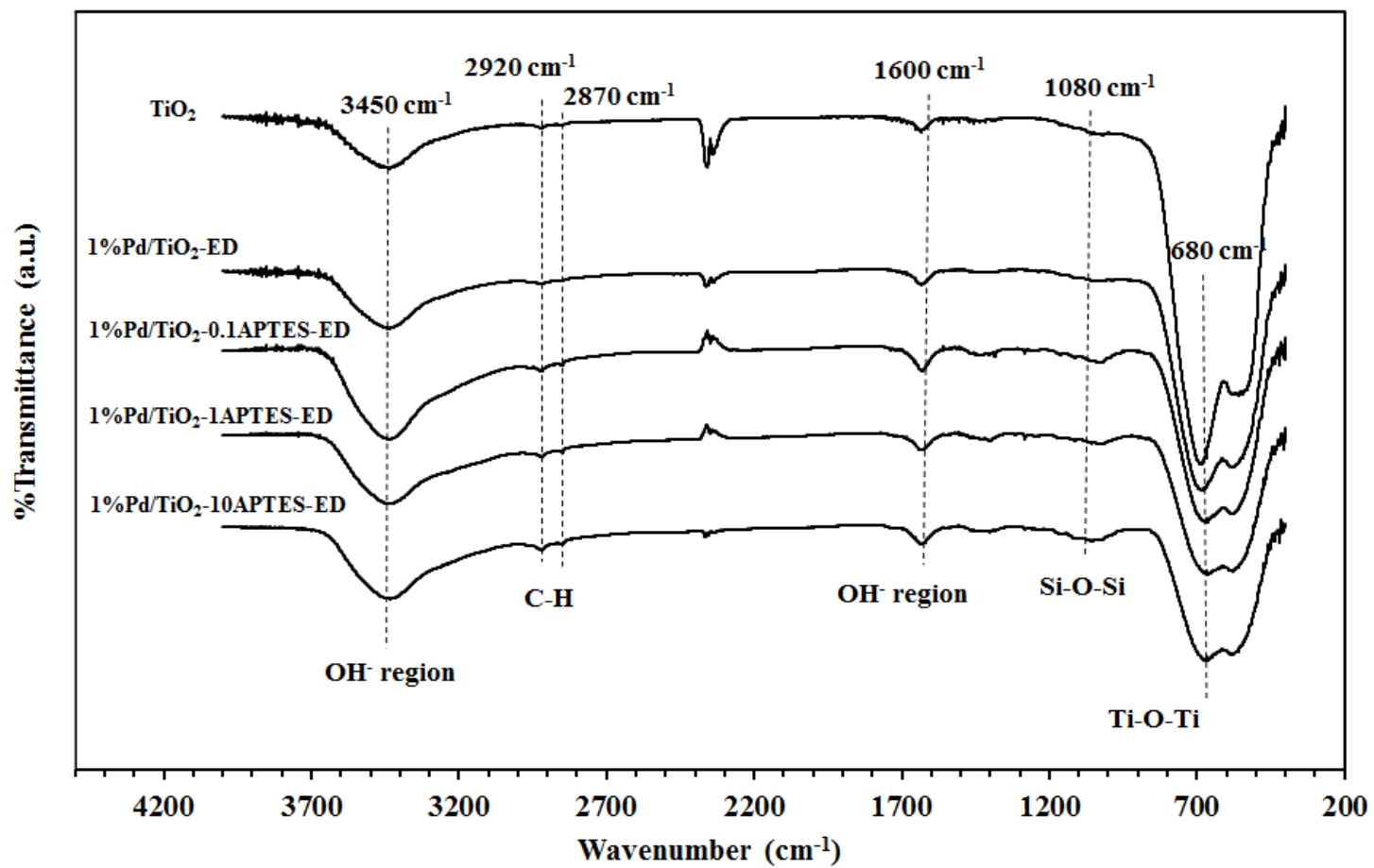


Figure 5.12 FTIR spectra of pristine TiO₂ and 1%Pd/TiO₂ catalysts prepared by electroless deposition method

5.2.2 The catalytic activity of 1%Pd/TiO₂ catalysts prepared by electroless deposition in the solvent-free selective oxidation of benzyl alcohol.

The catalytic performances of all 1%Pd/TiO₂ catalysts prepared by electroless deposition were evaluated in the solvent-free selective oxidation of benzyl alcohol under molecular O₂ (pO₂-1 bar) at 120°C. The conversion of benzyl alcohol and selectivity of benzaldehyde and the other byproducts obtained over 1%Pd/TiO₂ catalysts at 7 h reaction time are summarized in **Table 5.5**. Generally for selective oxidation of benzyl alcohol, benzaldehyde is produced as the main product along with trace amount of toluene, benzoic acid, benzyl benzoate and benzene as the byproducts. The highest benzyl alcohol conversion was obtained from 1%Pd/TiO₂-0.1APTES-ED (61.8%), followed by 1%Pd/TiO₂-ED (57.6%), 1%Pd/TiO₂-10APTES-ED (19.7%) and 1%Pd/TiO₂-1APTES-ED (8.2%) catalysts, respectively. Higher selectivity of benzaldehyde (> 80%) was obtained over the Pd catalysts supported on APTES modified TiO₂, comparing to that produced by 1%Pd/TiO₂-ED catalyst (selectivity of benzaldehyde 74%). Among the catalysts studied, the 1%Pd/TiO₂-0.1APTES-ED exhibited the best catalytic performances in the solvent-free selective oxidation of benzyl alcohol (conversion 61.8% and selectivity of benzaldehyde 89.8%). For the 1%Pd/TiO₂-ED catalyst, although high catalytic activity was achieved with the conversion at 57.6%, but lower selectivity of benzaldehyde at 74% was obtained. Furthermore, relatively large amount of toluene (ca. 20%) was obtained as the byproduct for the 1%Pd/TiO₂-ED catalyst from the disproportionation of benzyl alcohol. According to the literature [89], acidity/basicity of reaction mixture or the catalytic surface plays a crucial role in controlling catalysis of disproportionation in the benzyl alcohol oxidation. Formation of toluene by the disproportionation of

benzyl alcohol is favored when active metal particles are supported on acidic material and does not occur when basic supports are used. Thus, mildly acidic surface of the non-modified TiO_2 supported Pd catalyst (1%Pd/ TiO_2 -ED) facilitated the disproportionation reaction. Modification of TiO_2 supports by APTES increased basicity of the catalyst surface via the hydrolysis of amino groups ($-\text{NH}_2$). As a consequence, lower amount of toluene were produced on all the APTES modified catalysts. The surface basicity promoted the formation of benzoic acid while suppressed the formation of toluene. Increasing of surface basicity is suggested to enhance the dehydrogenation of benzyl alcohol.

High catalytic activity of Pd/ TiO_2 in the benzyl alcohol oxidation is correlated well with the formation of uniform Pd nanoclusters, especially on the 1%Pd/ TiO_2 -0.1APTES where the highest amount of Pd being deposited on the TiO_2 surface. However, it is interesting to note that the lower surface atomic ratios of Pd^0/PdO_x on the catalyst surface (as found on 1%Pd/ TiO_2 -0.1APTES-ED) did not lower the catalyst activity in the benzyl alcohol oxidation. Metallic Pd^0 has often been regarded as the active species for the benzyl alcohol oxidation and is known to be more active than the oxide forms of palladium [6, 62, 90]. In the present work, all the prepared catalysts contained Pd^0 and PdO_x species. A recent study by Wang et al. [24] revealed that reconstruction of PdO to metallic Pd^0 sites by hydrogen spillover occurred during the benzyl alcohol oxidation. The metallic Pd^0 appeared to be necessary at the beginning of reaction. Benzyl alcohol adsorbed on the metallic Pd^0 sites and then hydrogen spillover from β -C-H bond subsequently reduced most of PdO_x species to metallic Pd^0 , leading to more metallic Pd^0 sites. The dehydrogenation of benzyl alcohol then occurred and benzaldehyde was released

to the liquid-phase as the final product. Hence, high conversion of benzyl alcohol with high selectivity of benzaldehyde can be obtained on the catalysts with high Pd dispersion even though they contained both Pd^0/PdO_x species (in our case, the 1%Pd/TiO₂-0.1APTES-ED). Wang et al. [24] also suggested that PdO_x converted to different types of Pd metallic sites; defect sites, bridge sites, and hollow sites. Nevertheless, the oxidative dehydrogenation of alcohol to the corresponding aldehyde occurred on all exposed metallic Pd^0 faces. The mechanism for the *in-situ* reduction of PdO_x to metallic Pd^0 by hydrogen spillover from the benzyl alcohol during the reaction is illustrated in Figure 5.13.

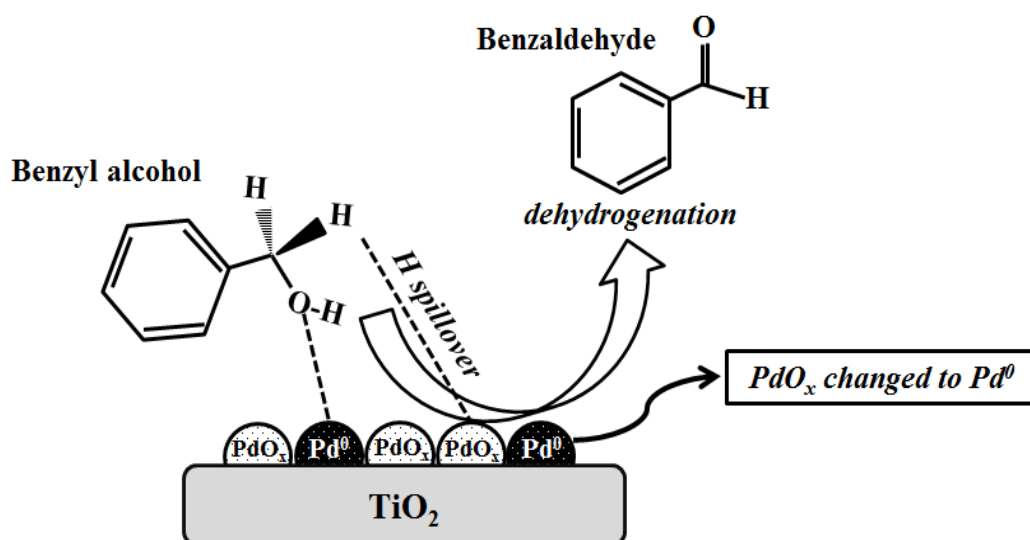


Figure 5.13 The mechanism for *in-situ* reduction of PdO_x to metallic Pd^0 by hydrogen spillover from the benzyl alcohol during the benzyl alcohol oxidation.

Table 5.5 Solvent-free liquid-phase selective oxidation of benzyl alcohol to benzaldehyde for 1%Pd/TiO₂ catalysts prepared by electroless deposition method at 7h.^a

| Catalysts | Conversion (%) | Product selectivity (%) ^b | | | | | Yield (%) ^c |
|------------------------------------|----------------|--------------------------------------|---------|--------------|-----------------|---------|------------------------|
| | | Benzaldehyde | Toluene | Benzoic acid | Benzyl benzoate | Benzene | |
| 1%Pd/TiO ₂ -ED | 57.6 | 74.1 | 20.2 | 3.5 | 2.0 | 0.2 | 42.7 |
| 1%Pd/TiO ₂ -0.1APTES-ED | 61.8 | 89.8 | 6.6 | 1.2 | 2.0 | 0.4 | 55.5 |
| 1%Pd/TiO ₂ -1APTES-ED | 8.2 | 84.1 | 0.4 | 4.8 | 10.7 | 0.0 | 6.9 |
| 1%Pd/TiO ₂ -10APTES-ED | 19.7 | 89.5 | 6.8 | 10.7 | 1.9 | 0.4 | 17.6 |

^a Reaction conditions: benzyl alcohol 10 cm³, 25 mg of catalyst, $T=120^{\circ}\text{C}$, $p\text{O}_2 = 1$ bar, stirring speed 1000 rpm. The errors for the conversion and selectivity measurements were $\pm 5\%$.

^b Selectivity of toluene, benzoic acid, benzyl benzoate and benzene present as byproducts.

^c %Yield of benzaldehyde which is the main product for this reaction.

5.2.3 Catalytic activity of 1%Pd/TiO₂ catalysts prepared by electroless deposition method in the liquid phase selective hydrogenation of 3-hexyn-1-ol

The catalytic performances of the 1%Pd/TiO₂ catalysts prepared by electroless deposition were evaluated in the liquid phase selective hydrogenation of 3-hexyn-1-ol to cis-3-hexen-1-ol using 100 ml stainless steel autoclave reactor under mild reaction conditions (p_{H_2} 2 bar and temperature 40°C). **Figure 5.14** illustrates the conversion of 3-hexyn-1-ol as a function of reaction time. The hydrogenation rates were found to be in the order 1%Pd/TiO₂-0.1APTES-ED > 1%Pd/TiO₂-10APTES-ED ≥ 1%Pd/TiO₂-1APTES-ED > 1%Pd/TiO₂-ED. Complete conversion (100%) of 3-hexyn-1-ol can be achieved from all 1%Pd/TiO₂ catalysts prepared by electroless deposition after 30 minutes of reaction time. However, it was clearly seen that APTES modified catalysts exhibited higher catalytic hydrogenation rates than the non-modified one. These results may possibly due to electron donating from NH₂ termination of APTES molecules to the metallic Pd⁰ facilitate the strong interaction between metal and support. Then alkyne molecules were weakly adsorbed on catalyst surface resulting in an increase of hydrogenation rate. Nevertheless, the order of catalytic activity for APTES modified 1%Pd/TiO₂ catalysts prepared by electroless deposition depended on the total amounts of Pd on catalyst surface as shown in the XPS results. The atomic concentration of Pd for Pd supported on APTES modified TiO₂ catalysts were in the order 1%Pd/TiO₂-0.1APTES-ED (0.98%) > 1%Pd/TiO₂-1APTES-ED (0.57%) > 1%Pd/TiO₂-10APTES-ED (0.51%), respectively. These results were corresponded with the catalytic activity of 3-hexyn-1-ol hydrogenation.

Figure 5.15 shows the selectivity of cis-3-hexen-1-ol for all 1%Pd/TiO₂ catalysts prepared by electroless deposition as a function of reaction time. Higher

selectivity of cis-3-hexen-1-ol (80-93%) was obtained on the catalysts when the reaction time was lower than 15 min. However after complete conversion of 3-hexyn-1-ol, the selectivity of cis-3-hexen-1-ol dramatically decreased to 22-44% for APTES modified catalysts whereas that of non-modified catalyst was slightly dropped to 63%. The major byproduct for this reaction is trans-3-hexen-1-ol followed by 1-hexanol.

The catalytic performances of 1%Pd/TiO₂ catalysts prepared by electroless deposition method are demonstrated in **Figure 5.16**. The selectivity of cis-3-hexen-1-ol for all 1%Pd/TiO₂ catalysts were not significant different at low conversion (less than 50%). However, after conversion reached 80%, the selectivity of cis-3-hexen-1-ol dropped to 70% for 1%Pd/TiO₂-1APTES-ED and 1%Pd/TiO₂-10APTES-ED catalysts. The highest catalytic performance in the liquid-phase selective hydrogenation of 3-hexyn-1-ol was obtained from the non-modified 1%Pd/TiO₂-ED catalyst. The non-modified 1%Pd/TiO₂-ED catalyst shows the highest catalytic performance (conversion of 3-hexyn-1-ol 100%, selectivity of cis-3-hexen-1-ol 88%), probably because the lowest hydrogenation rate retarded cis-3-hexen-1-ol hydrogenation. For 1%Pd/TiO₂-0.1APTES-ED catalysts, the highest hydrogenation rate with high catalytic performance can be obtained at 100% of 3-hexyn-1-ol conversion with 86% cis-3-hexen-1-ol selectivity.

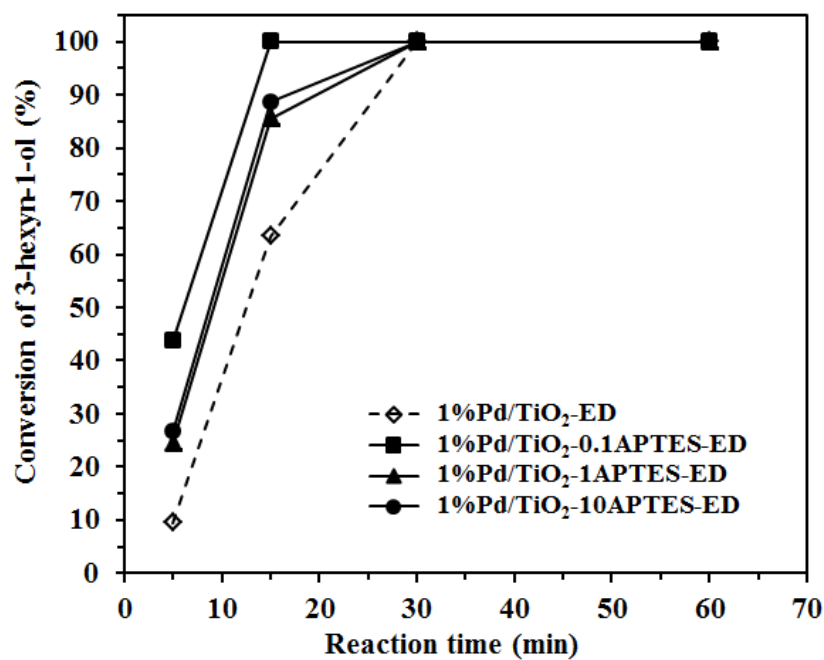


Figure 5.14 Conversion of 3-hexyn-1-ol for 1%Pd/TiO₂ catalysts prepared by electroless deposition with different reaction times

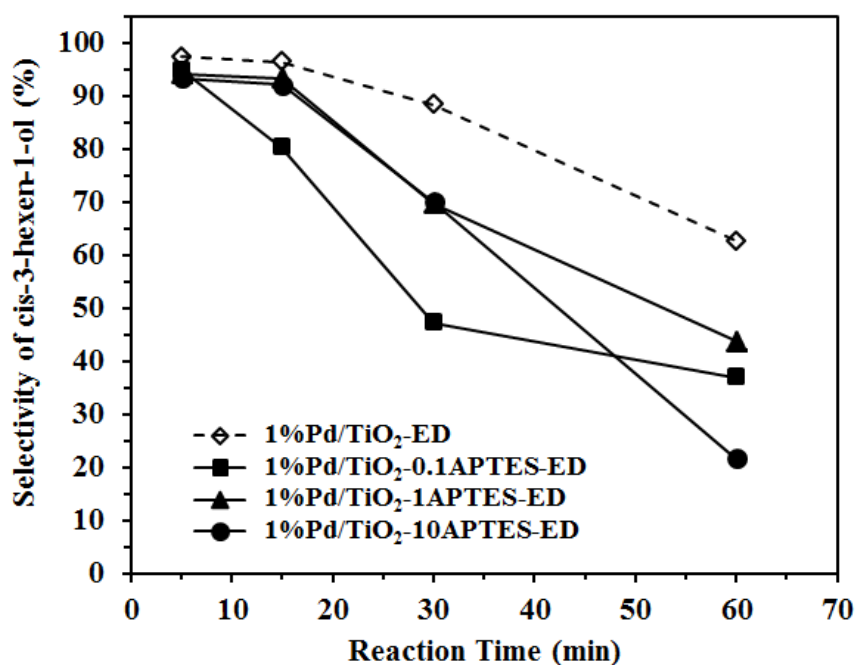


Figure 5.15 Selectivity of cis-3-hexen-1-ol for 1%Pd/TiO₂ catalysts prepared by electroless deposition with different reaction times

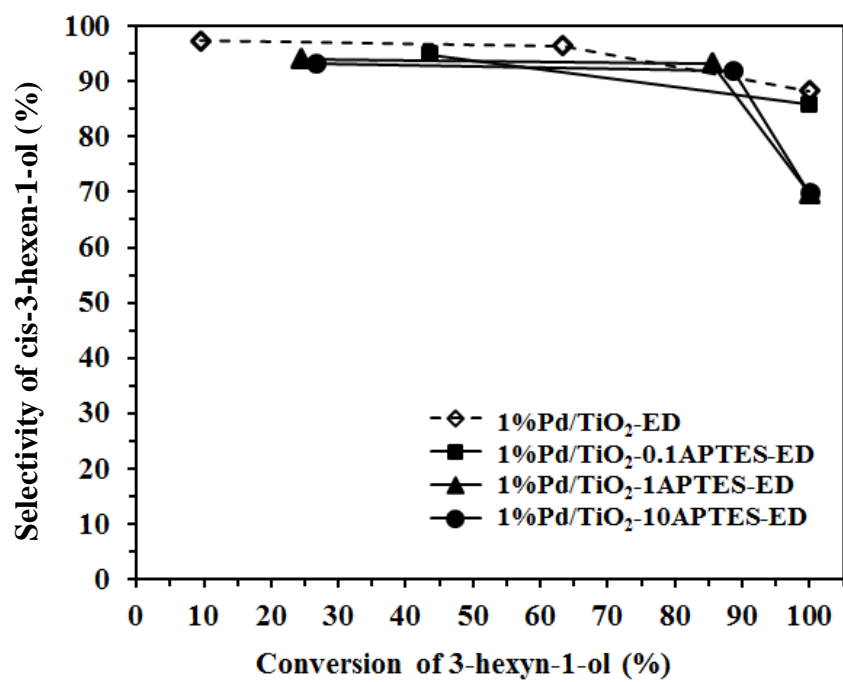


Figure 5.16 The catalytic performance for 1%Pd/TiO₂ catalysts prepared by electroless depositions in the liquid phase selective hydrogenation of 3-hexyn-1-ol

5.3 The characteristics and catalytic properties of 1%Pd/TiO₂ catalysts prepared by sonochemical method

The characteristics of 1%Pd/TiO₂ catalysts prepared by sonochemical method are illustrated in the section 5.3.1. The catalytic performances for all 1%Pd/TiO₂ catalysts were evaluated in the solvent-free selective oxidation of benzyl alcohol and the liquid phase selective hydrogenation of 3-hexyn-1-ol and the results are demonstrated in section 5.3.2 and 5.3.3, respectively.

5.3.1 Catalyst characterizations

5.3.1.1 X-ray diffraction (XRD)

The XRD patterns of the 1%Pd/TiO₂ catalysts prepared by sonochemical method are illustrated in **Figure 5.17**. All the catalysts exhibited the characteristic peaks of pure anatase TiO₂ at $2\theta=25^\circ$ (major), 37° , 48° , 55° , 56° , 62° , and 69° . The XRD characteristic peaks corresponding to PdO specie at $2\theta=33.5^\circ$ or metallic Pd⁰ at $2\theta=40.9^\circ$ were not detected for all catalysts due probably to the low amount of Pd present and/or very small Pd⁰/PdO crystallite size. Moreover, the peak position of anatase TiO₂ (101), d-spacing and the lattice parameters calculated from Bragg's law of all 1%Pd/TiO₂ catalysts prepared by sonochemical method are shown in **Table 5.6**. The value of 2-theta for all catalysts were not significant changed compared to the original TiO₂ supports. The d-spacing values and the lattice parameters for all Pd/TiO₂ catalysts were also not altered from those original TiO₂ supports suggesting that Pd was deposited only on the TiO₂ surface not inserted in the TiO₂ lattice.

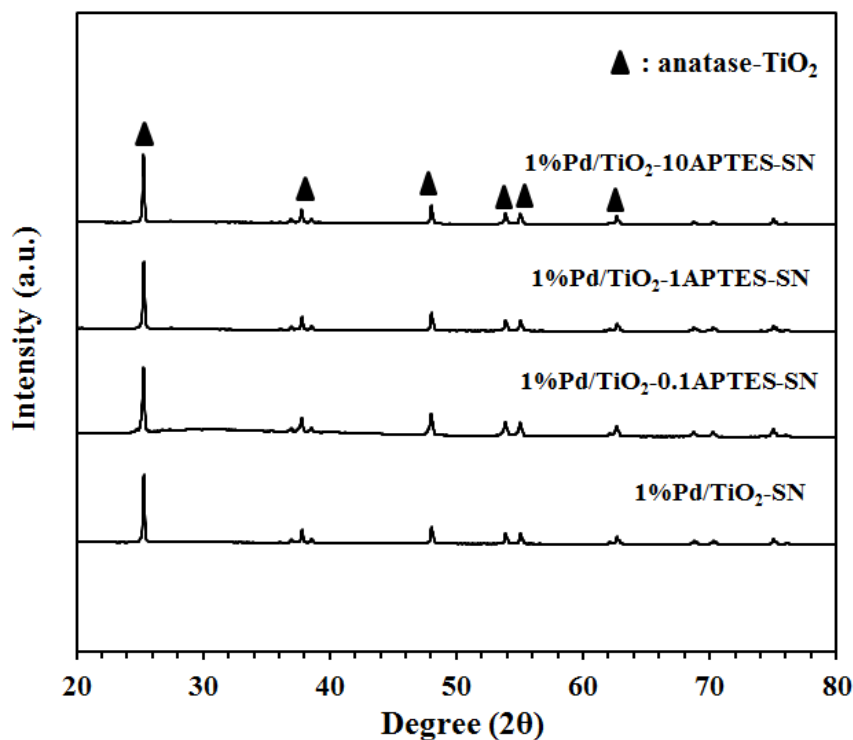


Figure 5.17 The XRD patterns of 1%Pd/TiO₂ catalysts prepared by sonochemical method

Table 5.6 The peak position of anatase (101) TiO₂, d-spacing and the lattice parameters of TiO₂ for 1%Pd/TiO₂ catalysts prepared by sonochemical method.

| Catalysts | Peak position of anatase (101) TiO ₂ (2θ, degree) | d-spacing (nm) | Lattice parameters ^a (Å) | | |
|------------------------------------|--|----------------|-------------------------------------|----------|------------|
| | | | <i>a</i> (=b) | <i>c</i> | <i>c/a</i> |
| 1%Pd/TiO ₂ -SN | 25.32 | 0.3515 | 3.7845 | 9.4778 | 2.50 |
| 1%Pd/TiO ₂ -0.1APTES-SN | 25.30 | 0.3517 | 3.7860 | 9.5091 | 2.51 |
| 1%Pd/TiO ₂ -1APTES-SN | 25.32 | 0.3515 | 3.7845 | 9.4778 | 2.50 |
| 1%Pd/TiO ₂ -10APTES-SN | 25.30 | 0.3517 | 3.7860 | 9.5091 | 2.51 |

^a calculated from Bragg's law using the diffraction peaks of anatase (101) and (200) TiO₂.

5.3.1.2 Transmission electron microscopy (TEM)

The morphologies of 1%Pd/TiO₂ catalysts prepared by sonochemical method were investigated by using the transmission electron microscopy (TEM). **Figure 5.18** illustrates the TEM micrographs and the Pd particles size distribution of (a) 1%Pd/TiO₂-SN, (b) 1%Pd/TiO₂-0.1APTES-SN, (c) 1%Pd/TiO₂-1APTES-SN, and (d) 1%Pd/TiO₂-10APTES-SN, respectively. It was clearly seen that small Pd nanoparticles were agglomerated to form a larger Pd cluster size on all TiO₂ supports, non-modify and APTES modified TiO₂ supports. These may possibly due to during the reduction of PdO precursor to metallic Pd⁰ by chemical reduction without stabilizing agent for sonochemical method resulting in agglomeration of metallic Pd⁰ even used the ultrasonic assisted. The average Pd particle size for Pd catalysts supported on APTES modified TiO₂ were c.a. 7.5-7.9 nm while those of Pd catalyst supported on non-modified TiO₂ was 7.9 nm. The average Pd particle size obtained from sonochemical method were found to be not significant different. However, large Pd nanoclusters (≥10 nm) with a broader particles size distribution in mean of standard deviation (S.D.) (c.a. 3.1-3.5 nm) were found for 1%Pd/TiO₂-1APTES-SN and 1%Pd/TiO₂-10APTES-SN catalysts. This can be suggested that excess amount of APTES tended to occur a higher variation of Pd particles size.

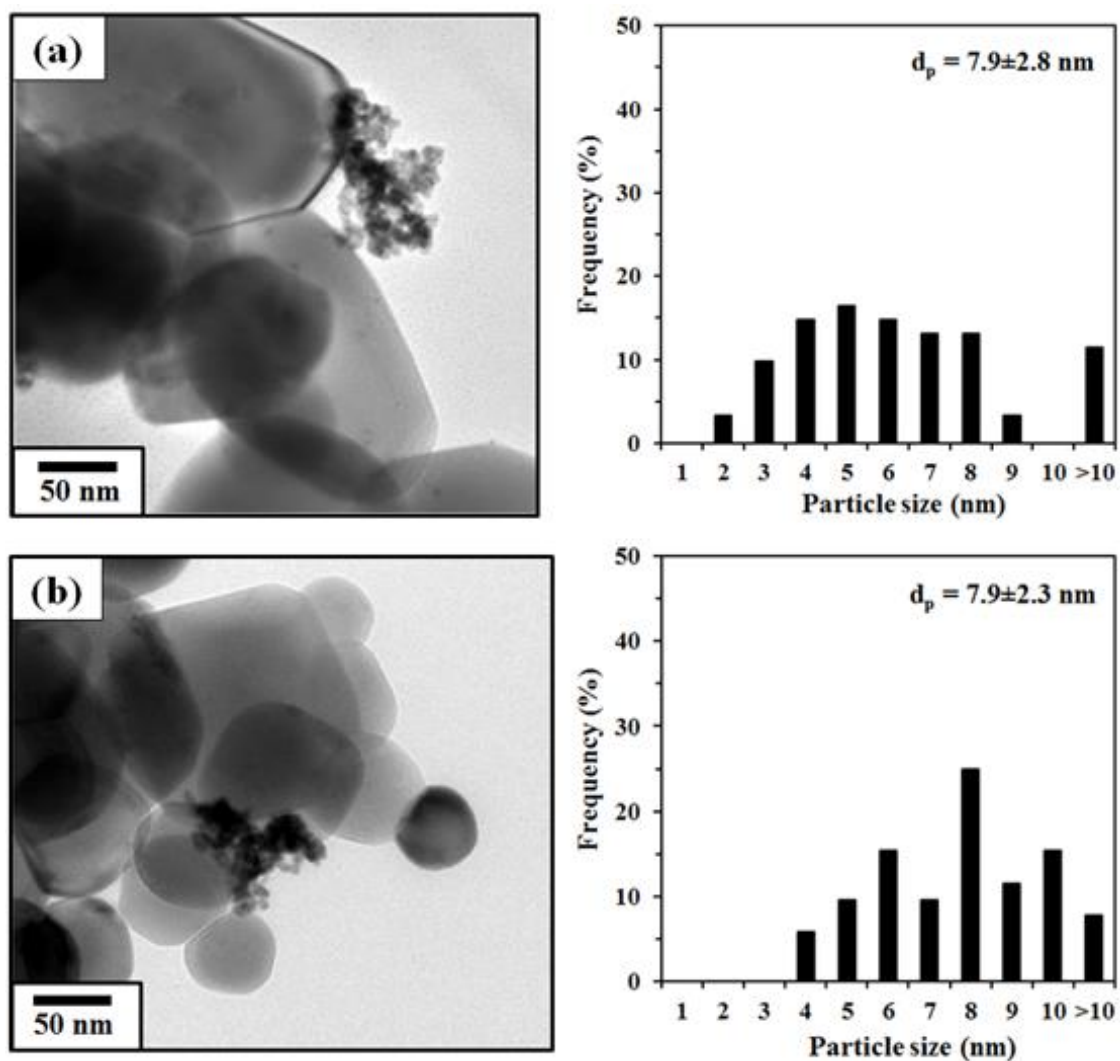


Figure 5.18 TEM micrographs and Pd particles size distributions of 1%Pd/TiO₂ catalysts prepared by sonochemical method (a) 1%Pd/TiO₂-SN, (b) 1%Pd/TiO₂-0.1APTES-SN, (c) 1%Pd/TiO₂-1APTES-SN, and (d) 1%Pd/TiO₂-10APTES-SN

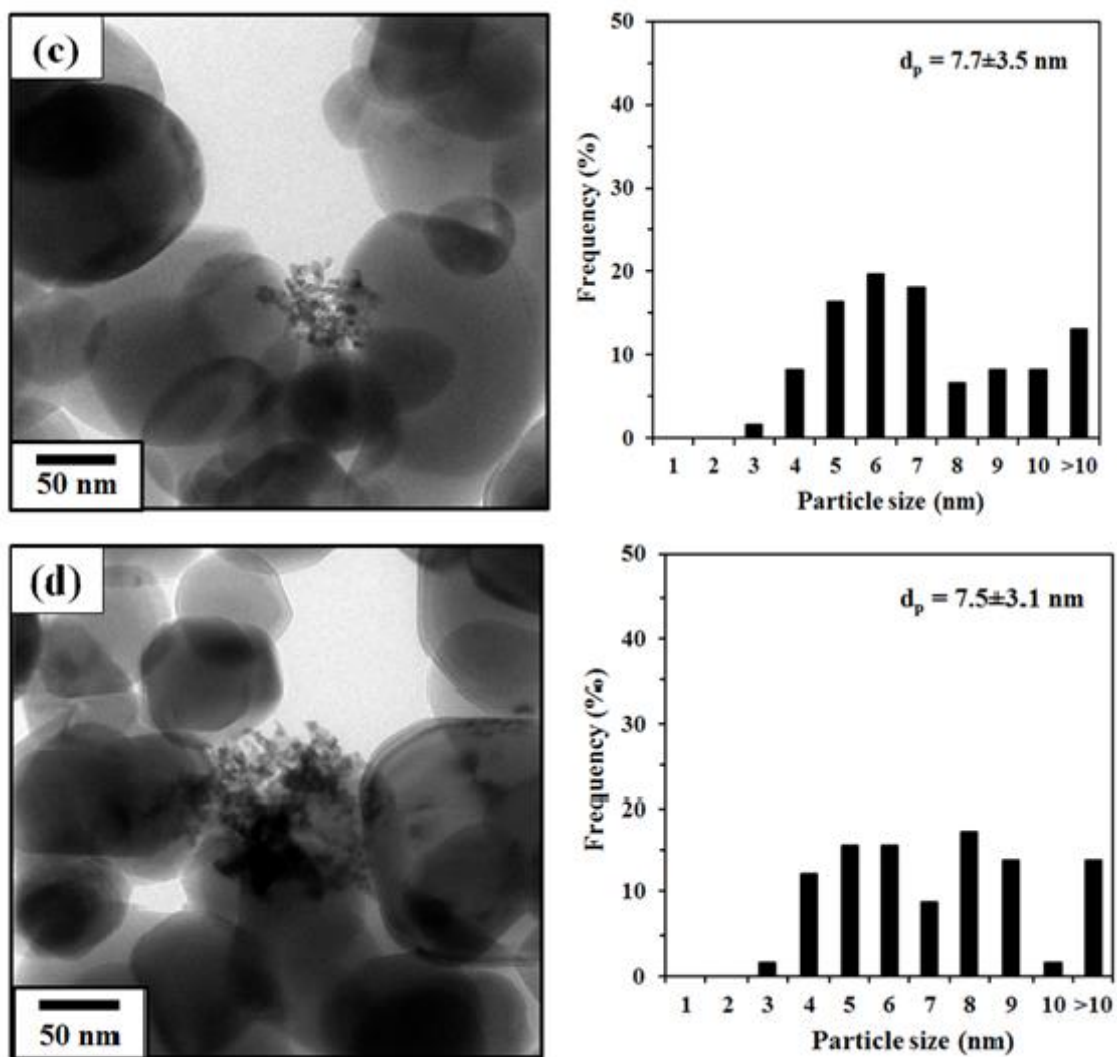


Figure 5.18 (cont.) TEM micrographs and Pd particles size distributions of 1%Pd/TiO₂ catalysts prepared by sonochemical method (a) 1%Pd/TiO₂-SN, (b) 1%Pd/TiO₂-0.1APTES-SN, (c) 1%Pd/TiO₂-1APTES-SN, and (d) 1%Pd/TiO₂-10APTES-SN

5.3.1.3 X-ray photoelectron spectroscopy (XPS)

The structural and electronic properties of Pd nanoparticles/clusters on 1%Pd/TiO₂ catalysts prepared by sonochemical method were further investigated by X-ray photoelectron spectroscopy (XPS). **Figure 5.19** illustrates the Pd 3d XPS spectra of 1%Pd/TiO₂ catalysts derived from sonochemical method. All samples show a typical doublet peaks of Pd 3d core level center around 335-337 eV and 340-342 eV, which were assigned to Pd 3d_{5/2} and Pd 3d_{3/2}, respectively. The Pd 3d core level could be fitted with two main doublets of the Pd 3d_{5/2} peaks at around 334.6, 336.3 eV, which can be assigned to metallic Pd⁰ and PdO, respectively [40, 81]. Highly oxidizing Pd species (PdO₂ or Pd⁴⁺) was not detected on all 1%Pd/TiO₂ catalysts derived by sonochemical method. Moreover, the surface composition and relative abundance of Pd species of all 1%Pd/TiO₂ catalysts prepared by sonochemical method are summarized in **Table 5.7**. The binding energy of Ti 2p around 458 eV and O 1s around 530 eV for all samples can be attributed to Ti⁴⁺ and oxygen lattice of TiO₂ support, respectively. The percentages of surface atomic concentration of Pd species were found to be in the order 1%Pd/TiO₂-SN (0.78) > 1%Pd/TiO₂-0.1APTES-SN (0.61) > 1%Pd/TiO₂-10APTES-SN (0.43) > 1%Pd/TiO₂-1APTES-SN (0.24). It can be noted that Pd contents on the catalyst surface decreased when Pd supported on APTES modified TiO₂ catalysts. However, the actual amount of Pd loading determined by inductive coupled plasma optical emission spectrometer (ICP-OES) for all 1%Pd/TiO₂ catalysts derived by sonochemical method were not significant different (c.a. 1.0-1.3 %) indicating that there were different Pd dispersions on various Pd/TiO₂ catalysts. Furthermore, it was clearly seen that the proportion of metallic Pd⁰ to PdO species increased for Pd catalysts supported on APTES modified TiO₂. Comparing the relative

abundance of Pd species, Pd supported on APTES modified TiO₂ catalysts exhibited higher amount of metallic Pd⁰ than PdO whereas the non-modified catalyst gave higher amount of PdO than metallic Pd⁰. This may possibly due to electron donating from nitrogen of amine group to metallic Pd⁰ facilitated the electronic interaction resulting to increase the proportion of metallic Pd⁰. Our results were consistent with the recently report by Radkevich et al. [91]. They showed that the amino groups possessing electron donor properties can increase the proportion of Pd⁰ and resistance against re-oxidation of Pd⁰ due to the electronic interactions between nitrogen atom and metallic Pd⁰ nanoparticles, which are active centers for hydrogenation-dehydrogenation reactions.

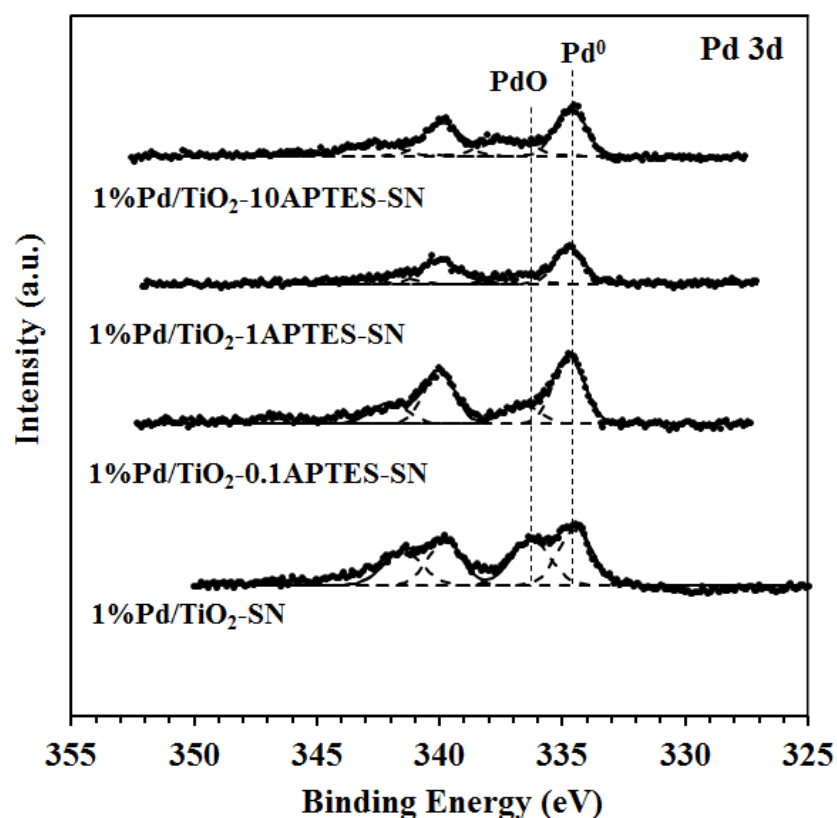


Figure 5.19 The XPS spectra of Pd 3d for 1%Pd/TiO₂ catalysts prepared by sonochemical method

Table 5.7 Surface compositions and the relative abundance of Pd species of 1%Pd/TiO₂ catalysts prepared by sonochemical method

| Catalysts | Binding Energy (eV) | | | | | At. (%) Pd | ICP ^a (%) Pd | Relative abundance of Pd ⁰ and PdO ^b (%) | | Surface atomic ratio | | |
|------------------------------------|---------------------|-------|-------|-------|-------|---------------|----------------------------|---|-------|----------------------|-------|----------------------|
| | Ti 2p | O 1s | Pd 3d | N 1s | Si 2p | | | Pd ⁰ | PdO | Ti/O | Pd/Ti | Pd ⁰ /PdO |
| 1%Pd/TiO ₂ -SN | 458.8 | 530.1 | 334.5 | - | - | 0.78 | 1.18 | 48.65 | 51.35 | 0.28 | 0.04 | 0.95 |
| 1%Pd/TiO ₂ -0.1APTES-SN | 458.9 | 530.2 | 334.8 | n.d. | 101.8 | 0.61 | 1.35 | 74.15 | 25.85 | 0.25 | 0.03 | 2.87 |
| 1%Pd/TiO ₂ -1APTES-SN | 458.4 | 529.9 | 334.6 | n.d. | 101.7 | 0.24 | 1.33 | 74.53 | 25.47 | 0.32 | 0.01 | 2.93 |
| 1%Pd/TiO ₂ -10APTES-SN | 458.4 | 529.8 | 334.6 | 400.8 | 101.9 | 0.43 | 0.99 | 63.31 | 36.69 | 0.27 | 0.02 | 1.73 |

^a The actual amount of the Pd loading determined by a Perkin Elmer Optima 2100DV AS93 PLUS inductive coupled plasma optical emission spectrometer.

^b Obtained from the deconvoluted area of XPS spectra of Pd 3d using Origin program.

5.3.1.4 Fourier transforms infrared spectroscopy (FTIR)

The functional groups of 1%Pd/TiO₂ catalysts prepared by sonochemical method compared with pristine TiO₂ were investigated by Fourier Transform Infrared Spectroscopy with a transmittance mode and the results are illustrated in **Figure 5.20**. The typical IR band at 680 cm⁻¹, which was assigned to the symmetric stretching vibration of Ti-O-Ti bonds in the TiO₂ lattice, was found on all samples [75, 76]. As similar as the IR bands at ca. 1600 cm⁻¹ and 3450 cm⁻¹, which were attributed to H-OH stretching vibration of physisorbed water and the stretching vibration of hydroxyl group of Ti-OH bonds [75], were be observed on pristine TiO₂ and all 1%Pd/TiO₂ catalysts. Moreover, the small IR peaks at 1460 cm⁻¹ and 1390 cm⁻¹ assigned to the characteristic of C-H and C-N stretching vibration of APTES [19, 77] and the broad typical IR band at 1080 cm⁻¹ which attributed to the asymmetric stretching vibration of Si-O-Si bridge achieved from the APTES molecules coupling [77, 78], were clearly more pronounced for all Pd catalysts supported on APTES modified TiO₂ supports. However, The IR band at around 900 cm⁻¹ assigned to the stretching vibration of Ti-O-Si became smaller after Pd deposition on the APTES modified TiO₂ support.

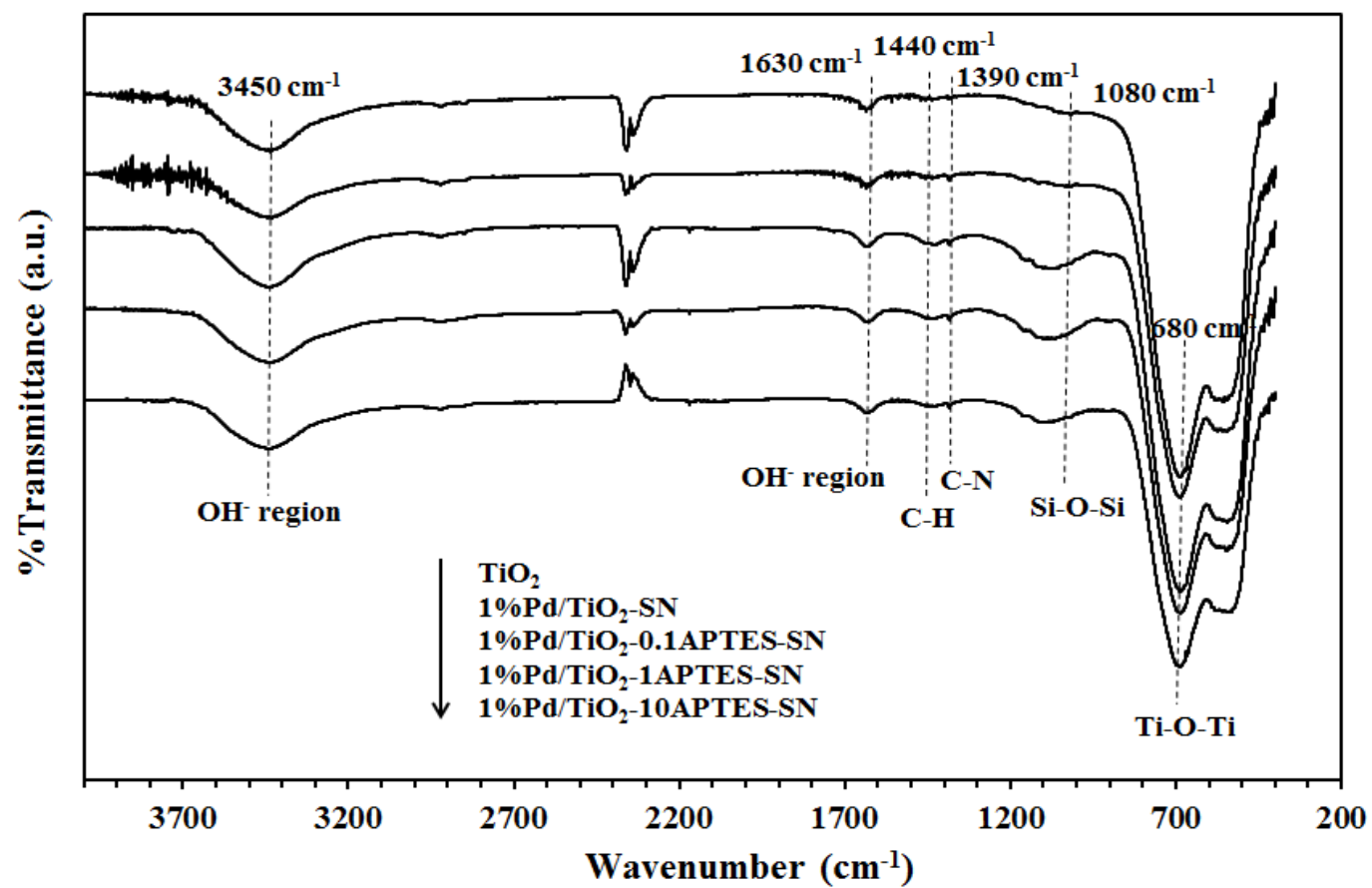


Figure 5.20 FTIR spectra of pristine TiO₂ and 1%Pd/TiO₂ catalysts prepared by sonochemical method

5.3.2 Reaction study in the solvent-free selective oxidation of benzyl alcohol to benzaldehyde

The catalytic performances of 1%Pd/TiO₂ catalysts prepared by sonochemical method were evaluated in the solvent-free selective oxidation of benzyl alcohol using molecular O₂ (pO₂ 1 bar) at 120 °C. **Table 5.8** summarized the conversion of benzyl alcohol, the selectivity of benzaldehyde and other byproducts for all 1%Pd/TiO₂ catalysts prepared by sonochemical method at 7h of reaction time. The conversion of benzyl alcohol was found to be in the order 1%Pd/TiO₂-SN (57.5%) > 1%Pd/TiO₂-1APTES-SN (52.2%) > 1%Pd/TiO₂-0.1APTES-SN (47.2%) > 1%Pd/TiO₂-10APTES-SN (27.2%). It was clearly seen that lower catalytic activity was obtained from Pd supported on APTES modified TiO₂ catalysts. This may be because of lower amount of surface atomic concentration of Pd on the Pd catalysts supported on APTES modified TiO₂. Actual amount of Pd loading from ICP-OES for all catalysts were around 1 wt. %, however, the surface metallic Pd⁰ specie which is essential active metal specie for benzyl alcohol oxidation were difference. Moreover previous studies from 1%Pd/TiO₂ catalysts derived by electroless deposition method, the catalyst containing high surface atomic concentration of Pd which possessed both metallic Pd⁰ and PdO_x species exhibited high catalytic activity in benzyl alcohol oxidation. Therefore, it was possible to suggest that the 1%Pd/TiO₂-SN catalyst gave the highest catalytic activity of benzyl alcohol oxidation because it had the highest surface atomic concentration of Pd.

In term of benzaldehyde selectivity at 7h of reaction time, similar selectivity of benzaldehyde around 58-60% was found on all 1%Pd/TiO₂ catalysts derived by sonochemical method, except 1%Pd/TiO₂-10APTES-SN catalyst. The highest

selectivity of benzaldehyde at 81.4% was obtained from 1%Pd/TiO₂-10APTES-SN catalyst. The lowest catalytic conversion of benzyl alcohol (27.2%) on 1%Pd/TiO₂-10APTES-SN retarded the dehydrogenation rate of benzaldehyde to benzoic acid; hence higher selectivity of benzaldehyde was obtained. For other byproducts, toluene was found to be the major byproduct, following by benzoic acid benzyl benzoate and benzene.

Besides the conversion of benzyl alcohol and selectivity of benzaldehyde, the percentage of yield for benzaldehyde was calculated to evaluate the catalytic performance of 1%Pd/TiO₂ derived by sonochemical method and the results are summarized in **Table 5.8**. The highest catalytic performance of benzyl alcohol oxidation for sonochemical catalysts was achieved from 1%Pd/TiO₂-SN catalyst at 34% yield. The order of yield was 1%Pd/TiO₂-SN > 1%Pd/TiO₂-1APTES-SN > 1%Pd/TiO₂-0.1APTES-SN > 1%Pd/TiO₂-10APTES-SN.

Table 5.8 Solvent-free selective oxidation of benzyl alcohol to benzaldehyde for 1%Pd/TiO₂ catalysts prepared by sonochemical method at 7h.^a

| Catalysts | Conversion (%) | Product selectivity ^b (%) | | | | | Yield ^c (%) |
|------------------------------------|----------------|--------------------------------------|---------|--------------|-----------------|---------|------------------------|
| | | Benzaldehyde | Toluene | Benzoic acid | Benzyl benzoate | Benzene | |
| 1%Pd/TiO ₂ -SN | 57.5 | 59.1 | 38.4 | 1.1 | 1.1 | 0.3 | 34.0 |
| 1%Pd/TiO ₂ -0.1APTES-SN | 47.2 | 60.2 | 36.7 | 1.3 | 1.5 | 0.4 | 28.4 |
| 1%Pd/TiO ₂ -1APTES-SN | 52.2 | 58.8 | 38.7 | 0.9 | 1.2 | 0.4 | 30.7 |
| 1%Pd/TiO ₂ -10APTES-SN | 27.2 | 81.4 | 9.5 | 3.9 | 4.5 | 0.7 | 22.1 |

^a Reaction conditions: benzyl alcohol 10 cm³, 25 mg of catalyst, $T=120^{\circ}\text{C}$, $p\text{O}_2 = 1$ bar, stirring speed 1000 rpm. The errors for the conversion and selectivity measurements were $\pm 5\%$.

^b Selectivity of toluene, benzoic acid, benzyl benzoate and benzene present as byproducts.

^c %Yield of benzaldehyde which is the main product for this reaction.

5.3.3 Reaction study in the liquid phase selective hydrogenation of 3-hexyn-1-ol to cis-3-hexen-1-ol

The catalytic performances of all 1%Pd/TiO₂ catalyst prepared by sonochemical method were also evaluated in the liquid phase selective hydrogenation of 3-hexyn-1-ol to cis-3-hexen-1-ol using 100 ml stainless steel autoclave reactor under mild reaction conditions (p_{H_2} 2 bar and temperature 40°C). **Figure 5.21** illustrates the conversion of 3-hexyn-1-ol as a function of reaction times. The hydrogenation activities were found to be in the order 1%Pd/TiO₂-1APTES-SN > 1%Pd/TiO₂-10APTES-SN > 1%Pd/TiO₂-0.1APTES-SN > 1%Pd/TiO₂-SN. Complete conversion of 3-hexyn-1-ol (100%) for all Pd supported on APTES modified TiO₂ catalysts occurred within 30-60 min. of reaction time while for Pd supported on non-modified TiO₂ catalyst, complete conversion was obtained after 90 min of reaction time. These should be remarked that Pd supported on APTES modified TiO₂ catalysts showed the higher catalytic hydrogenation rates than non-modified one. Typically, the hydrogenation activity is depended on the amount of active Pd species. However, all Pd/TiO₂ catalysts derived by sonochemical method showed the similar actual amount of Pd loading. Moreover prior to start of the reaction, the catalysts were pretreated in H₂ flow at 40°C for 2h, thus it can be assumed that PdO species should be reduced to metallic Pd⁰. Hence, it is possible to suggest that higher catalytic activity of Pd supported on APTES modified TiO₂ catalysts were obtained because electrons donating from NH₂ termination of APTES molecules to the metallic Pd⁰ facilitated the strong interaction between metal and support. Then alkynes molecules were weakly adsorbed on catalyst surface resulting in an increase of the hydrogenation rate.

The selectivity to cis-3-hexen-1-ol for all 1%Pd/TiO₂ catalysts prepared by sonochemical method as a function of reaction times is illustrated in **Figure 5.22**. High selectivity of cis-3-hexen-1-ol more than 93% was obtained on all catalysts when the reaction time was lower than 15 min. After complete conversion of 3-hexyn-1-ol (100%) with different reaction time (30-90 min), the selectivity of cis-3-hexen-1-ol dramatically decreased to 41-60% for Pd supported on APTES modified TiO₂ catalysts whereas it was sharply dropped to 0% for Pd supported on non-modified TiO₂ catalyst. The major byproduct for this reaction was trans-3-hexen-1-ol followed by 1-hexanol.

The catalytic performances of 1%Pd/TiO₂ catalysts prepared by sonochemical method are demonstrated in **Figure 5.23**. The selectivity of cis-3-hexen-1-ol for all 1%Pd/TiO₂ catalysts were not significant difference at low conversion (less than 50%). However, after conversion reached 90%, the selectivity of cis-3-hexen-1-ol was dramatically dropped to 0% for 1%Pd/TiO₂-SN catalyst whereas for Pd supported on APTES modified TiO₂ catalysts, the selectivity of cis-3-hexen-1-ol were around 41-60%. The results indicated that higher catalytic performances were obtained from all Pd supported on APTES modified TiO₂ catalysts compared with non-modified one. These may be because of the interaction between metallic Pd⁰ and nitrogen promoted desorption of alkene molecules, hence higher selectivity of cis-3-hexen-1-ol can be obtained. The orders of catalytic performance of 1%Pd/TiO₂ catalysts prepared by sonochemical method were 1%Pd/TiO₂-10APTES-SN > 1%Pd/TiO₂-0.1APTES-SN > 1%Pd/TiO₂-1APTES-SN > 1%Pd/TiO₂-SN.

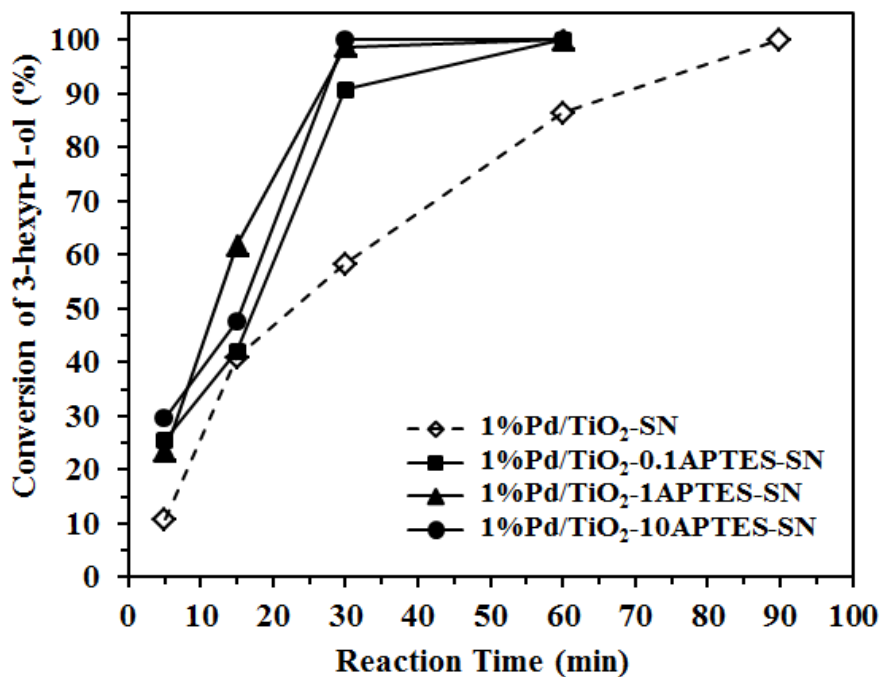


Figure 5.21 Conversion of 3-hexyn-1-ol for 1%Pd/TiO₂ catalysts prepared by sonochemical method with different reaction times

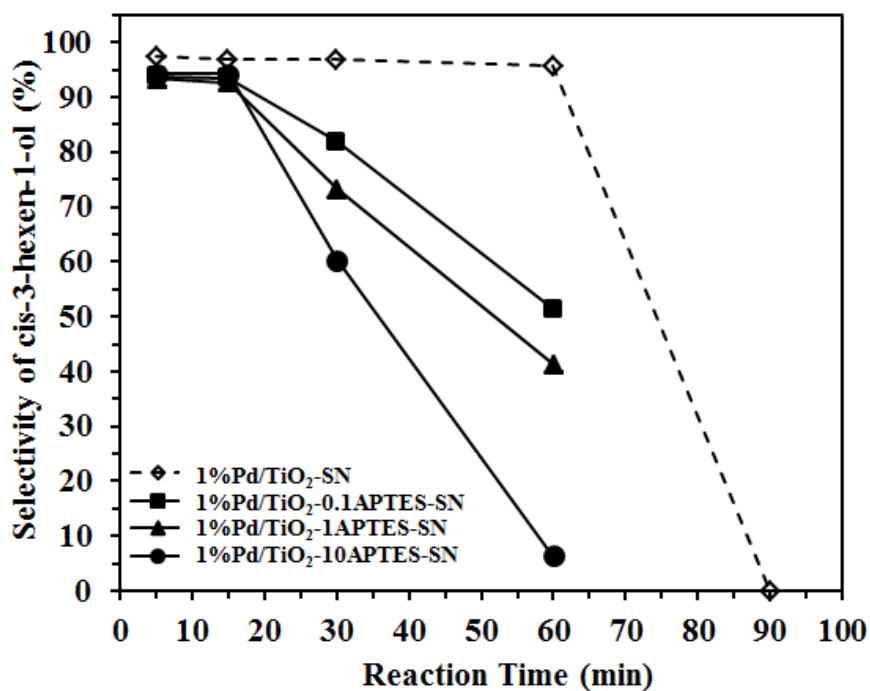


Figure 5.22 Selectivity of cis-3-hexen-1-ol for 1%Pd/TiO₂ catalysts prepared by sonochemical method with different reaction times

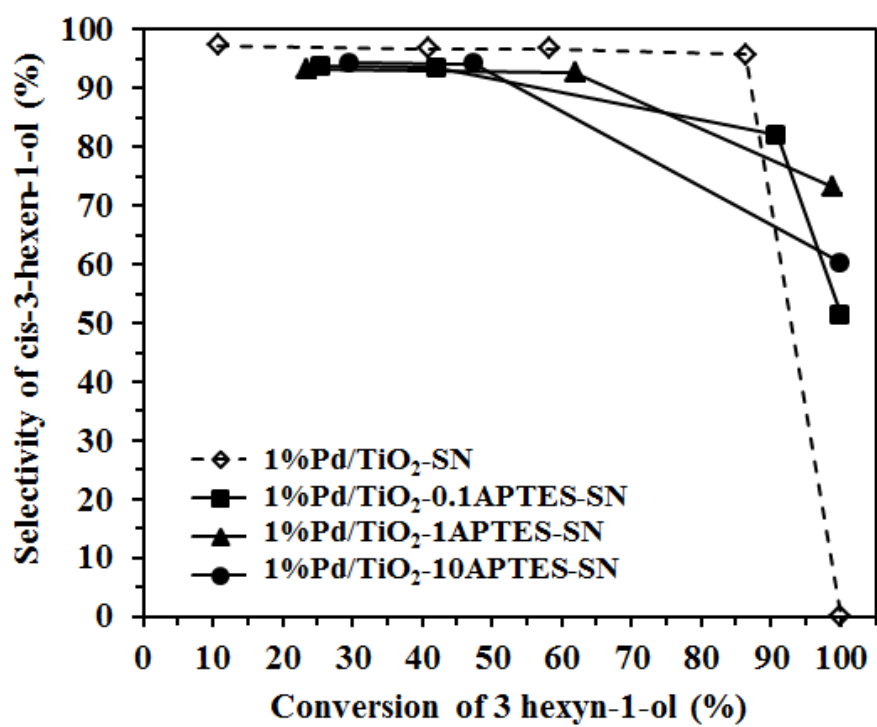


Figure 5.23 The catalytic performance for 1%Pd/TiO₂ catalysts prepared by sonochemical in the liquid phase selective hydrogenation of 3-hexyn-1-ol

5.4 The characteristics and catalytic properties of 1%Pd/TiO₂ catalysts prepared by sol immobilization method

The characteristics of 1%Pd/TiO₂ catalysts prepared by sol immobilization method are illustrated in the section 5.4.1. The catalytic performances for all 1%Pd/TiO₂ catalysts evaluated in solvent-free selective oxidation of benzyl alcohol and the liquid phase selective hydrogenation of 3-hexyn-1-ol are demonstrated in section 5.4.2 and 5.4.3, respectively.

5.4.1 Catalyst characterizations

5.4.1.1 X-ray diffraction (XRD)

The XRD patterns of the 1%Pd/TiO₂ catalysts prepared by sol immobilization method are illustrated in **Figure 5.24**. All catalysts exhibited the characteristic peaks of pure anatase TiO₂ at $2\theta=25^\circ$ (major), 37° , 48° , 55° , 56° , 62° , and 69° . The XRD characteristic peaks corresponding to PdO specie at $2\theta=33.5^\circ$ or metallic Pd⁰ at $2\theta=40.9^\circ$ were not detected for all catalysts due probably to the low amount of Pd present and/or very small Pd⁰/PdO crystallite size. Moreover, the peak position of anatase TiO₂ (101), d-spacing and the lattice parameters calculated from Bragg's law of all 1%Pd/TiO₂ catalysts prepared by sol immobilization method are shown in **Table 5.9**. The value of 2-theta for all catalysts did not changed compared to the original TiO₂ supports. The d-spacing values and the lattice parameters for all 1%Pd/TiO₂ catalysts were also not altered from those original TiO₂ supports suggesting that Pd was deposited only on the TiO₂ surface not inserted in the TiO₂ lattice.

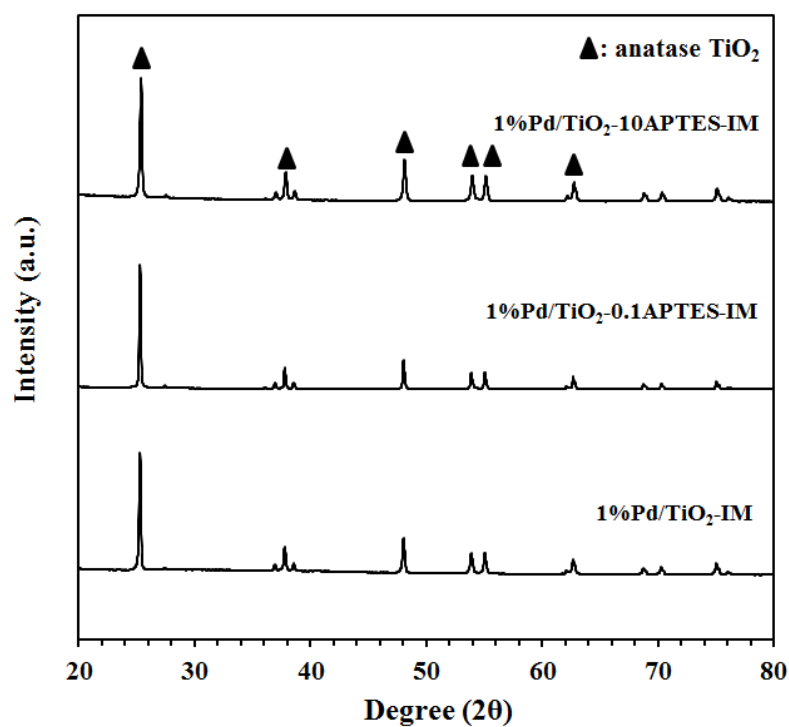


Figure 5.24 The XRD patterns of 1%Pd/TiO₂ catalysts prepared sol immobilization method

Table 5.9 The peak position of anatase (101) TiO₂, d-spacing and the lattice parameters of TiO₂ for 1%Pd/TiO₂ catalysts prepared by sol immobilization method.

| Catalysts | Peak position of anatase (101) TiO ₂ (2θ, degree) | d-spacing (nm) | Lattice parameters ^a (Å) | | |
|------------------------------------|--|----------------|-------------------------------------|--------|------|
| | | | a (=b) | c | c/a |
| 1%Pd/TiO ₂ -IM | 25.32 | 0.3515 | 3.7845 | 9.4778 | 2.50 |
| 1%Pd/TiO ₂ -0.1APTES-IM | 25.32 | 0.3515 | 3.7845 | 9.4778 | 2.50 |
| 1%Pd/TiO ₂ -10APTES-IM | 25.32 | 0.3515 | 3.7845 | 9.4778 | 2.50 |

^a calculated from Bragg's law using the diffraction peaks of anatase (101) and (200) TiO₂

5.4.1.2 Transmission electron microscopy (TEM)

The morphologies of 1%Pd/TiO₂ catalysts prepared by sol immobilization method were investigated by using the transmission electron microscopy (TEM). **Figure 5.25** illustrates the TEM micrographs and the Pd particles size distribution of (a) 1%Pd/TiO₂-IM, (b) 1%Pd/TiO₂-0.1APTES-IM, and (c) 1%Pd/TiO₂-10APTES-IM, respectively. All 1%Pd/TiO₂ catalysts derived by sol immobilization method show small and uniform Pd nanoparticles size with average Pd particle size around 2.4-2.6 nm. It was clearly seen that most of Pd nanoparticles obtained from sol immobilization were in uniform size. This because of during formation of Pd colloids, polyvinyl alcohol (PVA) was added to stabilize the Pd colloid, therefore small and uniform Pd nanoparticles were generated. High amount of Pd nanoparticles dispersed on catalyst surface can be observed on 1%Pd/TiO₂-IM and 1%Pd/TiO₂-0.1APTES-IM micrographs whereas low amount of Pd nanoparticles dispersed on catalyst surface was clearly seen on 1%Pd/TiO₂-10APTES-IM micrograph. This may be because of multilayer and reversed attachment of APTES on TiO₂-10APTES surface affected the lower amount of Pd deposition.

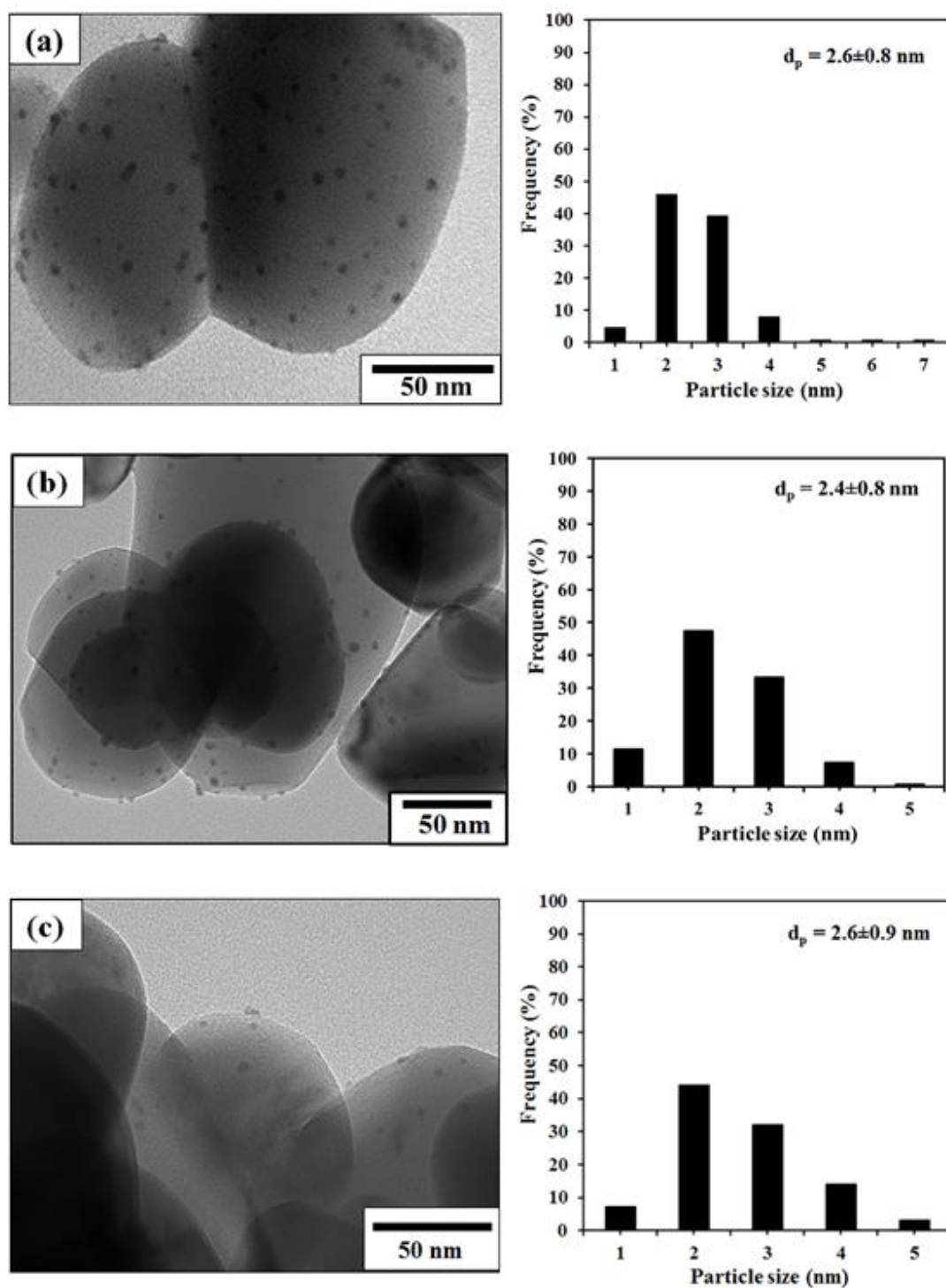


Figure 5.25 TEM micrographs and Pd particles size distributions of 1%Pd/TiO₂ catalysts prepared by sol immobilization method (a) 1%Pd/TiO₂-IM, (b) 1%Pd/TiO₂-0.1APTES-IM, and (c) 1%Pd/TiO₂-10APTES-IM

5.4.1.3 X-ray photoelectron spectroscopy (XPS)

The structural and electronic properties of Pd nanoparticles/clusters on 1%Pd/TiO₂ catalysts prepared by sol immobilization method were further investigated by X-ray photoelectron spectroscopy (XPS). **Figure 5.26** illustrates the Pd 3d XPS spectra of 1%Pd/TiO₂ catalysts derived from sol immobilization method. A typical doublet peaks of Pd 3d core level center around 335-337 eV and 340-342 eV, which were assigned to Pd 3d_{5/2} and Pd 3d_{3/2}, was clearly observed only on 1%Pd/TiO₂-IM catalyst whereas these peaks became flat and hardly to be observed on 1%Pd/TiO₂-0.1APTES-IM and 1%Pd/TiO₂-10APTES-IM catalysts. The Pd 3d core level could be fitted into two main doublets of the Pd 3d_{5/2} peaks at around 335, 336.9 eV, which can be assigned to metallic Pd⁰ and PdO, respectively [40, 81]. Highly oxidizing Pd species (PdO₂ or Pd⁴⁺) was not detected on all 1%Pd/TiO₂ catalysts derived by sol immobilization method. Moreover, the surface composition and relative abundance of Pd species of all 1%Pd/TiO₂ catalysts prepared by sol immobilization method are summarized in **Table 5.10**. The binding energy of Ti 2p around 458.9 eV and O 1s around 530.2 eV for all samples can be attributed to Ti⁴⁺ and oxygen lattice of TiO₂ support, respectively. The percentage of surface atomic concentration of Pd species were found to be in the order 1%Pd/TiO₂-IM (0.55) > 1%Pd/TiO₂-0.1APTES-IM (0.10) ~ 1%Pd/TiO₂-10APTES-IM (0.10). It can be noted that Pd contents on the catalyst surface decreased when Pd supported on APTES modified TiO₂ catalysts. However, as revealed by TEM micrograph, Pd supported on TiO₂-0.1APTES catalyst showed well dispersed of Pd nanoparticles on catalyst surface.

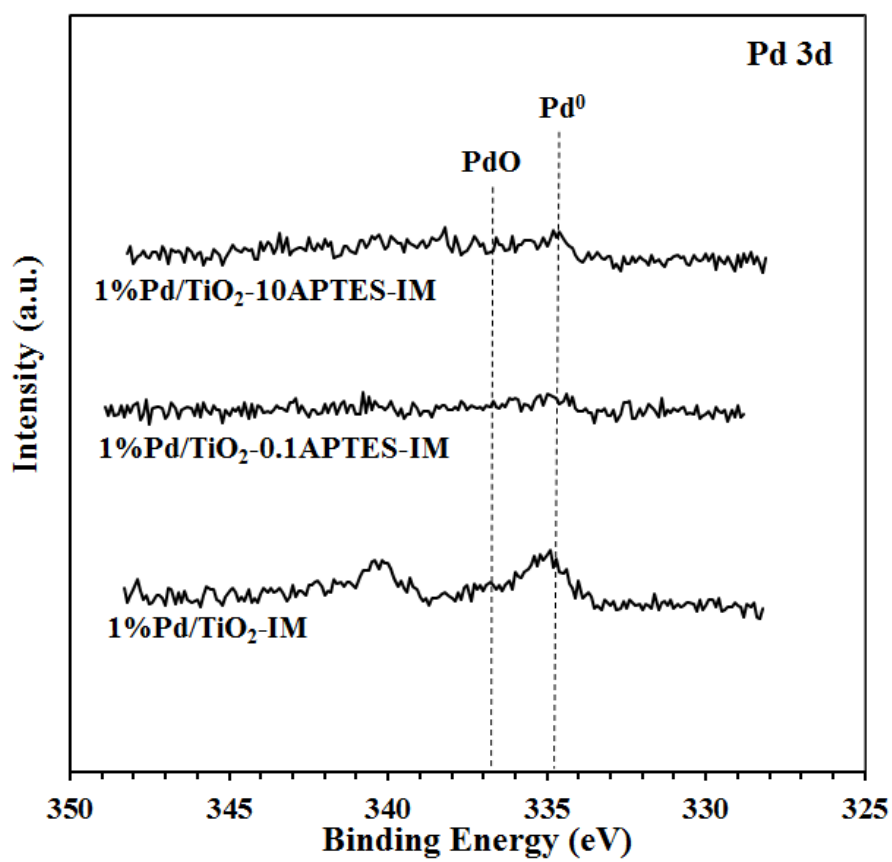


Figure 5.26 The XPS spectra of Pd 3d for 1%Pd/TiO₂ catalysts prepared by sol immobilization method

Table 5.10 Surface compositions and the relative abundance of Pd species of 1%Pd/TiO₂ catalysts prepared by sol immobilization method

| Catalysts | Binding Energy (eV) | | | | | At. (%) | Relative abundance of Pd ⁰ and PdO ^a (%) | | Surface atomic ratio | | |
|------------------------------------|---------------------|-------|-------|-------|-------|---------|--|-----------------|----------------------|------|-------|
| | Ti 2p | O 1s | Pd 3d | N 1s | Si 2p | | Pd | Pd ⁰ | PdO | Ti/O | Pd/Ti |
| 1%Pd/TiO ₂ -IM | 458.9 | 530.2 | 335.5 | - | - | 0.55 | 70.5 | 29.5 | 0.24 | 0.03 | 2.39 |
| 1%Pd/TiO ₂ -0.1APTES-IM | 458.9 | 530.2 | 335.2 | n.d. | n.d. | 0.10 | 100.0 | 0.0 | 0.23 | 0.01 | - |
| 1%Pd/TiO ₂ -10APTES-IM | 458.9 | 530.1 | 334.9 | 400.9 | 102.4 | 0.10 | 100.0 | 0.0 | 0.21 | 0.01 | - |

^a Obtained from the deconvoluted area of XPS spectra of Pd 3d using Origin program.

n.d.; not determined

5.4.2 Reaction study in the solvent-free selective oxidation of benzyl alcohol to benzaldehyde

The catalytic performances of 1%Pd/TiO₂ catalysts prepared by sol immobilization method were evaluated in the solvent-free liquid phase selective oxidation of benzyl alcohol using molecular O₂ (pO₂ 1 bar) at 120°C. **Table 5.11** summarizes the conversion of benzyl alcohol, the selectivity of benzaldehyde and other byproducts for all 1%Pd/TiO₂ catalysts prepared by sol immobilization method at 7h of reaction time. The conversion of benzyl alcohol was found to be in the order 1%Pd/TiO₂-IM (23.9%) > 1%Pd/TiO₂-0.1APTES-IM (11.3%) > 1%Pd/TiO₂-10APTES-IM (8.6%). All catalysts derived by sol immobilization method exhibited quite low catalytic activities in benzyl alcohol oxidation, especially for Pd supported on APTES modified TiO₂ catalysts. This may be because of low amount of Pd being deposited on catalyst surface as shown in XPS results. Generally, Pd colloids were synthesis by using polyvinyl alcohol as a ligand polymer stabilized. After Pd colloid generated, they would adsorb on the metal oxide support with hydrogen bond or electrostatic bond which a weak interaction. Thus, it was possible to achieve low amount of Pd deposited on TiO₂ support when the catalyst was prepared by sol immobilization. For APTES modified TiO₂ support, it is difficult to transfer electron from amino group to metallic Pd⁰ via a polymer stabilized, hence lower Pd deposited was found on Pd supported on APTES modified TiO₂ catalysts.

In term of benzaldehyde selectivity at 7h of reaction time, similar selectivity of benzaldehyde around 86% was found on all 1%Pd/TiO₂-IM and 1%Pd/TiO₂-0.1APTES-IM catalyst. The lowest catalytic activity of benzyl alcohol oxidation with selectivity of benzaldehyde was found on 1%Pd/TiO₂-10APTES-IM catalyst because

low amount of Pd deposition on catalyst surface. For other byproducts of all catalysts, benzoic acid was found to be the major byproduct, following by benzyl benzoate, benzene and toluene. Small amount of toluene occurred in this reaction demonstrated that sol immobilization catalysts can suppress the disproportionation of benzyl alcohol pathway and promote the oxidation pathway of benzaldehyde.

Besides the conversion of benzyl alcohol and selectivity of benzaldehyde, the percentage of yield for benzaldehyde was calculated to evaluate the catalytic performance of 1%Pd/TiO₂ derived by sol immobilization method and the results are summarized in **Table 5.11**. The highest catalytic performance of benzyl alcohol oxidation for sol immobilization catalysts was achieved from 1%Pd/TiO₂-IM catalyst at 20.6% yield. The order of yield was 1%Pd/TiO₂-IM (20.6%) > 1%Pd/TiO₂-0.1APTES-IM (9.8%) > 1%Pd/TiO₂-10APTES-IM (5.5%), respectively.

Table 5.11 Solvent-free selective oxidation of benzyl alcohol to benzaldehyde for 1%Pd/TiO₂ catalysts prepared by sol immobilization method at 7h.^a

| Catalysts | Conversion (%) | Product selectivity ^b (%) | | | | | Yield ^c (%) |
|------------------------------------|----------------|--------------------------------------|---------|--------------|-----------------|---------|------------------------|
| | | Benzaldehyde | Toluene | Benzoic acid | Benzyl benzoate | Benzene | |
| 1%Pd/TiO ₂ -IM | 23.9 | 86.1 | 2.9 | 4.2 | 5.6 | 1.2 | 20.6 |
| 1%Pd/TiO ₂ -0.1APTES-IM | 11.3 | 86.4 | 1.0 | 5.0 | 6.5 | 1.2 | 9.8 |
| 1%Pd/TiO ₂ -10APTES-IM | 8.6 | 64.6 | 0.0 | 15.3 | 20.1 | 0.0 | 5.5 |

^a Reaction conditions: benzyl alcohol 10 cm³, 25 mg of catalyst, $T=120^{\circ}\text{C}$, $p\text{O}_2 = 1$ bar, stirring speed 1000 rpm. The errors for the conversion and selectivity measurements were $\pm 5\%$.

^b Selectivity of toluene, benzoic acid, benzyl benzoate and benzene present as byproducts.

^c %Yield of benzaldehyde which is the main product for this reaction.

5.4.3 Reaction study in the liquid phase selective hydrogenation of 3-hexyn-1-ol to cis-3-hexen-1-ol

The catalytic performances of all 1%Pd/TiO₂ catalyst prepared by sol immobilization method were also evaluated in the liquid phase selective hydrogenation of 3-hexyn-1-ol to cis-3-hexen-1-ol using 100 ml stainless steel autoclave reactor under mild reaction conditions (p_{H_2} 2 bar and temperature 40°C). **Figure 5.27** illustrates the conversion of 3-hexyn-1-ol as a function of reaction times. The hydrogenation activities were found to be in the order 1%Pd/TiO₂-IM > 1%Pd/TiO₂-0.1APTES-IM > 1%Pd/TiO₂-10APTES-IM. Complete conversion of 3-hexyn-1-ol (100%) for 1%Pd/TiO₂-IM occurred within 30 min of reaction time while for 1%Pd/TiO₂-0.1APTES-IM and 1%Pd/TiO₂-10APTES-IM catalyst, complete conversion were obtained after 60 min of reaction time. These should be remarked that Pd supported on APTES modified TiO₂ catalysts showed the lower catalytic hydrogenation rates than non-modified one. Typically, the hydrogenation activity depended on the amount of active metallic Pd⁰ species. As revealed by TEM and XPS results, the higher amount of Pd loading with uniform and small Pd particles size for 1%Pd/TiO₂-IM catalyst was obtained; therefore 1%Pd/TiO₂-IM catalyst showed the highest catalytic activity in the liquid phase selective hydrogenation of 3-hexyn-1-ol. For 1%Pd/TiO₂-0.1APTES-IM and 1%Pd/TiO₂-10APTES-IM catalyst, lower interaction between Pd metal to TiO₂ support affected the strong adsorption of alkynes and H₂ molecules, so that the hydrogenation rate decreased.

Figure 5.28 illustrates the selectivity of benzaldehyde for all 1%Pd/TiO₂ prepared by sol immobilization as a function of reaction time. High selectivity of cis-3-hexen-1-ol more than 95% was obtained on all catalysts when the reaction time

was lower than 15 min. After complete conversion of 3-hexyn-1-ol (100%) with different reaction time (30-60 min), the selectivity of cis-3-hexen-1-ol dramatically decreased to 47% for Pd/TiO₂-IM catalysts whereas it was slowly dropped to 80% and 69% for 1%Pd/TiO₂-0.1APTES-IM and 1%Pd/TiO₂-10APTES-IM, respectively. The major byproduct for this reaction is trans-3-hexen-1-ol followed by 1-hexanol.

The catalytic performances of 1%Pd/TiO₂ catalysts prepared by sol immobilization method are demonstrated in **Figure 5.29**. The selectivity of cis-3-hexen-1-ol for all 1%Pd/TiO₂ catalysts were not significant different at low conversion (less than 50%). However, after conversion reached 70%, the selectivity of cis-3-hexen-1-ol was dramatically dropped to 47% for 1%Pd/TiO₂-IM catalyst whereas for Pd supported on APTES modified TiO₂ catalysts, the selectivity of cis-3-hexen-1-ol were around 69-80%. The results indicated that higher catalytic performances were obtained from all Pd supported on APTES modified TiO₂ catalysts compared with non-modified one. The orders of catalytic performance for 1%Pd/TiO₂ catalysts derived by sol immobilization method were 1%Pd/TiO₂-0.1APTES-IM > 1%Pd/TiO₂-10APTES-IM > 1%Pd/TiO₂-IM.

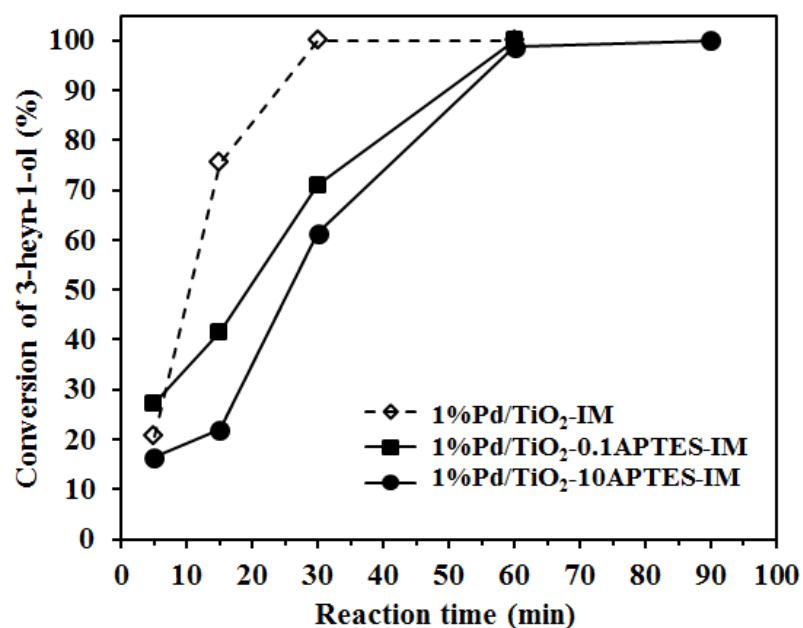


Figure 5.27 Conversion of 3-hexyn-1-ol for 1%Pd/TiO₂ catalysts prepared by sol immobilization method with different reaction times

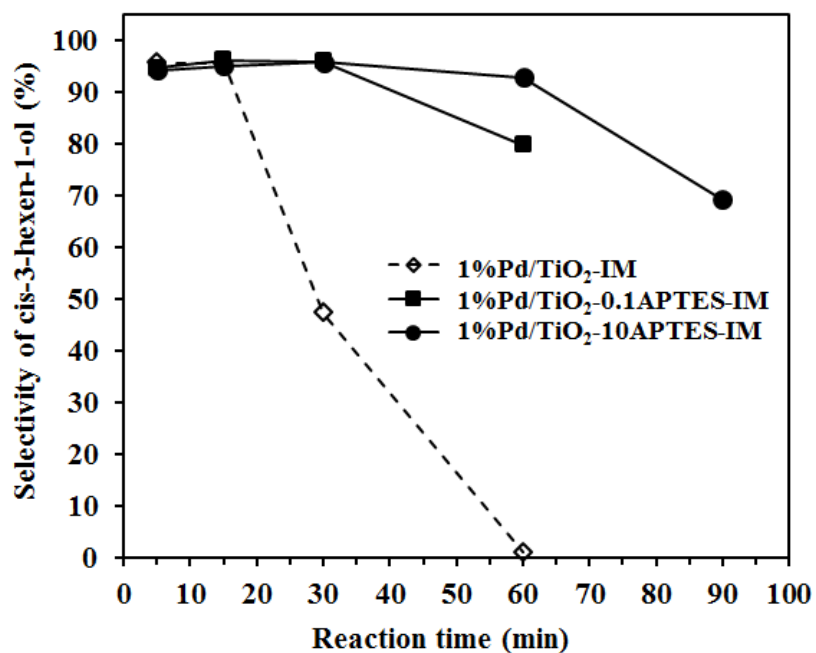


Figure 5.28 Selectivity of cis-3-hexen-1-ol for 1%Pd/TiO₂ catalysts prepared by sol immobilization method with different reaction times

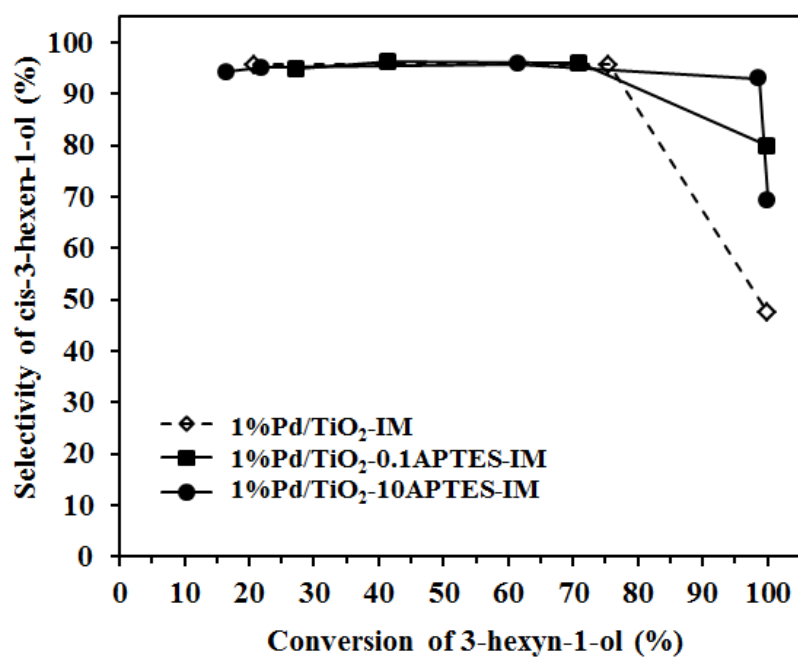


Figure 5.29 The catalytic performance for 1%Pd/TiO₂ catalysts prepared by sol immobilization method in the liquid phase selective hydrogenation of 3-hexyn-1-ol

5.5 Comparative study the catalytic behavior for 1%Pd/TiO₂ catalysts prepared by three different preparation methods

5.5.1 The Pd supported on non-modified TiO₂ catalysts

The catalytic behaviors of three 1%Pd/TiO₂ catalysts prepared by electroless deposition (ED), sonochemical (SN), and sol immobilization (IM) methods were investigated and compared in the solvent free liquid phase selective oxidation of benzyl alcohol (in section 5.5.1.1) and liquid phase selective hydrogenation of 3-hexyn-1-ol (in section 5.5.1.2).

5.5.1.1 Reaction study in solvent-free selective oxidation of benzyl alcohol to benzaldehyde

The catalytic performance of all 1%Pd/TiO₂ catalysts prepared by different preparation methods were evaluated in the solvent-free liquid phase selective oxidation of benzyl alcohol with molecular O₂ by using 50 ml round bottom flask reactor from Radleys. Typically, the oxidation of benzyl alcohol is always used as a model reaction for alcohol oxidation, not only due to the relatively high activity but also because of the existence of a complex reaction pathway. The desired product for this reaction is benzaldehyde, but other byproducts including to benzoic acid, benzyl benzoate, toluene, and benzene can be formed depending on the reaction condition and the catalyst used. The conversions of benzyl alcohol as a function of reaction times for all 1%Pd/TiO₂ catalysts are illustrated in **Figure 5.30**. Such results are clearly seen that the benzyl alcohol conversions increased with prolonged reaction time from 0.5 to 7 h. After the first 0.5 h of reaction, the highest benzyl alcohol conversion at 6.2% was achieved from 1%Pd/TiO₂-SN catalyst, followed by 3.2% of 1%Pd/TiO₂-IM and 1.4% of 1%Pd/TiO₂-ED catalyst, respectively. When the

reaction time reached 3 h, the conversion of benzyl alcohol monotonically enhanced and was found to be in the order: 1%Pd/TiO₂-ED > 1%Pd/TiO₂-SN > 1%Pd/TiO₂-IM. After 7 h of reaction, the highest conversion at 57.6% was achieved over 1%Pd/TiO₂-ED and 1%Pd/TiO₂-SN catalysts, while only 23.9% conversion was achieved over 1%Pd/TiO₂-IM catalyst. There are many factors which has an impact on catalytic activity of benzyl alcohol oxidation such as the nature of supports [19, 92], the metal particle size [40, 93], and/or the geometric of metal species [24]. Base on the XPS results, the 1%Pd/TiO₂-ED catalyst exhibited the highest surface atomic concentration of Pd at 0.96%, followed by 0.78% of 1%Pd/TiO₂-SN and 0.55% of 1%Pd/TiO₂-IM, respectively. In our case, the order of catalytic activity after 3 h of reaction were found to be in good agreement with the order of surface atomic concentrations of Pd. Therefore, it can be considered that the majority factor determining catalyst activity under this reaction condition is the surface atomic Pd concentration. However, the presence of higher amount of palladium oxide species (PdO and PdO₂) than metallic Pd⁰ for 1%Pd/TiO₂-ED catalyst was seem to be not corresponded with the highest activity of benzyl alcohol oxidation. Because of metallic Pd⁰ is generally known to be more active than palladium oxide species for benzyl alcohol oxidation [90, 94, 95]. Nevertheless, Wang et al. [24] demonstrated that the in situ reduction of palladium oxide to metallic Pd⁰ via a hydrogen spill over from benzyl alcohol adsorption created a higher amount of defective metallic Pd⁰ sites or linear bond CO on Pd (111), which proved to be the primary site for benzyl alcohol oxidation, resulting in an enhancement of catalytic activity of benzyl alcohol oxidation. Hence it is possible to propose that higher catalytic activity at first 0.5 h of reaction for the 1%Pd/TiO₂-SN and 1%Pd/TiO₂-IM catalysts than 1%Pd/TiO₂-ED

catalyst have an influence from higher metallic Pd⁰ species, which appeared to be an essential species for starting the reaction. During the reaction, PdO_x species were reduced to metallic Pd⁰ via a hydrogen spill from benzyl alcohol adsorbed resulting in an increasing of active metallic Pd⁰ sites. Therefore higher catalytic activity on 1%Pd/TiO₂-ED and 1%Pd/TiO₂-SN catalysts can be obtained when prolonged the reaction time. Besides the high benzyl alcohol conversion, the selectivity of benzaldehyde can be improved during the reconstruction of PdO_x because the hydrogen spill over from benzyl alcohol adsorbed effect to break C-H bond in benzyl alkoxide resulting to release the benzaldehyde as the final product.

Figure 5.31 and **Figure 5.32** illustrate the selectivity of benzaldehyde and toluene of all 1%Pd/TiO₂ catalysts as a function of reaction time. In term of products selectivity, benzaldehyde was produced as the main product following by trace amounts of toluene and benzoic acid as byproducts. High selectivity to benzaldehyde at 0.5 h was found to be in the order of 1%Pd/TiO₂-ED (87.9%) > 1%Pd/TiO₂-IM (86.3%) > 1%Pd/TiO₂-SN (77.4%). When prolonged the reaction time to 7h, increasing of benzyl alcohol conversion for 1%Pd/TiO₂-ED (57.6%) and 1%Pd/TiO₂-SN (57.6%) catalysts affected to monotonically decrease in the selectivity of benzaldehyde (74.1% for 1%Pd/TiO₂-ED and 58.9% for 1%Pd/TiO₂-SN) whereas higher toluene formation obviously occurred. In this case, it can be noted that the 1%Pd/TiO₂ catalysts prepared by sonochemical and electroless deposition methods facilitated the disproportionation of benzyl alcohol as the side reaction which involved in toluene formation more than consecutive benzaldehyde oxidation to benzoic acid hence, higher amount of toluene than benzoic acid was obtained on both catalysts. In contrast, for 1%Pd/TiO₂-IM catalyst, increasing of benzyl alcohol

conversion from 3.2% to 23.9% was not significant changed the benzaldehyde selectivity (ca. 86%). It is attributed that the 1%Pd/TiO₂-IM catalyst shows the preferable benzaldehyde oxidation pathway to produce benzoic acid as the side reaction rather than disproportionation of benzyl alcohol to produce toluene. The formation of toluene by disproportionation necessarily involves the cleavage of the C-O bond of benzyl alcohol and may also indicate the presence of surface hydrogen on the Pd surface. As suggested by Enache et al. [67], toluene mainly comes from the disproportionation of benzyl alcohol via either a hydrogen transfer step or an oxygen transfer step. Moreover, Corma and coworkers also suggested that the Au-H and Pd-H species which formed on supported Au and Pd catalysts are important in the toluene formation [96, 97]. It should be considered that if catalyst contains higher amount of Pd sites, it is possible that a higher amount of Pd-H species will exist during reaction, so that facilitating the toluene formation.

However, the preferable issue for benzyl alcohol oxidation is the presence of high benzyl alcohol conversion with high benzaldehyde selectivity. Hence, the most active catalyst for the oxidation of benzyl alcohol was the 1%Pd/TiO₂ catalyst synthesized by the electroless deposition method which exhibited the highest conversion of benzyl alcohol at 57.6% with high selectivity of benzaldehyde at 74.1%. In addition, the highest %yield of benzaldehyde at 42.7% was also obtained from the 1%Pd/TiO₂-ED catalyst.

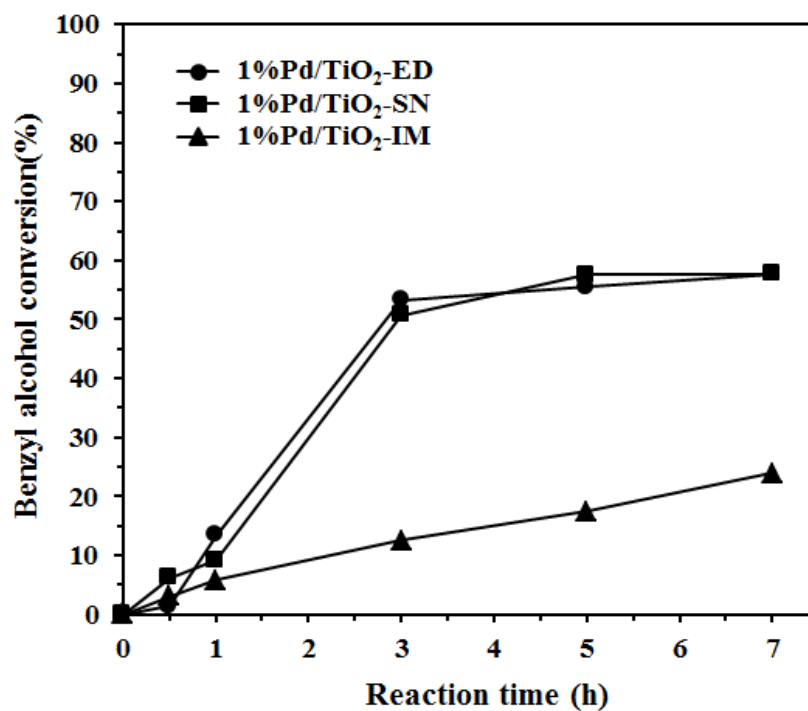


Figure 5.30 Conversion of benzyl alcohol as a function of reaction time for 1%Pd/TiO₂ catalysts

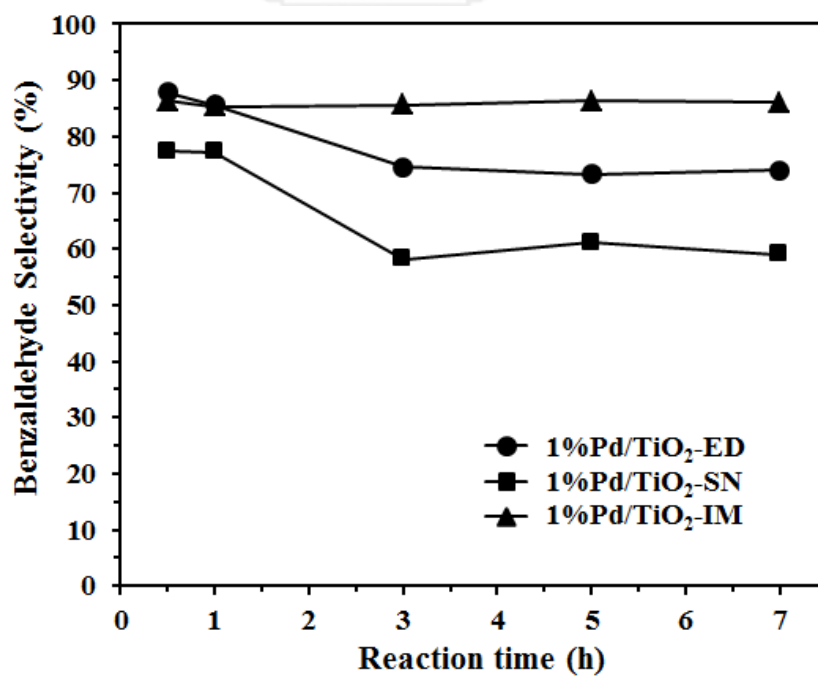


Figure 5.31 Selectivity of benzaldehyde as a function of reaction time for 1%Pd/TiO₂ catalysts

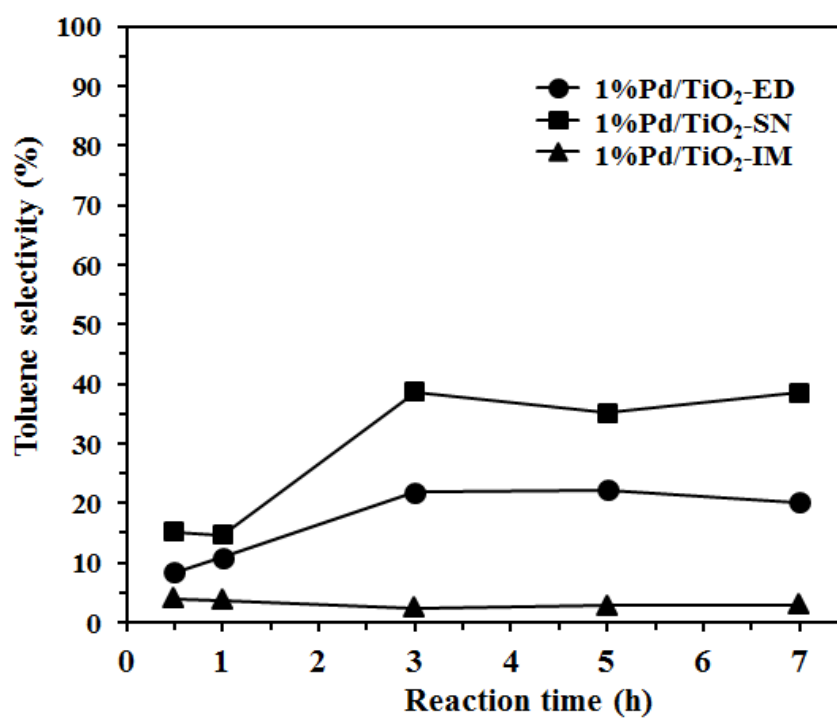


Figure 5.32 Selectivity of toluene as a function of reaction time for 1%Pd/TiO₂ catalysts

5.5.1.2 Reaction study in the liquid phase selective hydrogenation of 3-hexyn-1-ol to cis-3-hexen-1-ol

The catalytic performance of all 1%Pd/TiO₂ catalysts prepared by different preparation methods were evaluated and compared in the liquid phase selective hydrogenation of 3-hexyn-1-ol to cis-3-hexen-1-ol by using 100 ml batch type stainless steel autoclave reactor at mild reaction conditions (pH₂-2 bar, 40°C). Prior to reaction tested, the catalysts were reduced in H₂ stream at 40°C for 2h. Typically, the selective hydrogenation of 3-hexyn-1-ol is one of the most important reactions for the fragrance industry. The desired product is leaf fragrance alcohol or cis-3-hexen-1-ol. When prolonged the reaction time, isomerization of cis-3-hexen-1-ol to trans-3-hexen-1-ol can occur. Furthermore, the other byproducts from this reaction are 1-hexanol and hexane [98]. **Figure 5.33** shows the conversion of 3-hexyn-1-ol as a function of reaction time for the 1%Pd/TiO₂ catalysts. The conversion of 3-hexyn-1-ol for 1%Pd/TiO₂-ED and 1%Pd/TiO₂-IM catalysts was 100% after 30 min of reaction time, except 1%Pd/TiO₂-SN catalyst. The catalytic hydrogenation rates of catalysts were in the order 1%Pd/TiO₂-IM > 1%Pd/TiO₂-ED > 1%Pd/TiO₂-SN. The lowest catalytic hydrogenation rate on 1%Pd/TiO₂-SN catalyst has been attributed to low dispersion of Pd with a broader range of particles size distribution. However, the conversion of 3-hexyn-1-ol for 1%Pd/TiO₂-SN catalyst can reach 100% when prolonged the reaction time to 90 minutes. However, the higher catalytic activity obtained from 1%Pd/TiO₂-IM and 1%Pd/TiO₂-ED catalyst should be attributed to higher Pd dispersion with more uniform Pd particle size around 2-4 nm.

Figure 5.34 illustrates the selectivity of cis-3-hexen-1-ol as a function of reaction time for the 1%Pd/TiO₂ catalysts. Before reaction time reached 15 min, the

selectivity of cis-3-hexen-1-ol for all 1%Pd/TiO₂ catalysts were found to be more than 90%. When prolonged the reaction time to 30, 60, and 90 min, the selectivity of cis-3-hexen-1-ol for all catalysts were significantly decreased in different trends, especially for 1%Pd/TiO₂-SN catalyst. These results indicated different catalytic behavior over the 1%Pd/TiO₂ catalysts prepared by different methods.

The catalytic performances of the 1%Pd/TiO₂ catalysts in the liquid phase selective hydrogenation of 3-hexyn-1-ol to cis-3-hexen-1-ol are shown in **Figure 5.35**. After complete conversion of 3-hexyn-1-ol (100%), the selectivity of cis-3-hexen-1-ol on three 1%Pd/TiO₂ catalysts were significant different. The highest catalytic performance was obtained from 1%Pd/TiO₂-ED catalyst with 100% conversion of 3-hexyn-1-ol and 88% selectivity of cis-3-hexen-1-ol, following by 1%Pd/TiO₂-IM and 1%Pd/TiO₂-SN catalysts.

From these catalytic results, we can conclude that the Pd supported on non-modified TiO₂ catalysts prepared by electroless deposition exhibited the highest catalytic performance in both of solvent-free liquid phase selective oxidation of benzyl alcohol and liquid phase selective hydrogenation of 3-hexyn-1-ol.

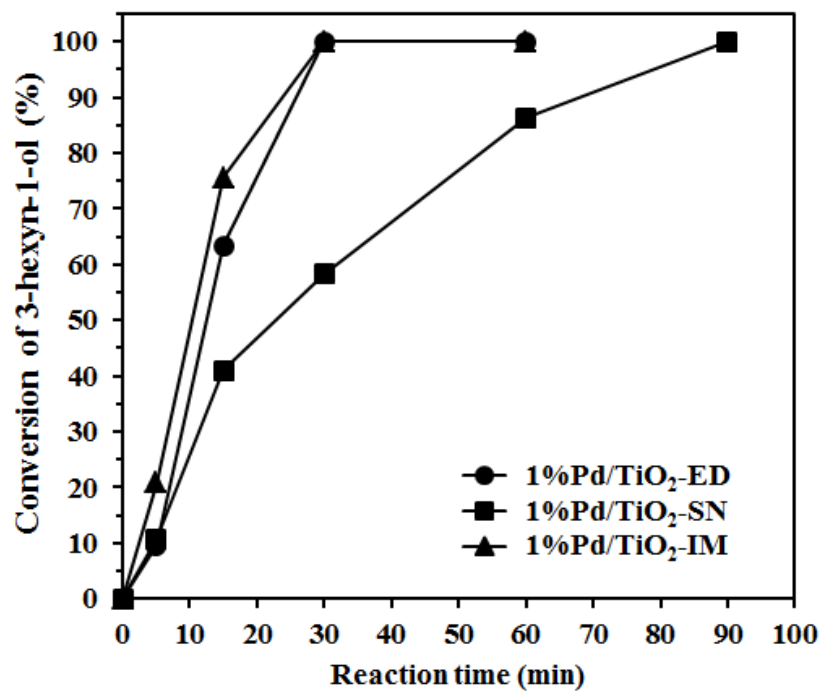


Figure 5.33 Conversion of 3-hexyn-1-ol as a function of reaction time for 1%Pd/TiO₂ catalysts

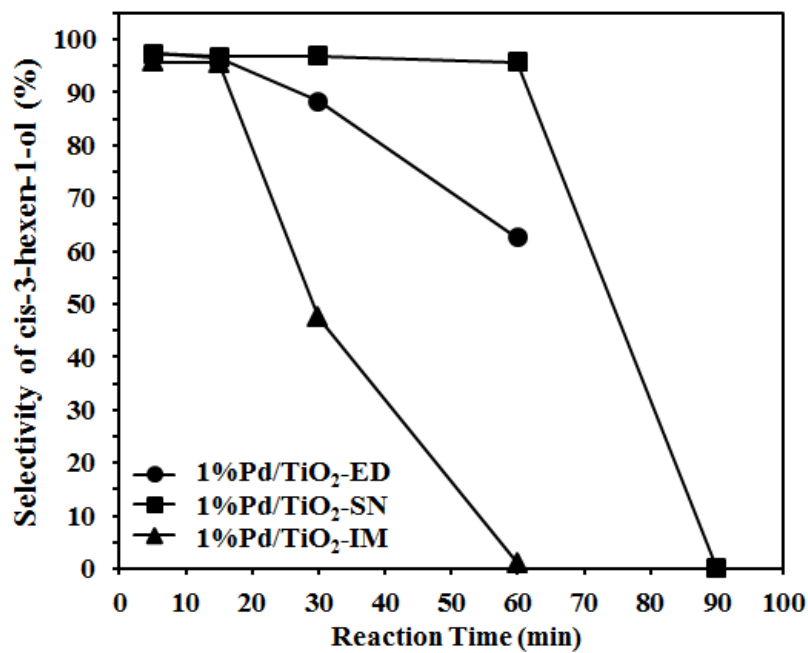


Figure 5.34 Selectivity of cis-3-hexen-1-ol as a function of reaction time for 1%Pd/TiO₂ catalysts

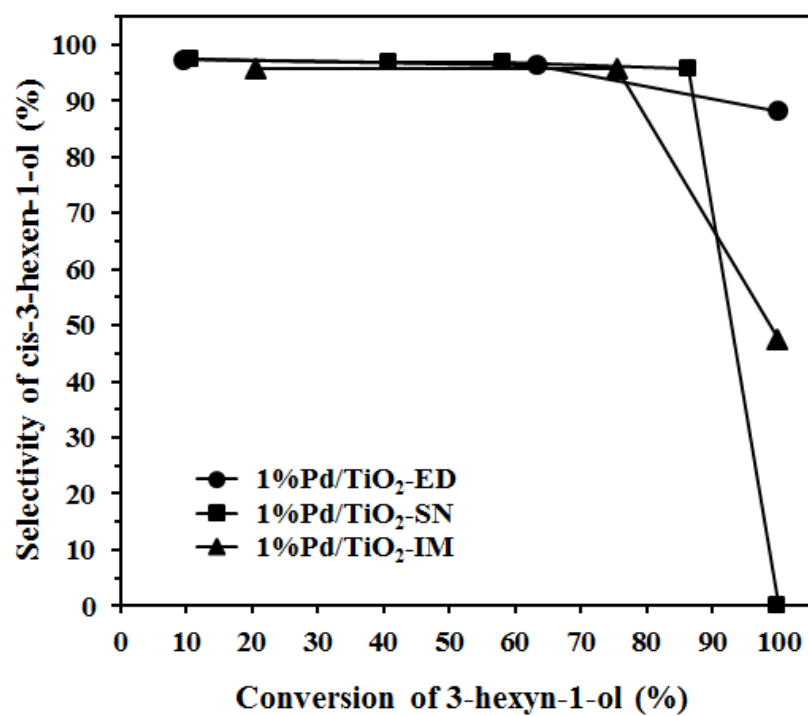


Figure 5.35 The catalytic performance of 1%Pd/TiO₂ catalysts in the liquid phase selective hydrogenation of 3-hexyn-1ol

5.5.2 The Pd supported on APTES modified TiO₂ catalysts

In this section, the catalytic behaviors of Pd supported on TiO₂-0.1APTES catalysts prepared by electroless deposition (ED), sonochemical (SN), and sol immobilization (IM) methods were investigated and compared in the solvent free selective oxidation of benzyl alcohol (in section 5.5.2.1) and the liquid phase selective hydrogenation of 3-hexyn-1-ol (in section 5.5.2.2).

5.5.2.1 Reaction study in solvent-free selective oxidation of benzyl alcohol to benzaldehyde

The catalytic performance of all 1%Pd/TiO₂-0.1APTES catalysts prepared by different preparation methods were evaluated in the solvent-free selective oxidation of benzyl alcohol with molecular O₂ by using 50 ml round bottom flask reactor (p_{O_2} 1 bar, 120^oC). The conversions of benzyl alcohol for all 1%Pd/TiO₂-0.1APTES catalysts as a function of reaction times are shown in **Figure 5.36**. The conversion of benzyl alcohol for all 1%Pd/TiO₂-0.1APTES catalysts increased when prolonged the reaction time from 0.5-7 h. The catalytic activity trend was in the order 1%Pd/TiO₂-0.1APTES-ED > 1%Pd/TiO₂-0.1APTES-SN > 1%Pd/TiO₂-0.1APTES-IM. After reaction time reached to 7h, the highest conversion of benzyl alcohol achieved from 1%Pd/TiO₂-0.1APTES-ED was found to be 61.8%, following by 47.2% for 1%Pd/TiO₂-0.1APTES-SN and 11.3% for 1%Pd/TiO₂-0.1APTES-IM, respectively. Typically, the catalytic activity of benzyl alcohol is known to be depended on amount of metallic Pd⁰ sites. As revealed by XPS results, the surface atomic concentrations of Pd on different catalysts were 0.98% for 1%Pd/TiO₂-0.1APTES-ED, following by 0.61% for 1%Pd/TiO₂-0.1APTES-SN, and 0.10% for 1%Pd/TiO₂-0.1APTES-IM, respectively. Therefore, it can

be suggested that different catalytic activity of benzyl alcohol for all 1%Pd/TiO₂-0.1APTES catalysts were depended on various amounts of surface atomic Pd concentrations. The catalysts that contained PdO_x species, however, they can be converted to metallic Pd⁰ which acts as the active species in benzyl alcohol oxidation by in-situ reduction of benzyl alcohol (discussed in section 5.2.2).

Figure 5.37 and **Figure 5.38** illustrate the selectivity of benzaldehyde and toluene as a function of reaction times for all 1%Pd/TiO₂-0.1APTES catalysts. In term of products selectivity, benzaldehyde was produced as the main product following by trace amounts of toluene and benzoic acid as byproducts. After reaction time reached 7h, the selectivity to benzaldehyde was found to be in the order 1%Pd/TiO₂-0.1APTES-ED (89.8%) > 1%Pd/TiO₂-0.1APTES-IM (86.4%) > 1%Pd/TiO₂-0.1APTES-SN (60.2%). In this case, the highest selectivity of benzaldehyde from 1%Pd/TiO₂-0.1APTES-ED catalyst may be consequent of the catalyst possessed more PdO_x species which would be reduced to metallic Pd⁰ during benzyl alcohol oxidation and then desorbed benzaldehyde as a final product. Therefore, higher benzaldehyde selectivity could be obtained from 1%Pd/TiO₂-0.1APTES-ED catalyst. The lowest selectivity of benzaldehyde with high amount of toluene byproducts was found on 1%Pd/TiO₂-0.1APTES-SN catalyst. This can be suggested that the 1%Pd/TiO₂-0.1APTES-SN catalysts facilitated the disproportionation of benzyl alcohol to toluene as a major side reaction more than consecutive benzaldehyde oxidation to benzoic acid. For 1%Pd/TiO₂-0.1APTES-IM catalyst, high benzaldehyde selectivity ca. 86% may be obtained because low catalytic activity of benzyl alcohol retarded the oxidation of benzaldehyde.

However, the preferable issue for benzyl alcohol oxidation is the presence of high benzyl alcohol conversion with high benzaldehyde selectivity. Hence, the most active catalyst for the oxidation of benzyl alcohol was the 1%Pd/TiO₂-0.1APTES-ED catalyst which possessed the highest conversion of benzyl alcohol at 61.8% with high selectivity of benzaldehyde at 89.8%. The highest %yield of benzaldehyde at 55.5% was also obtained from the 1%Pd/TiO₂-0.1APTES-ED catalyst.

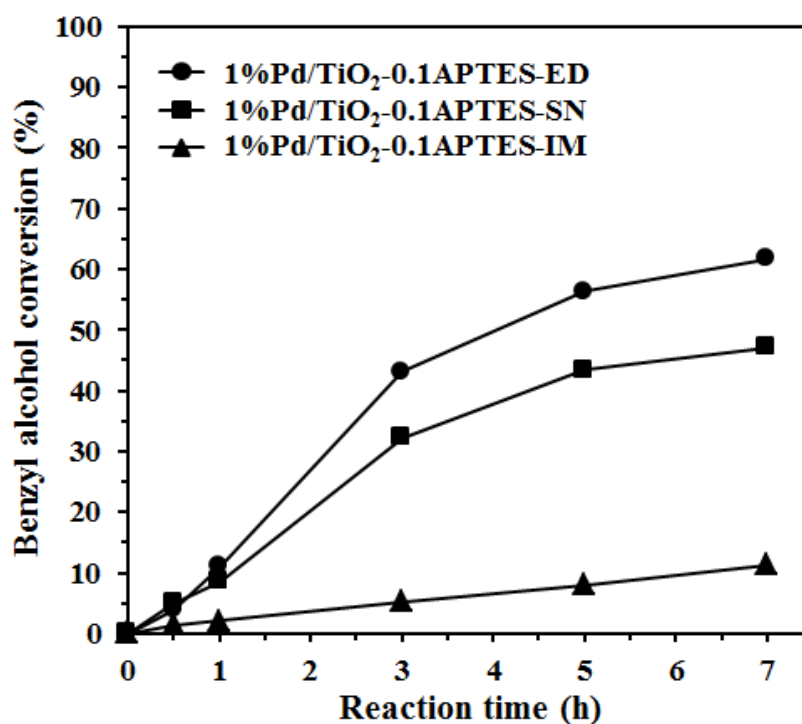


Figure 5.36 Conversion of benzyl alcohol as a function of reaction time for 1%Pd/TiO₂-0.1APTES catalysts

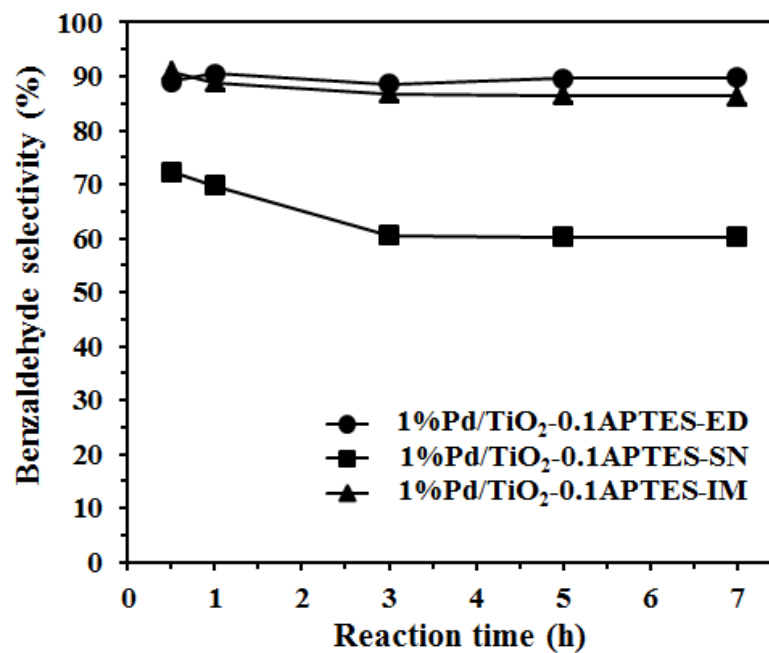


Figure 5.37 Selectivity of benzaldehyde as a function of reaction time for 1%Pd/TiO₂-0.1APTES catalysts

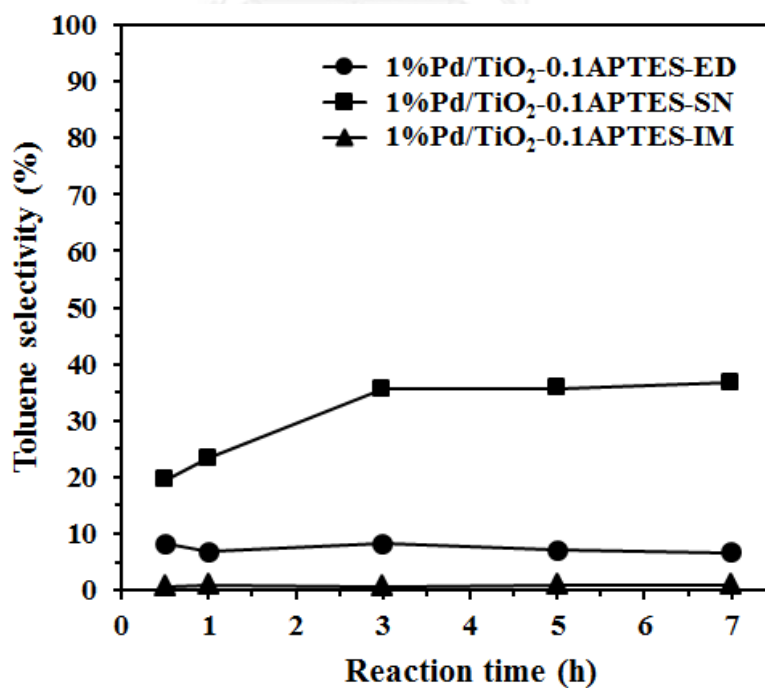


Figure 5.38 Selectivity of toluene as a function of reaction time for 1%Pd/TiO₂-0.1APTES catalysts

5.5.2.2 Reaction study in the liquid phase selective hydrogenation of 3-hexyn-1-ol to cis-3-hexen-1-ol

The catalytic performance of all 1%Pd/TiO₂-0.1APTES catalysts prepared by different preparation methods were evaluated and compared in the liquid phase selective hydrogenation of 3-hexyn-1-ol to cis-3-hexen-1-ol by using 100 ml batch type stainless steel autoclave reactor at mild reaction conditions (p_{H_2} -2 bar, 40°C). Prior to reaction tested, the catalysts were reduced in H₂ stream at 40°C for 2h. **Figure 5.39** shows the conversion of 3-hexyn-1-ol as a function of reaction time for all 1%Pd/TiO₂-0.1APTES catalysts. The catalytic hydrogenation rates of catalysts were in the order 1%Pd/TiO₂-0.1APTES-ED > 1%Pd/TiO₂-0.1APTES-SN > 1%Pd/TiO₂-0.1APTES-IM. Such results indicated that different Pd loading methods have an influence to catalytic activity although using the same TiO₂-0.1APTES support. As revealed by TEM and XPS results, the morphologies and electronic states of Pd on three 1%Pd/TiO₂-0.1APTES catalysts were significant different. The lowest catalytic hydrogenation rate on 1%Pd/TiO₂-0.1APTES-IM catalyst has been attributed to the lowest amount of Pd deposited on TiO₂-0.1APTES support since Pd colloids became weak interaction on the APTES modified TiO₂ support compared with metallic Pd⁰ on 1%Pd/TiO₂-0.1APTES-SN or SnO₂ stabilized metallic Pd⁰ on 1%Pd/TiO₂-0.1APTES-ED catalyst. However, all 1%Pd/TiO₂-0.1APTES catalyst can achieve 100% conversion of 3-hexyn-1-ol when the reaction time reached to 60 min. **Figure 5.40** illustrates the selectivity of cis-3-hexen-1-ol as a function of reaction time for 1%Pd/TiO₂-0.1APTES catalysts. The selectivity of cis-3-hexen-1-ol for all 1%Pd/TiO₂-0.1APTES catalysts were significant decreased when the reaction time increased from 5-60 min.

The catalytic performances of all 1%Pd/TiO₂-0.1APTES catalysts in the liquid phase selective hydrogenation of 3-hexyn-1-ol to cis-3-hexen-1-ol are shown in **Figure 5.41**. After complete conversion of 3-hexyn-1-ol (100%), the selectivity of cis-3-hexen-1-ol on three 1%Pd/TiO₂-0.1APTES catalysts were significant different. The highest catalytic performance was obtained from 1%Pd/TiO₂-0.1APTES-ED catalyst with 100% conversion of 3-hexyn-1-ol and 86% selectivity of cis-3-hexen-1-ol, following by 1%Pd/TiO₂-0.1APTES-IM and 1%Pd/TiO₂-0.1APTES-SN catalysts.

From these catalytic results, we can conclude that the Pd supported on 0.1 mM APTES modified TiO₂ catalysts prepared by electroless deposition exhibits the highest catalytic performance in both of solvent-free liquid phase selective oxidation of benzyl alcohol and liquid phase selective hydrogenation of 3-hexyn-1-ol.

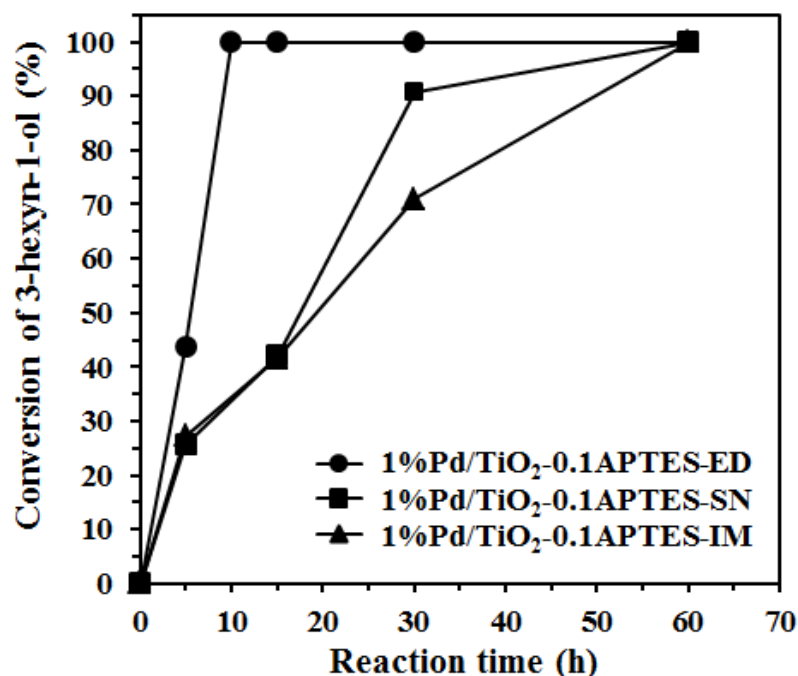


Figure 5.39 Conversion of 3-hexyn-1-ol as a function of reaction time for APTES modified 1%Pd/TiO₂ catalysts

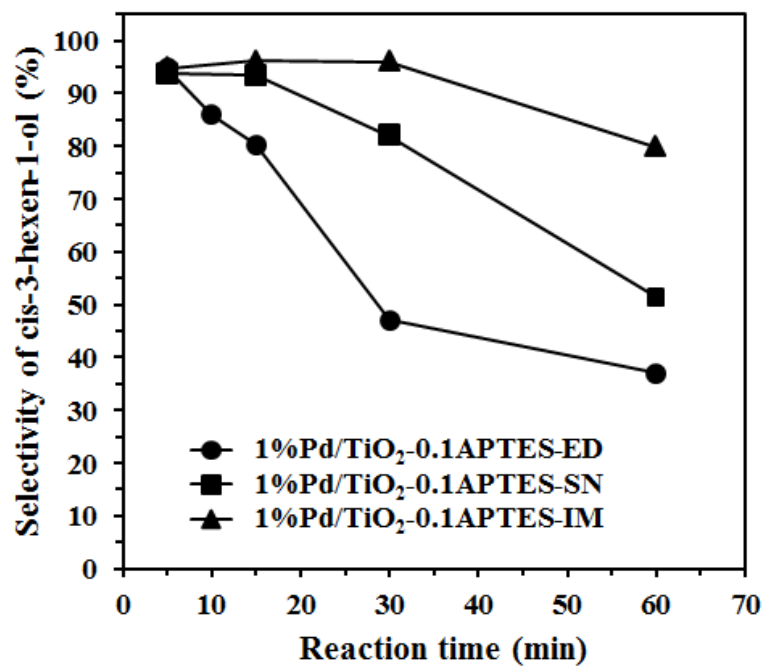


Figure 5.40 Selectivity of cis-3-hexen-1-ol as a function of reaction time for APTES modified 1%Pd/TiO₂ catalysts

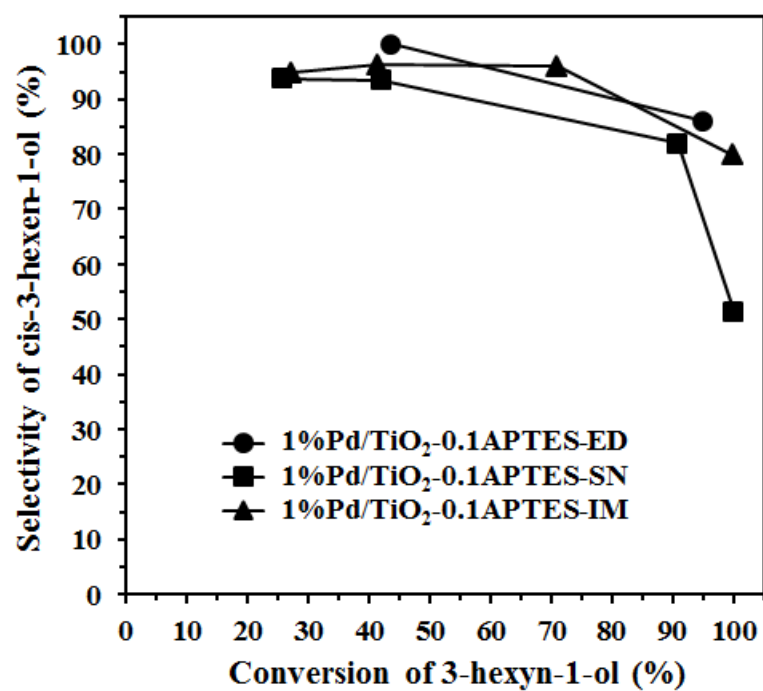


Figure 5. 41 The catalytic performance of 1%Pd/TiO₂-0.1APTES catalysts in the liquid-phase selective hydrogenation of 3-hexyn-1-ol

Part III

Comparative study the characteristics and catalytic properties of 1%Pd/TiO₂ catalysts prepared by sonochemical method with H₂ reduction and incipient wetness impregnation method

In this part, the characteristic of 1%Pd/TiO₂ catalyst prepared by sonochemical method with H₂ reduction has been investigated and compared with one prepared by incipient wetness impregnation method. Section 5.6.1, the mechanism of the metal-support interaction on 1%Pd/TiO₂ catalysts prepared by different methods were investigated by means of X-ray photoelectron spectroscopy (XPS), CO pulse chemisorption, and transmission electron microscopy (TEM). Section 5.6.2, their catalytic behaviors were evaluated in the liquid phase selective hydrogenation of phenylacetylene to styrene under mild reaction conditions.

5.6 The characteristics and catalytic properties of 1%Pd/TiO₂ catalysts prepared by sonochemical with H₂ reduction and incipient wetness impregnation method

1 wt. % of Pd was deposited on TiO₂ support by sonochemical with H₂ reduction and incipient wetness impregnation method and they were denoted as 1%Pd/TiO₂ (S) and 1%Pd/TiO₂ (I), respectively. In order to study the metal-support interaction, the 1%Pd/TiO₂ catalysts were reduced at either 40°C or 500°C under H₂ flow (rate 50 cm³/min) before reaction study and they were denoted as 1%Pd/TiO₂(S)-R40, 1%Pd/TiO₂(S)-R500, 1%Pd/TiO₂(I)-R40 and 1%Pd/TiO₂(I)-R500. The catalysts were characterized by several techniques as results show in section 5.6.1. The catalytic performances of the catalysts are demonstrated in section 5.6.2.

5.6.1 Catalyst characterizations

5.6.1.1 X-ray diffraction (XRD)

The XRD patterns of TiO_2 support and 1%Pd/ TiO_2 catalysts are shown in **Figure 5.42**. All the samples exhibited the characteristic peaks of pure anatase TiO_2 at $2\theta=25^\circ$ (major), 37° , 48° , 55° , 56° , 62° , 71° , and 75° . The average crystallite size of the TiO_2 support calculated from the full width at half maximum of the XRD peak at $2\theta=25^\circ$ using Scherrer equation was about 66 nm. After Pd loading, the peak intensity of TiO_2 was lower especially for the 1%Pd/ TiO_2 (S) because Pd nanoparticles may act as X-ray scattered. The XRD characteristic peaks corresponding to PdO at $2\theta = 33.5^\circ$ or metallic Pd⁰ at $2\theta = 40.9^\circ$, however, were not observed for all the catalysts due probably to the low amount of Pd present and/or high Pd dispersion.

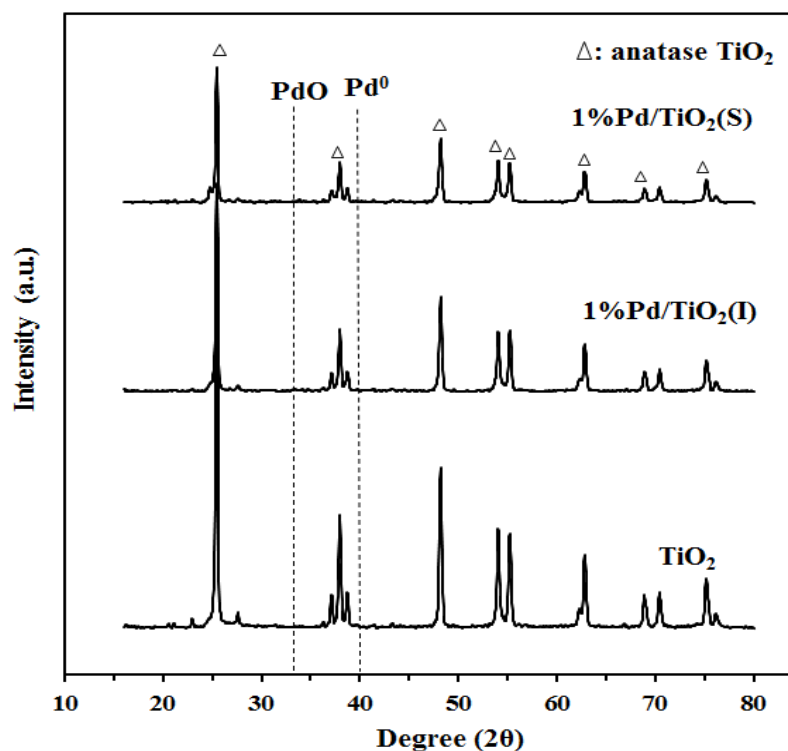


Figure 5.42 The XRD patterns of TiO_2 support and 1%Pd/ TiO_2 catalysts

5.6.1.2 Transmission electron microscopy (TEM)

The degree of Pd dispersion and Pd⁰ particle size was investigated by TEM analysis and the results are shown in **Figure 5.43**. The crystallite size of the TiO₂ supports was consistent to the XRD results. Higher Pd dispersion and more uniform Pd⁰ particle size were clearly observed on the 1%Pd/TiO₂(S) compared to 1%Pd/TiO₂(I). The use of ultrasonic has been proven to be beneficial for high dispersion of metal on various supported catalyst systems.[99, 100] From the Pd⁰ particle size distribution plots (**Figure 5.44**), the average Pd⁰ particle sizes of 1%Pd/TiO₂(I)-R40 and 1%Pd/TiO₂(S)-R40 were 5.7 and 3.9 nm, respectively. Increasing reduction temperature to 500°C did not strongly affect the Pd⁰ particle size of the 1%Pd/TiO₂(S) catalysts, in which most of the Pd⁰ particles fell in the same range (2-9 nm) after reduction at either 40°C or 500°C. On the other hand, for the 1%Pd/TiO₂(I), sintering of Pd⁰ metals was clearly observed by the presence of relatively large Pd⁰ particles (> 20 nm) on the catalysts after reduction at 500°C (1%Pd/TiO₂(I)-R500).

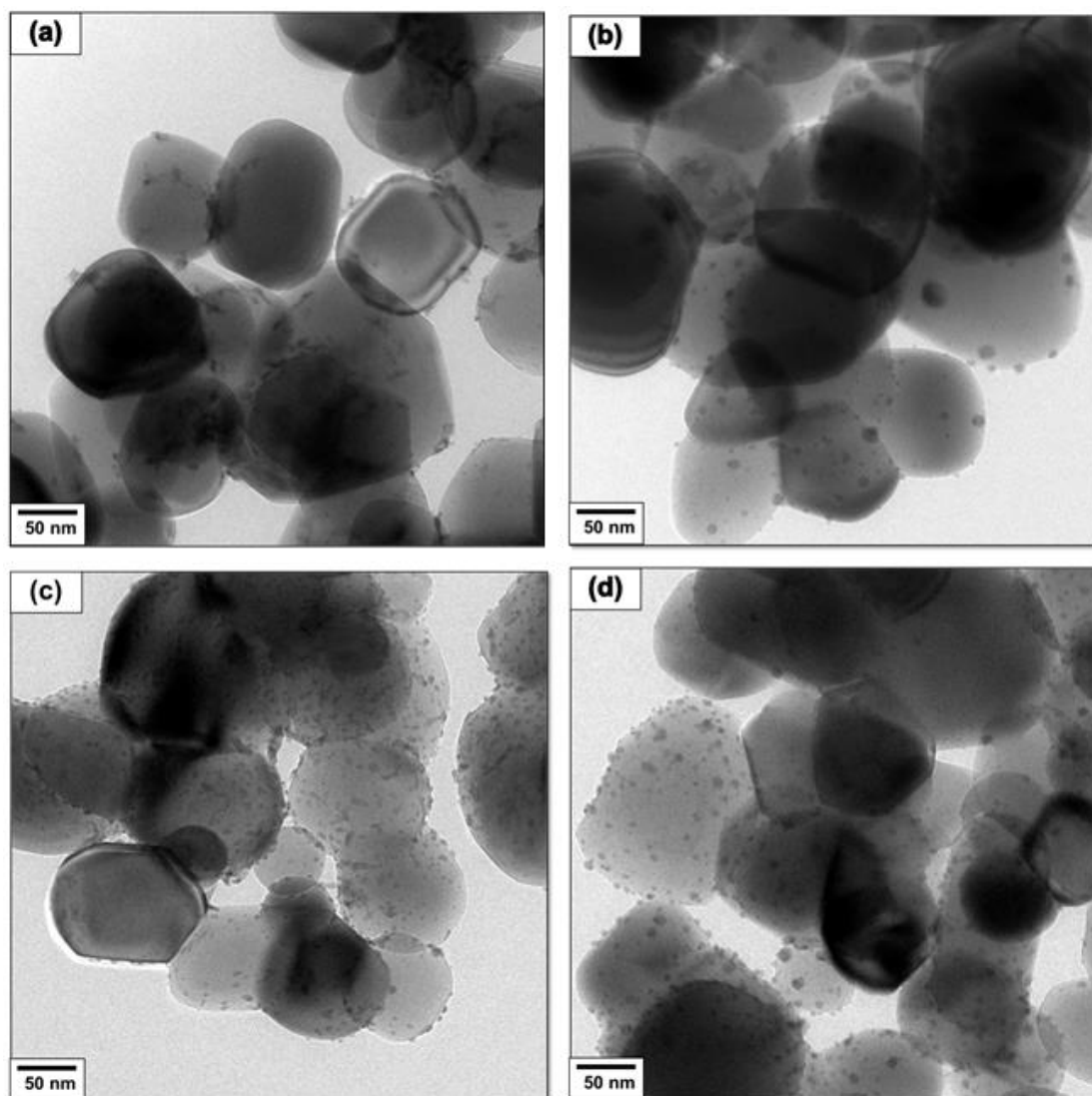


Figure 5.43 TEM micrographs of (a) 1%Pd/TiO₂(I)-R40, (b) 1%Pd/TiO₂(I)-R500, (c) 1%Pd/TiO₂(S)-R40, and (d) 1%Pd/TiO₂(S)-R500 catalysts

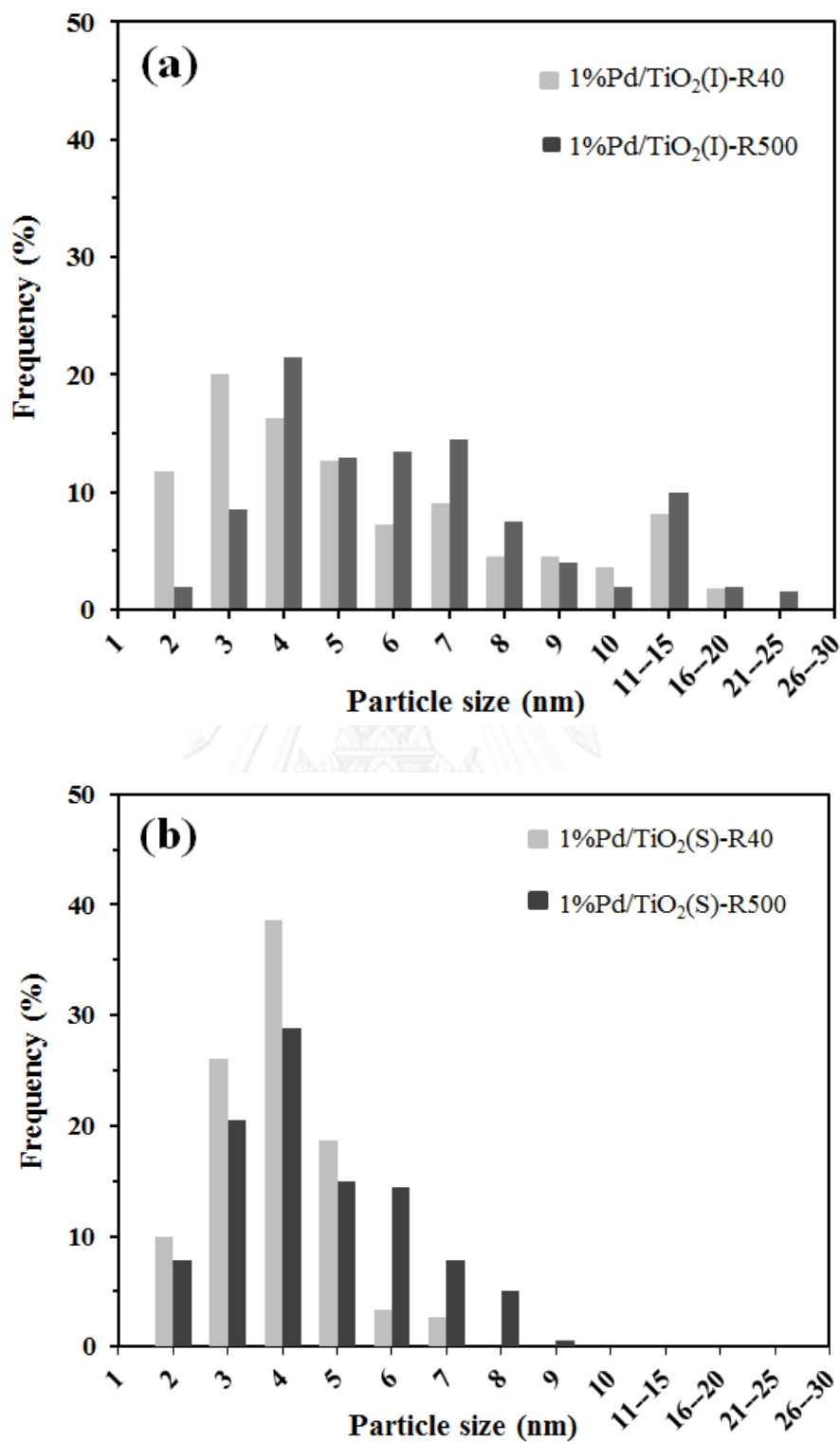


Figure 5.44 Particle sizes distribution of (a) 1%Pd/TiO₂(I) and (b) 1%Pd/TiO₂(S) catalysts.

5.6.1.3 CO pulse chemisorption

The CO chemisorption ability of 1%Pd/TiO₂(l) and 1%Pd/TiO₂(s) catalysts were first measured after reduction by H₂ at 40 and 500°C. Then the reduced catalysts were re-calcined at 450°C and re-reduced at 40°C to recover their active surface. The results of CO chemisorption on the catalysts in different states are illustrated in **Figure 5.45**. Reduction at high temperature caused significant loss of the chemisorption ability for both catalysts. For the 1%Pd/TiO₂(l)-R500, the lower CO chemisorption was probably due to sintering of Pd⁰ metal as observed from TEM analysis. On the other hand, the loss of CO chemisorption capacity on 1%Pd/TiO₂(s)-R500 was attributed to the presence of the SMSI effect and not due to metal agglomeration/metal sintering since there were no significant changes in the Pd⁰ particle size.

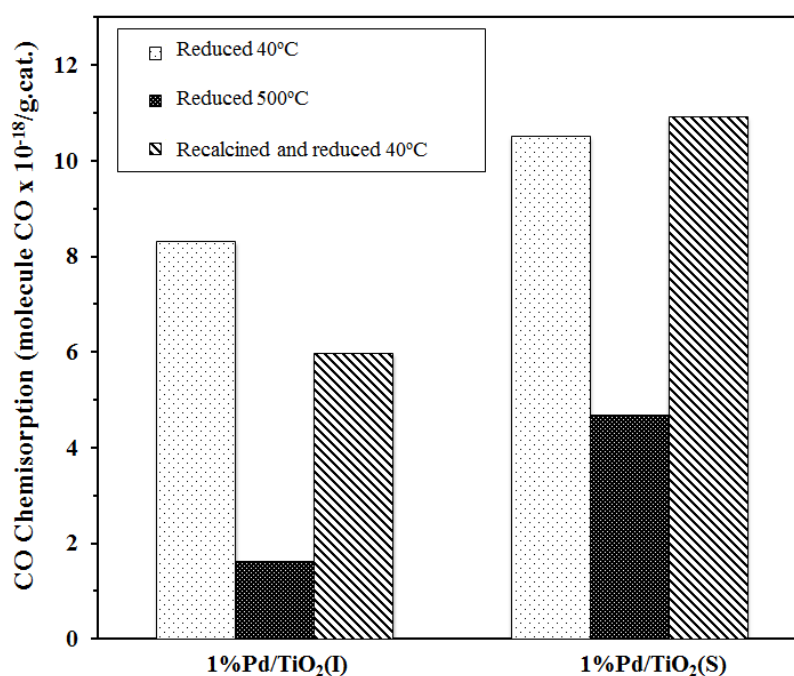


Figure 5.45 The CO chemisorption results for 1%Pd/TiO₂(l) and 1%Pd/TiO₂(s) catalysts

5.6.1.4 X-Ray photoelectron spectroscopy (XPS)

The SMSI effect on TiO₂ supported catalysts has known to occur via either the decoration of metal surface by partially reducible of TiO₂ or electron transfer between metal and TiO₂ support [21, 26, 101]. Surface compositions and electronic properties of the catalysts were investigated by means of XPS analysis. The binding energy (B.E.) and atomic concentrations of Ti 2p, O 1s, and Pd 3d on various 1%Pd/TiO₂ catalysts are summarized in **Table 5.12**. The binding energy of Ti 2p_{3/2} and Ti 2p_{1/2} for the TiO₂ support was found to be ca. 458.7 and 464.3 eV respectively, with a spin-orbit splitting of 5.6 eV, which was assigned to Ti⁴⁺ in anatase TiO₂ support [81, 102]. The binding energy of O 1s in all the samples were at ca. 530.0 eV, which were assigned to Ti-O-Ti lattice oxygen of TiO₂ [81, 102]. The binding energy of Pd 3d_{5/2} of the 1%Pd/TiO₂(l) and 1%Pd/TiO₂(s) in the calcined state were in the range of 336.5-336.7 eV, indicating that palladium was in the form of PdO (**Figure 5.46**). After reduced at 40^oC, the binding energy of Pd 3d_{5/2} for both catalysts were found at 335.0-335.1 eV, which can be attributed to the metallic Pd⁰. Reduction at 500^oC resulted in a slightly shift of Pd 3d_{5/2} binding energy towards lower values at ca. 335.1 to 334.8 eV. A shift of metal binding energy is influenced not only by electronic interaction between metal and support but also by metal crystallite size effect [21]. However, for the 1%Pd/TiO₂(s)-R500 there was no significant change in the Pd⁰ particle size after reduction at 500^oC, so the shift of binding energy indicated that more negative charges were presented on the Pd⁰ metal particles or/and there was electron transfer from TiO₂ support to Pd⁰ metal. In addition, the atomic ratio of Pd/Ti was higher for the 1%Pd/TiO₂(s) than the 1%Pd/TiO₂(l), suggesting higher Pd dispersion on the catalyst prepared by the sonochemical method. Elevation of

reduction temperature from 40°C to 500°C led to decreased Pd/Ti atomic ratios by 40 and 29% for 1%Pd/TiO₂(l)-R500 and 1%Pd/TiO₂(s)-R500, respectively.

The oxygen concentration ratio of O⁻/O²⁻ calculated from the atomic concentration of O 1s peak at binding energy ca. 532 and 530 eV were assigned to the oxygen vacancies (O⁻) (or so-called Ti³⁺ defective sites) and oxygen in the lattice (O²⁻) of TiO₂, respectively. The O⁻/O²⁻ ratio was higher for 1%Pd/TiO₂(s) than 1%Pd/TiO₂(l). In other words, the catalysts derived by sonochemical method had higher amount of oxygen vacancies or Ti³⁺ defective sites. Moreover, the highest O⁻/O²⁻ ratio was obtained over the 1%Pd/TiO₂(s)-R500 catalyst, indicating the highest amount of surface Ti³⁺. Because the catalysts prepared by sonochemical method possessed more uniform and smaller Pd⁰ particles (higher Pd dispersion), they would adsorb more hydrogen during reduction step. Under excess H₂, there may be some hydrogen spillover from Pd⁰ metal surface to TiO₂ support, resulting in reduction of Ti⁴⁺ to Ti³⁺. According to the literature, Ti³⁺ can migrate to Pd surface under high reduction temperature conditions, resulting in the SMSI [27, 28, 99].

Table 5.12 The XPS results of TiO₂ and 1%Pd/TiO₂ catalysts reduced at 40 and 500°C

| Samples | Binding Energy (eV) | | | | Atomic concentration |
|--------------------------------|---------------------|-------|-------|-------|---------------------------------|
| | Ti 2p | O 1s | Pd 3d | Pd/Ti | O ⁻ /O ²⁻ |
| TiO ₂ | 458.7 | 529.9 | - | - | 0.567 |
| 1%Pd/TiO ₂ (l) | 458.9 | 530.2 | 336.5 | 0.080 | 0.235 |
| 1%Pd/TiO ₂ (l)-R40 | 458.8 | 530.1 | 335.1 | 0.064 | 0.280 |
| 1%Pd/TiO ₂ (l)-R500 | 458.8 | 530.1 | 334.8 | 0.048 | 0.276 |
| 1%Pd/TiO ₂ (s) | 459.0 | 530.2 | 336.7 | 0.127 | 0.304 |
| 1%Pd/TiO ₂ (s)-R40 | 459.0 | 530.2 | 335.0 | 0.106 | 0.377 |
| 1%Pd/TiO ₂ (s)-R500 | 458.9 | 530.1 | 334.8 | 0.090 | 0.482 |

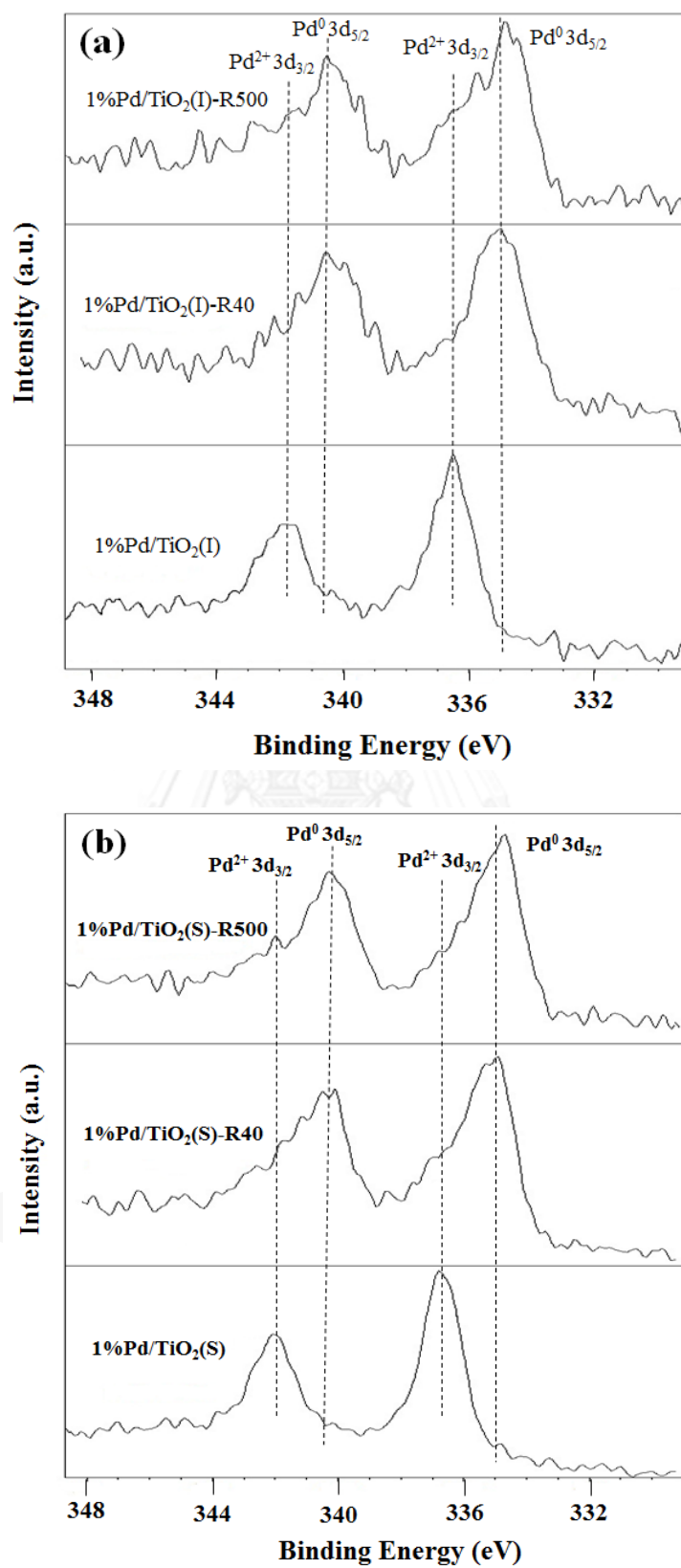


Figure 5.46 The Pd 3d XPS spectra of (a) 1%Pd/TiO₂(l) and (b) 1%Pd/TiO₂(S)

5.6.2 Catalytic performance of 1%Pd/TiO₂(l) and 1%Pd/TiO₂(s) catalysts in the liquid phase selective hydrogenation of phenylacetylene to styrene

The performance of 1%Pd/TiO₂ catalysts were evaluated in the liquid-phase selective hydrogenation of phenylacetylene to styrene under mild reaction conditions (p_{H_2} 3 bar and 40°C). **Figure 5.47** shows the conversion of phenylacetylene as a function of reaction time. The hydrogenation activities were found to be in the order: 1%Pd/TiO₂(l)-R40 > 1%Pd/TiO₂(s)-R40 > 1%Pd/TiO₂(l)-R500 > 1%Pd/TiO₂(s)-R500. In all cases, complete conversion of phenylacetylene occurred within 30 min. The lower initial activity of 1%Pd/TiO₂(s)-R40 catalyst could be explained by the particle size effect in which smaller Pd particle exhibited lower hydrogenation activity, especially when the average Pd particle size is very small (\leq 3-5nm) [103, 104]. Diminishing activity of small metal particles was probably due to the different band structure characteristics of nano-sized metal compared to bulk metals and that they appear to be electron deficient [105]. **Figure 5.48** shows the selective of styrene as a function of reaction time. High styrene selectivity (81-93%) was obtained on all the catalysts when the reaction time was lower than 20 min. After complete conversion of phenylacetylene (100% conversion), the styrene selectivity of 1%Pd/TiO₂ catalysts reduced at 40°C dramatically dropped to 57% for 1%Pd/TiO₂(l) whereas that of 1%Pd/TiO₂(s) was slightly dropped to 81%. The styrene selectivity was improved to 79% and 87% for 1%Pd/TiO₂(l) and 1%Pd/TiO₂(s), respectively when the catalysts were reduced at 500°C. The better catalytic performance of 1%Pd/TiO₂(s)-R500 was attributed to the presence of SMSI effect. Charges transfer from the TiO₂ support to Pd during high temperature reduction

could weaken the adsorption strength of styrene on the Pd surface; hence higher styrene selectivity was obtained [4, 27].

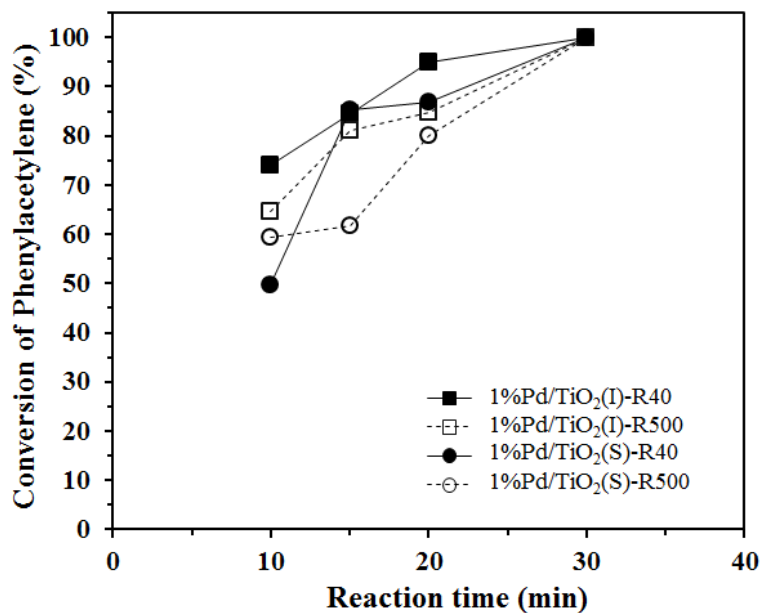


Figure 5.47 The conversion of phenylacetylene for 1%Pd/TiO₂(I) and 1%Pd/TiO₂(S) catalysts as a function of reaction time.

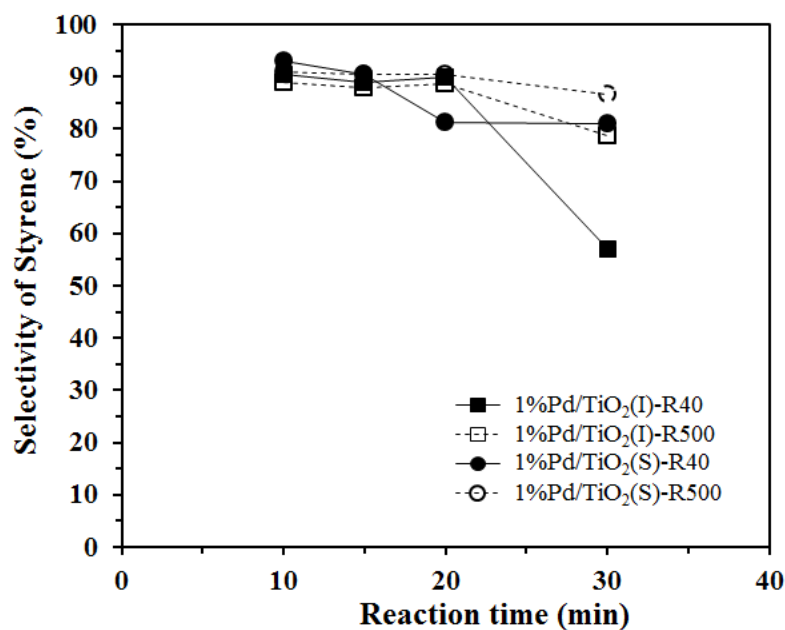


Figure 5.48 The selectivity of styrene for 1%Pd/TiO₂(I) and 1%Pd/TiO₂(S) catalysts as a function of reaction time.

CHAPTER VI

CONCLUSIONS AND RECOMMENDATIONS

6.1 Conclusions

Part I: Surface modification of TiO₂ support with APTES

- Surface modification of TiO₂ with monolayer APTES grafting was obtained by using 0.1 mM of APTES on 1.5 g of TiO₂ support. Excess APTES concentrations (e.g. 1, 10 mM) resulted in both multilayer APTES grafting and reversed attachment, which NH₂-groups attached on TiO₂ surface rather than giving free NH₂ termination.

Part II: Comparative study the effect of catalyst preparation methods

- The different characteristics of 1%Pd/TiO₂ catalysts which were influenced by Pd deposition methods are summarized in **Table 6.1**.

Table 6.1 The characteristics of 1%Pd/TiO₂ catalysts prepared by different methods

| Characteristics | Electroless deposition | Sonochemical | Sol immobilization |
|---------------------|---------------------------------------|-------------------------------|----------------------------|
| Pd morphology | small Pd nanoclusters | agglomerated Pd nanoparticles | spherical Pd nanoparticles |
| Pd dispersion | Well dispersed | Low dispersed | High dispersed |
| Pd particle size | 3.4-4.1 nm | 7.5-7.9 nm | 2.4-2.6 nm |
| State of Pd | Pd ⁰ /PdO/PdO ₂ | Pd ⁰ /PdO | Pd ⁰ /PdO |
| Dominant Pd species | PdO ₂ | Pd ⁰ | Pd ⁰ |

- For the liquid-phase selective oxidation of benzyl alcohol, 1%Pd/TiO₂-0.1APTES-ED catalyst exhibited the highest catalytic performance because it had the highest atomic concentrations of Pd surface. Furthermore, the presence of both Pd⁰ and PdO_x (1 ≤ x ≤ 2) gave high catalytic activity in the benzyl alcohol oxidation. Additional metallic Pd⁰ sites were formed via the *in-situ* reduction of PdO/PdO₂ by the adsorbed benzyl alcohol.
- For the liquid-phase selective hydrogenation of 3-hexyn-1-ol, 1%Pd/TiO₂-0.1APTES-ED catalyst exhibited the best catalytic performance and the highest hydrogenation rate because it had the highest atomic concentrations of Pd surface. Moreover, electron donating from NH₂ termination of APTES molecules to the metallic Pd⁰ species facilitated the metal-support interaction. So that alkyne molecules became weakly adsorbed and easy to be hydrogenated resulting in an increase of the hydrogenation rate.
- Such effect was not found on Pd catalysts supported on APTES modified TiO₂ prepared by sol immobilization method. Because Pd particles were stabilized by polyvinyl alcohol (PVA) molecules so it was difficult for electron donating from NH₂ groups to metallic Pd⁰, resulting in lower hydrogenation rate.

Part III: Comparative study the characteristics and catalytic properties of 1%Pd/TiO₂ catalysts prepared by sonochemical method with H₂ reduction and incipient wetness impregnation method

- The uniform and small size of Pd particles for 1%Pd/TiO₂(S) catalyst prepared by the sonochemical method with H₂ reduction promoted the SMSI effect during high temperature reduction at 500°C whereas the

conventional 1%Pd/TiO₂(I) catalyst derived by incipient wetness impregnation method showed the absence of SMSI and sintering of metallic Pd⁰ particles was observed instead. The presence of SMSI resulted in improved catalytic performances of 1%Pd/TiO₂(S)-R500 catalysts in the liquid phase selective hydrogenation of phenylacetylene under mild conditions.

6.2 Recommendations

- 1) Other TiO₂ supports with higher surface area should be used to modify with APTES in order to confirm the results in this work.
- 2) Other organic functional groups such as thiol group (-SH) or diamine group modified on TiO₂ support should be studied in the future work.

REFERENCES

- [1] Leyva-Pérez, A., Cabrero-Antonino, J.R., and Corma, A. Bifunctional solid catalysts for chemoselective hydrogenation–cyclisation–amination cascade reactions of relevance for the synthesis of pharmaceuticals. Tetrahedron 66(41) (2010): 8203-8209.
- [2] Semikolenov, V.A., et al. Design of selective 1-ethyl-2-nitromethylenepyrrolidine hydrogenation for pharmaceuticals production. in Studies in Surface Science and Catalysis, pp. 255-262: Elsevier, 1997.
- [3] Komhom, S., Mekasuwandumrong, O., Praserthdam, P., and Panpranot, J. Improvement of Pd/Al₂O₃ catalyst performance in selective acetylene hydrogenation using mixed phases Al₂O₃ support. Catalysis Communications 10(1) (2008): 86-91.
- [4] Weerachawanasak, P., Praserthdam, P., Arai, M., and Panpranot, J. A comparative study of strong metal-support interaction and catalytic behavior of Pd catalysts supported on micron- and nano-sized TiO₂ in liquid-phase selective hydrogenation of phenylacetylene. Journal of Molecular Catalysis A: Chemical 279(1) (2008): 133-139.
- [5] Hou, Y., et al. Immobilization of palladium in N-heterocyclic carbene functionalized SBA-15 for the catalytic application in aerobic oxidation of benzyl alcohol. Catalysis Communications 10(10) (2009): 1459-1462.
- [6] Chen, Y., et al. Solvent-free aerobic oxidation of benzyl alcohol over Pd monometallic and Au–Pd bimetallic catalysts supported on SBA-16 mesoporous molecular sieves. Applied Catalysis A: General 380(1–2) (2010): 55-65.
- [7] Sheldon, R.A., Arends, I.W.C.E., and Dijkstra, A. New developments in catalytic alcohol oxidations for fine chemicals synthesis. Catalysis Today 57(1–2) (2000): 157-166.
- [8] Dimitratos, N., Villa, A., Wang, D., Porta, F., Su, D., and Prati, L. Pd and Pt catalysts modified by alloying with Au in the selective oxidation of alcohols. Journal of Catalysis 244(1) (2006): 113-121.
- [9] Dimitratos, N., Lopez-Sanchez, J.A., and Hutchings, G.J. Selective liquid phase oxidation with supported metal nanoparticles. Chemical Science 3(1) (2012): 20-44.

- [10] Guzzi, L., Borkm, L., Schay, Z., Rao, T.S.R.P., and Dhar, G.M. Some problems on environmental catalysis. in Studies in Surface Science and Catalysis, pp. 69-80: Elsevier, 1998.
- [11] Hutchings, G.J. Supported gold and gold palladium catalysts for selective chemical synthesis. Catalysis Today 138(1-2) (2008): 9-14.
- [12] Pálincó, I. Effects of surface modifiers on the liquid-phase hydrogenation of alkenes over silica-supported platinum, palladium and rhodium catalysts I. Quinoline and carbon tetrachloride. Applied Catalysis A: General 126(1) (1995): 39-49.
- [13] Beier, M.J., Hansen, T.W., and Grunwaldt, J.-D. Selective liquid-phase oxidation of alcohols catalyzed by a silver-based catalyst promoted by the presence of ceria. Journal of Catalysis 266(2) (2009): 320-330.
- [14] Chen, H., Xu, Z., Wan, H., Zheng, J., Yin, D., and Zheng, S. Aqueous bromate reduction by catalytic hydrogenation over Pd/Al₂O₃ catalysts. Applied Catalysis B: Environmental 96(3-4) (2010): 307-313.
- [15] Chinayon, S., Mekasuwandumrong, O., Praserthdam, P., and Panpranot, J. Selective hydrogenation of acetylene over Pd catalysts supported on nanocrystalline [alpha]-Al₂O₃ and Zn-modified [alpha]-Al₂O₃. Catalysis Communications 9(14) (2008): 2297-2302.
- [16] Gómez-Quero, S., Cárdenas-Lizana, F., and Keane, M.A. Liquid phase catalytic hydrodechlorination of 2,4-dichlorophenol over Pd/Al₂O₃: Batch vs. continuous operation. Chemical Engineering Journal 166(3) (2011): 1044-1051.
- [17] Wongwaranon, N., Mekasuwandumrong, O., Praserthdam, P., and Panpranot, J. Performance of Pd catalysts supported on nanocrystalline [alpha]-Al₂O₃ and Ni-modified [alpha]-Al₂O₃ in selective hydrogenation of acetylene. Catalysis Today 131(1-4) (2008): 553-558.
- [18] Duca, D., Liotta, L.F., and Deganello, G. Liquid phase hydrogenation of phenylacetylene on pumice supported palladium catalysts. Catalysis Today 24(1-2) (1995): 15-21.
- [19] Wang, B., Lin, M., Ang, T.P., Chang, J., Yang, Y., and Borgna, A. Liquid phase aerobic oxidation of benzyl alcohol over Pd and Rh catalysts on N-doped mesoporous carbon: Effect of the surface acido-basicity. Catalysis Communications 25(0) (2012): 96-101.
- [20] Tiengchad, N., Mekasuwandumrong, O., Na-Chiangmai, C., Weerachawanasak, P., and Panpranot, J. Geometrical Confinement Effect in the Liquid-Phase

- Semihydrogenation of Phenylacetylene over Mesostructured Silica Supported Pd Catalysts. Catalysis Communications 12 (2011): 910-916.
- [21] Kang, J.H., Shin, E.W., Kim, W.J., Park, J.D., and Moon, S.H. Selective Hydrogenation of Acetylene on TiO₂-Added Pd Catalysts. Journal of Catalysis 208(2) (2002): 310-320.
- [22] Panpranot, J., Kontapakdee, K., and Praserthdam, P. Selective hydrogenation of acetylene in excess ethylene on micron-sized and nanocrystalline TiO₂ supported Pd catalysts. Applied Catalysis A: General 314(1) (2006): 128-133.
- [23] Gao, J., Zhu, Q., Wen, L., and Chen, J. TiO₂-modified nano-egg-shell Pd catalyst for selective hydrogenation of acetylene. Particuology 8(3) (2010): 251-256.
- [24] Wang, X., Wu, G., Guan, N., and Li, L. Supported Pd catalysts for solvent-free benzyl alcohol selective oxidation: Effects of calcination pretreatments and reconstruction of Pd sites. Applied Catalysis B: Environmental 115-116(0) (2012): 7-15.
- [25] Lu, C.-M., Lin, Y.-M., and Wang, I. Naphthalene hydrogenation over Pt/TiO₂-ZrO₂ and the behavior of strong metal-support interaction (SMSI). Applied Catalysis A: General 198(1-2) (2000): 223-234.
- [26] Bowker, M., et al. Model catalyst studies of the strong metal-support interaction: Surface structure identified by STM on Pd nanoparticles on TiO₂(110). Journal of Catalysis 234(1) (2005): 172-181.
- [27] Weerachawanasak, P., Mekasuwandumrong, O., Arai, M., Fujita, S.-I., Praserthdam, P., and Panpranot, J. Effect of strong metal-support interaction on the catalytic performance of Pd/TiO₂ in the liquid-phase semihydrogenation of phenylacetylene. Journal of Catalysis 262(2) (2009): 199-205.
- [28] Li, Y., et al. The effect of titania polymorph on the strong metal-support interaction of Pd/TiO₂ catalysts and their application in the liquid phase selective hydrogenation of long chain alkadienes. Journal of Molecular Catalysis A: Chemical 216(1) (2004): 107-114.
- [29] Albala, R., Olmos, D., Aznar, A.J., Baselga, J., and Gonzalez-Benito, J. Fluorescent labels to study thermal transitions in epoxy/silica composites. Journal of Colloid and Interface Science 277(1) (2004): 71-78.
- [30] Olmos, D., Aznar, A.J., Baselga, J., and Gonzalez-Benito, J. Kinetic study of epoxy curing in the glass fiber/epoxy interface using dansyl fluorescence. Journal of Colloid and Interface Science 267(1) (2003): 117-126.

- [31] Watson, H., Norstrom, A., Torrkulla, A., and Rosenholm, J. Aqueous Amino Silane Modification of E-glass Surfaces. Journal of Colloid and Interface Science 238(1) (2001): 136-146.
- [32] Phillips, L.G. and Barbano, D.M. The Influence of Fat Substitutes Based on Protein and Titanium Dioxide on the Sensory Properties of Lowfat Milk. Journal of Dairy Science 80 (1997): 2726.
- [33] Fujishima, A. Discovery and applications of photocatalysis: Creating a comfortable future by making use of light energy Japan Nanonet Bulletin 44 (2005).
- [34] Fujishima, A. Electrochemical Photolysis of Water at a Semiconductor Electrode. Nature 37 (1972): 238.
- [35] Martín, C., Rives, V., Sánchez-Escribano, V., Busca, G., Lorenzelli, V., and Ramis, G. Surface reactivity and morphology of vanadia-titania catalysts. Surface Science 251–252(0) (1991): 825-830.
- [36] Tauster, S.J. and Fung, S.C. Strong metal-support interactions: Occurrence among the binary oxides of groups IIA-VB. Journal of Catalysis 55(1) (1978): 29-35.
- [37] Bond, G.C. Catalysis, science and technology. Applied Catalysis 5(1) (1983): 134-134.
- [38] Volpe, M., Inguanta, R., Piazza, S., and Sunseri, C. Optimized bath for electroless deposition of palladium on amorphous alumina membranes. Surface and Coatings Technology 200(20–21) (2006): 5800-5806.
- [39] Cui, X., Hutt, D.A., Scurr, D.J., and Conway, P.P. The evolution of Pd/Sn catalytic surfaces in electroless copper deposition. Journal of The Electrochemical Society 158(3) (2011): D172-D177.
- [40] Chen, Y., Guo, Z., Chen, T., and Yang, Y. Surface-functionalized TUD-1 mesoporous molecular sieve supported palladium for solvent-free aerobic oxidation of benzyl alcohol. Journal of Catalysis 275(1) (2010): 11-24.
- [41] Zhan, G., et al. Liquid phase oxidation of benzyl alcohol to benzaldehyde with novel uncalcined bioreduction Au catalysts: High activity and durability. Chemical Engineering Journal 187(0) (2012): 232-238.
- [42] Dimitratos, N., et al. Solvent-free oxidation of benzyl alcohol using Au-Pd catalysts prepared by sol immobilisation. Physical Chemistry Chemical Physics 11(25) (2009): 5142-5153.
- [43] Köckritz, A., et al. Ru-catalyzed oxidation of primary alcohols. Journal of Molecular Catalysis A: Chemical 246(1–2) (2006): 85-99.

- [44] Yasu-eda, T., Kitamura, S., Ikenaga, N.-o., Miyake, T., and Suzuki, T. Selective oxidation of alcohols with molecular oxygen over Ru/CaO–ZrO₂ catalyst. Journal of Molecular Catalysis A: Chemical 323(1–2) (2010): 7-15.
- [45] Habibi, D. and Faraji, A.R. Preparation, characterization and catalytic activity of a nano-Co(II)-catalyst as a high efficient heterogeneous catalyst for the selective oxidation of ethylbenzene, cyclohexene, and benzyl alcohol. Comptes Rendus Chimie 16(10) (2013): 888-896.
- [46] Alhumaimess, M., et al. Oxidation of benzyl alcohol by using gold nanoparticles supported on ceria foam. ChemSusChem 5(1) (2012): 125-131.
- [47] Dimitratos, N., Lopez-Sanchez, J.A., Morgan, D., Carley, A., Prati, L., and Hutchings, G.J. Solvent free liquid phase oxidation of benzyl alcohol using Au supported catalysts prepared using a sol immobilization technique. Catalysis Today 122(3-4) (2007): 317-324.
- [48] Ma, C.Y., et al. Characteristics of Au/HMS catalysts for selective oxidation of benzyl alcohol to benzaldehyde. Catalysis Today 158(3–4) (2010): 246-251.
- [49] Tan, H.T., et al. Palladium nanoparticles supported on manganese oxide–CNT composites for solvent-free aerobic oxidation of alcohols: Tuning the properties of Pd active sites using MnO_x. Applied Catalysis B: Environmental 119–120(0) (2012): 166-174.
- [50] Harada, T., Ikeda, S., Miyazaki, M., Sakata, T., Mori, H., and Matsumura, M. A simple method for preparing highly active palladium catalysts loaded on various carbon supports for liquid-phase oxidation and hydrogenation reactions. Journal of Molecular Catalysis A: Chemical 268(1-2) (2007): 59-64.
- [51] Chen, Y., et al. Formation of monometallic Au and Pd and bimetallic Au–Pd nanoparticles confined in mesopores via Ar glow-discharge plasma reduction and their catalytic applications in aerobic oxidation of benzyl alcohol. Journal of Catalysis 289(0) (2012): 105-117.
- [52] Pritchard, J., et al. Direct synthesis of hydrogen peroxide and benzyl alcohol oxidation using Au-Pd catalysts prepared by sol immobilization. Langmuir 26(21) (2010): 16568-16577.
- [53] Arena, F., Cum, G., Gallo, R., and Parmaliana, A. Palladium catalysts supported on oligomeric aramides in the liquid-phase hydrogenation of phenylacetylene. Journal of Molecular Catalysis A: Chemical 110(3) (1996): 235-242.
- [54] Musolino, M.G., Cutrupi, C.M.S., Donato, A., Pietropaolo, D., and Pietropaolo, R. Liquid phase hydrogenation of 2-butyne-1,4-diol and 2-butene-1,4-diol isomers over Pd catalysts: roles of solvent, support and proton on activity

- and products distribution. Journal of Molecular Catalysis A: Chemical 195(1-2) (2003): 147-157.
- [55] Nijhuis, T.A., van Koten, G., and Moulijn, J.A. Optimized palladium catalyst systems for the selective liquid-phase hydrogenation of functionalized alkynes. Applied Catalysis A: General 238(2) (2003): 259-271.
- [56] Panpranot, J., Pattamakomsan, K., Goodwin Jr, J.G., and Praserthdam, P. A comparative study of Pd/SiO₂ and Pd/MCM-41 catalysts in liquid-phase hydrogenation. Catalysis Communications 5(10) (2004): 583-590.
- [57] Musolino, M.G., Apa, G., Donato, A., Pietropaolo, R., and Frusteri, F. Supported palladium catalysts for the selective conversion of cis-2-butene-1,4-diol to 2-hydroxytetrahydrofuran: effect of metal particle size and support. Applied Catalysis A: General 325(1) (2007): 112-120.
- [58] Campo, B.C., Volpe, M.A., and Gigola, C.E. Liquid-Phase Hydrogenation of Crotonaldehyde over Platinum- and Palladium-Based Catalysts. Industrial & Engineering Chemistry Research 48(23) (2009): 10234-10239.
- [59] Alvez-Manoli, G., et al. Stereo-selective hydrogenation of 3-hexyne over low-loaded palladium catalysts supported on mesostructured materials. Applied Catalysis A: General 387(1-2): 26-34.
- [60] Liotta, L.F., et al. Liquid phase selective oxidation of benzyl alcohol over Pd-Ag catalysts supported on pumice. Catalysis Today 66(2-4) (2001): 271-276.
- [61] Villa, A., et al. Tuning hydrophilic properties of carbon nanotubes: A challenge for enhancing selectivity in Pd catalyzed alcohol oxidation. Catalysis Today 186(1) (2012): 76-82.
- [62] Ma, Z., Yang, H., Qin, Y., Hao, Y., and Li, G. Palladium nanoparticles confined in the nanocages of SBA-16: Enhanced recyclability for the aerobic oxidation of alcohols in water. Journal of Molecular Catalysis A: Chemical 331(1-2) (2010): 78-85.
- [63] Johnston, E.V., et al. Highly Dispersed Palladium Nanoparticles on Mesocellular Foam: An Efficient and Recyclable Heterogeneous Catalyst for Alcohol Oxidation. Chemistry – A European Journal 18(39) (2012): 12202-12206.
- [64] Dandekar, A. and Vannice, M.A. Crotonaldehyde Hydrogenation on Pt/TiO₂ and Ni/TiO₂ SMSI Catalysts. Journal of Catalysis 183(2) (1999): 344-354.
- [65] Lee, D.C., Kim, J.H., Kim, W.J., Kang, J.H., and Moon, S.H. Selective hydrogenation of 1,3-butadiene on TiO₂-modified Pd/SiO₂ catalysts. Applied Catalysis A: General 244(1) (2003): 83-91.

- [66] Xu, J., Sun, K., Zhang, L., Ren, Y., and Xu, X. A highly efficient and selective catalyst for liquid phase hydrogenation of maleic anhydride to butyric acid. Catalysis Communications 6(7) (2005): 462-465.
- [67] Enache, D.I., et al. Solvent-free oxidation of benzyl alcohol using titania-supported gold-palladium catalysts: Effect of Au-Pd ratio on catalytic performance. Catalysis Today 122(3-4) (2007): 407-411.
- [68] Miedziak, P., et al. Oxidation of benzyl alcohol using supported gold-palladium nanoparticles. Catalysis Today 164(1) (2011): 315-319.
- [69] Sankar, M., et al. Controlling the duality of the mechanism in liquid-phase oxidation of benzyl alcohol catalysed by supported Au-Pd nanoparticles. Chemistry - A European Journal 17(23) (2011): 6524-6532.
- [70] Dimitratos, N., Lopez-Sanchez, J.A., Morgan, D., Carley, A., Prati, L., and Hutchings, G.J. Solvent free liquid phase oxidation of benzyl alcohol using Au supported catalysts prepared using a sol immobilization technique. Catalysis Today 122(3-4) (2007): 317-324.
- [71] Ukaji, E., Furusawa, T., Sato, M., and Suzuki, N. The effect of surface modification with silane coupling agent on suppressing the photo-catalytic activity of fine TiO₂ particles as inorganic UV filter. Applied Surface Science 254(2) (2007): 563-569.
- [72] Morrill, A.R., Duong, D.T., Lee, S.J., and Moskovits, M. Imaging 3-aminopropyltriethoxysilane self-assembled monolayers on nanostructured titania and tin (IV) oxide nanowires using colloidal silver nanoparticles. Chemical Physics Letters 473(1-3) (2009): 116-119.
- [73] Song, Y.-Y., Hildebrand, H., and Schmuki, P. Optimized monolayer grafting of 3-aminopropyltriethoxysilane onto amorphous, anatase and rutile TiO₂. Surface Science 604(3-4) (2010): 346-353.
- [74] Tan, G., Zhang, L., Ning, C., Liu, X., and Liao, J. Preparation and characterization of APTES films on modification titanium by SAMs. Thin Solid Films 519(15) (2011): 4997-5001.
- [75] Comsup, N., Panpranot, J., and Praserttham, P. The influence of Si-modified TiO₂ on the activity of Ag/TiO₂ in CO oxidation. Journal of Industrial and Engineering Chemistry 16(5) (2010): 703-707.
- [76] Adamczyk, A. and Długoń, E. The FTIR studies of gels and thin films of Al₂O₃-TiO₂ and Al₂O₃-TiO₂-SiO₂ systems. Spectrochimica Acta Part A: Molecular and Biomolecular Spectroscopy 89(0) (2012): 11-17.

- [77] Kim, J., Seidler, P., Wan, L.S., and Fill, C. Formation, structure, and reactivity of amino-terminated organic films on silicon substrates. Journal of Colloid and Interface Science 329(1) (2009): 114-119.
- [78] Shylesh, S. and Singh, A.P. Synthesis, characterization, and catalytic activity of vanadium-incorporated, -grafted, and -immobilized mesoporous MCM-41 in the oxidation of aromatics. Journal of Catalysis 228(2) (2004): 333-346.
- [79] Li, Z., et al. Comparative study of sol-gel-hydrothermal and sol-gel synthesis of titania-silica composite nanoparticles. Journal of Solid State Chemistry 178(5) (2005): 1395-1405.
- [80] Song, Y.-Y., Hildebrand, H., and Schmuki, P. Optimized monolayer grafting of 3-aminopropyltriethoxysilane onto amorphous, anatase and rutile TiO₂. Surface Science 604(3-4) (2010): 346-353.
- [81] Sohn, Y. Interfacial electronic structure and ion beam induced effect of anatase TiO₂ surface modified by Pd nanoparticles. Applied Surface Science 257(5) (2010): 1692-1697.
- [82] Sargeant, T.D., Rao, M.S., Koh, C.-Y., and Stupp, S.I. Covalent functionalization of NiTi surfaces with bioactive peptide amphiphile nanofibers. Biomaterials 29(8) (2008): 1085-1098.
- [83] J.W. Zheng, Z.H.Z., H.F. Chen, Z.F. Lui. Langmuir 16 (2000): 4409.
- [84] Kallury, K.M.R., Macdonald, P.M., and Thompson, M. Effect of Surface Water and Base Catalysis on the Silanization of Silica by (Aminopropyl)alkoxysilanes Studied by X-ray Photoelectron Spectroscopy and ¹³C Cross-Polarization/Magic Angle Spinning Nuclear Magnetic Resonance. Langmuir 10(2) (1994): 492-499.
- [85] Otto, K., Haack, L.P., and deVries, J.E. Identification of two types of oxidized palladium on γ -alumina by X-ray photoelectron spectroscopy. Applied Catalysis B: Environmental 1(1) (1992): 1-12.
- [86] Kibis, L.S., Stadnichenko, A.I., Koscheev, S.V., Zaikovskii, V.I., and Boronin, A.I. Highly oxidized palladium nanoparticles comprising Pd⁴⁺ species: Spectroscopic and structural aspects, thermal stability, and reactivity. Journal of Physical Chemistry C 116(36) (2012): 19342-19348.
- [87] Mirkelamoglu, B. and Karakas, G. The role of alkali-metal promotion on CO oxidation over PdO/SnO₂ catalysts. Applied Catalysis A: General 299(0) (2006): 84-94.

- [88] Kibis, L.S., Titkov, A.I., Stadnichenko, A.I., Koscheev, S.V., and Boronin, A.I. X-ray photoelectron spectroscopy study of Pd oxidation by RF discharge in oxygen. Applied Surface Science 255(22) (2009): 9248-9254.
- [89] Meenakshisundaram, S., et al. Oxidation of alcohols using supported gold and gold-palladium nanoparticles. Faraday Discussions 145 (2010): 341-356.
- [90] Grunwaldt, J.D., Caravati, M., and Baiker, A. Oxidic or metallic palladium: Which is the active phase in Pd-catalyzed aerobic alcohol oxidation? Journal of Physical Chemistry B 110(51) (2006): 25586-25589.
- [91] Radkevich, V.Z., Senko, T.L., Wilson, K., Grishenko, L.M., Zaderko, A.N., and Diyuk, V.Y. The influence of surface functionalization of activated carbon on palladium dispersion and catalytic activity in hydrogen oxidation. Applied Catalysis A: General 335(2) (2008): 241-251.
- [92] Sankar, M., et al. Controlling the duality of the mechanism in liquid-phase oxidation of benzyl alcohol catalysed by supported Au-Pd nanoparticles. Chemistry 17(23) (2011): 6524-32.
- [93] Li, F., Zhang, Q., and Wang, Y. Size dependence in solvent-free aerobic oxidation of alcohols catalyzed by zeolite-supported palladium nanoparticles. Applied Catalysis A: General 334(1-2) (2008): 217-226.
- [94] Mallat, T. and Baiker, A. Oxidation of Alcohols with Molecular Oxygen on Solid Catalysts. Chemical Reviews 104(6) (2004): 3037-3058.
- [95] Keresszegi, C., Grunwaldt, J.-D., Mallat, T., and Baiker, A. In situ EXAFS study on the oxidation state of Pd/Al₂O₃ and Bi-Pd/Al₂O₃ during the liquid-phase oxidation of 1-phenylethanol. Journal of Catalysis 222(1) (2004): 268-280.
- [96] Corma, A. and Domine, M.E. Gold supported on a mesoporous CeO₂ matrix as an efficient catalyst in the selective aerobic oxidation of aldehydes in the liquid phase. Chemical Communications (32) (2005): 4042-4044.
- [97] Abad, A., Almela, C., Corma, A., and Garcia, H. Unique gold chemoselectivity for the aerobic oxidation of allylic alcohols. Chemical Communications (30) (2006): 3178-3180.
- [98] Roelofs, J.C.A.A. and Berben, P.H. First example of high loaded polymer-stabilized nanoclusters immobilized on hydrotalcite: effects in alkyne hydrogenation. Chemical Communications (8) (2004): 970-971.
- [99] Torok, B., Szollosi, G., Balazsik, K., Felfoldi, K., Kun, I., and Bartok, M. Ultrasonics in heterogeneous metal catalysis: sonochemical chemo- and enantioselective hydrogenations over supported platinum catalysts. Ultrasonics Sonochemistry 6(1-2) (1999): 97-103.

- [100] Kumar, N., Masloboischikova, O.V., Kustov, L.M., Heikkila, T., Salmi, T., and Murzin, D.Y. Synthesis of Pt modified ZSM-5 and beta zeolite catalysts: Influence of ultrasonic irradiation and preparation methods on physico-chemical and catalytic properties in pentane isomerization. Ultrasonics Sonochemistry 14(2) (2007): 122-130.
- [101] Bernal, S., et al. Some contributions of electron microscopy to the characterisation of the strong metal-support interaction effect. Catalysis Today 77(4) (2003): 385-406.
- [102] J.F.Moulder, W.F.S., P.E. Sobol, K.D. Bomben. in J.Chastain (ed.)Handbook of X-Ray Photoelectron Spectroscopy Eden-Prairie, MN: Perkin-Elmer Corp., 1992.
- [103] Panpranot, J., Phandinthong, K., Sirikajorn, T., Arai, M., and Prasertthdam, P. Impact of palladium silicide formation on the catalytic properties of Pd/SiO₂ catalysts in liquid-phase semihydrogenation of phenylacetylene. Journal of Molecular Catalysis A: Chemical 261(1) (2007): 29-35.
- [104] Dominguez-Dominguez, S., Berenguer-Murcia, A., Linares-Solano, A., and Cazorla-Amoros, D. Inorganic materials as supports for palladium nanoparticles: Application in the semi-hydrogenation of phenylacetylene. Journal of Catalysis 257(1) (2008): 87-95.
- [105] Molnar, A.r., Sarkany, A., and Varga, M. Hydrogenation of carbon-carbon multiple bonds: chemo-, regio- and stereo-selectivity. Journal of Molecular Catalysis A: Chemical 173(1-2) (2001): 185-221.



APPENDICES

จุฬาลงกรณ์มหาวิทยาลัย
CHULALONGKORN UNIVERSITY

APPENDIX A

CALCULATION FOR SURFACE MODIFICATION OF TiO₂ WITH APTES

Surface modification of TiO₂ support with APTES various concentrations were prepared by post synthesis grafting method.

Reagents: - 3-(aminopropyl)triethoxysilane (APTES)

Mw = 221.37 g/mol, density= 0.946 g/ml at 25°C

- Anhydrous toluene (C₆H₅CH₃)

- Titanium dioxide (TiO₂)

Example calculation:

Preparation stock solution 100 ml of 50 mM APTES in anhydrous toluene

In solution 1000 ml consisted of APTES 50×10^{-3} mole

In solution 100 ml consisted of APTES $\frac{50 \times 10^{-3} \times 100}{1000} = 5 \times 10^{-3}$ mole

APTES required $5 \times 10^{-3} \times \frac{221.37}{0.946} = 1.170$ ml

So that pipette 1.170 ml mixed with anhydrous toluene in volumetric flask 100 ml.

➤ For modification of 1.5 g TiO₂ support with 25 ml of APTES solution

From $M_1V_1 = M_2V_2$

1) Prepared 25 ml of 0.1 mM APTES in anhydrous toluene

So that 0.1 mM APTES has been used 50 mM APTES stock solution (V₁)

$$(50\text{mM})(V_1) = (0.1\text{mM})(25\text{ml})$$

$$V_1 = 0.05 \text{ ml}$$

2) So that 1 mM APTES has been used 50 mM APTES stock solution V₁ = 0.5 ml

3) So that 10 mM APTES has been used 50 mM APTES stock solution V₁ = 5 ml

APPENDIX B

CALCULATION FOR PREPARATION OF 1%Pd/TiO₂ CATALYSTS BY
ELECTROLESS DEPOSITION

- Reagents:
- Titanium dioxide (TiO₂ and TiO₂-xAPTES)
 - Palladium chloride (PdCl₂), Mw = 177.32 g/mol
 - Hydrochloric acid (HCl 37%)
 - Sodium hypophosphite (NaH₂PO₂·H₂O), Mw = 105.99 g/mol

➤ Basic calculation of TiO₂ pretreating process

Prepared 50 ml of 14%HCl from 37%HCl for pretreated TiO₂ supports

$$M_1V_1 = M_2V_2$$

$$(14\%)(50\text{ml}) = (37\%)(V_2)$$

$$V_2 = \frac{14 \times 50}{37} = 18.92 \text{ ml}$$

So that we can prepare 14%HCl from pipetted 18.92 ml of 37%HCl diluted with DI-water in 50 ml volumetric flask.

➤ Calculations for 50 ml of Pd electroless plating bath

1) Preparation 1% wt. of Pd supported on TiO₂ catalyst (1 g of catalyst)

$$\text{TiO}_2 \text{ 99 g consisted of Pd} = 1 \text{ g}$$

$$\text{TiO}_2 \text{ 1 g consisted of Pd} = \frac{1}{99} \text{ g}$$

$$\text{Pd 106.42 g obtained from PdCl}_2 = 177.32 \text{ g}$$

$$\text{Pd } \frac{1}{99} \text{ g obtained from PdCl}_2 = \frac{177.32 \times (\frac{1}{99})}{106.42} = 0.0168 \text{ g}$$

In this method we used sodium hypophosphite as a reducing agent.

2) The ratio between Pd : NaH₂PO₂·H₂O = 1:10 (by mole)

$$\text{Mole of Pd used} = \frac{0.0168}{177.32} = 9.474 \times 10^{-5} \text{ mole}$$

$$\text{Mole of NaH}_2\text{PO}_2 \cdot \text{H}_2\text{O} = 10 \times 9.474 \times 10^{-5} = 9.474 \times 10^{-4} \text{ mole}$$

$$\text{Weight of NaH}_2\text{PO}_2 \cdot \text{H}_2\text{O} = 9.474 \times 10^{-4} \times 105.99 = 0.1004 \text{ g}$$

Therefore in a Pd electroless plating bath, we dissolved 0.0168 g of PdCl₂, 0.2 ml of HCl (37%), 8 ml of NH₄OH, and 0.1004 g of NaH₂PO₂·H₂O in 50 ml volumetric flask which was adjusted by DI-water.

APPENDIX C

CALCULATION FOR PREPARATION OF 1%Pd/TiO₂ CATALYSTS BY
SONOCHEMICAL METHOD

Reagents: - Titanium dioxide (TiO₂ and TiO₂-xAPTES)
 - Palladium nitrate hexahydrated (Pd(NO₃)₂. 6H₂O), Mw = 338.52 g/mol
 - Hydrazine hydrated (NH₂NH₂. H₂O)
 Mw = 50.06 g/mol, density = 1.032 g/ml at 25°C

➤ Basic calculation for preparation of 1% wt. of Pd for 1 g of TiO₂ support

$$\begin{aligned} \text{TiO}_2 \text{ 99 g consisted of Pd} &= 1 \text{ g} \\ \text{TiO}_2 \text{ 1 g consisted of Pd} &= \frac{1}{99} \text{ g} \\ \text{Pd 106.42 g obtained from Pd(NO}_3)_2 \cdot 6\text{H}_2\text{O} &= 338.52 \text{ g} \\ \text{Pd } \frac{1}{99} \text{ g obtained from Pd(NO}_3)_2 \cdot 6\text{H}_2\text{O} &= \frac{338.52 \times \frac{1}{99}}{106.42} = 0.0321 \text{ g} \end{aligned}$$

Therefore we dissolved 0.0321 g of Pd(NO₃)₂. 6H₂O in 25 ml of DI-water

➤ Calculation the quantitative of hydrazine hydrate

In this method, hydrazine hydrate was used as a reducing agent and the ratio between Pd : hydrazine hydrate = 1:10 (mole/mole)

$$\begin{aligned} \text{Mole of Pd used in the solution} &= \frac{0.0321}{338.52} = 9.482 \times 10^{-5} \text{ mole} \\ \text{Mole of hydrazine hydrate} &= 10 \times 9.482 \times 10^{-5} = 9.482 \times 10^{-4} \text{ mole} \\ \text{Thus hydrazine hydrate} &= 9.482 \times 10^{-4} \times \frac{50.06}{1.032} \text{ ml} \\ &= 0.0460 \text{ ml} \end{aligned}$$

Therefore, 25 ml of Pd solution was consisted of 0.046 ml of hydrazine hydrate.

APPENDIX D

CALCULATION FOR PREPARATION OF 1%Pd/TiO₂ CATALYSTS BY
SOL IMMOBILIZATION METHOD

- Reagents:
- TiO₂ and TiO₂-xAPTES
 - Palladium chloride (PdCl₂), Mw = 177.32 g/mol
 - Polyvinyl alcohol (PVA, 80% hydrolyzed), Mw 89,000-98,000
 - Sodium borohydride (NaBH₄), Mw=37.83 g/mol

- Calculation for preparation of 1% wt. of Pd for 1 g of TiO₂ support

$$\text{TiO}_2 \text{ 99 g consisted of Pd} = 1 \text{ g}$$

$$\text{TiO}_2 \text{ 1 g consisted of Pd} = \frac{1}{99} \text{ g}$$

$$\text{Pd 106.42 g obtained from PdCl}_2 = 177.32 \text{ g}$$

$$\text{Pd } \frac{1}{99} \text{ g obtained from PdCl}_2 = \frac{177.32 \times \frac{1}{99}}{106.42} = 0.0168 \text{ g}$$

From 6.25 g/dm³ of PdCl₂ stock solution, we have to pipette PdCl₂ solution;

$$\text{PdCl}_2 \text{ 6.25 g obtained from PdCl}_2 \text{ stock solution} \quad 1000 \text{ ml}$$

$$\text{PdCl}_2 \text{ 0.0168 g obtained from PdCl}_2 \text{ stock solution} \quad \frac{1000 \times 0.0168}{6.25} \text{ ml}$$

$$= 2.688 \text{ ml}$$

- Calculation for preparation of 1% wt. of PVA aqueous solution

$$\text{Solution 100 ml consisted of PVA} = 1 \text{ g}$$

$$\text{Solution 10 ml consisted of PVA} = \frac{1 \times 10}{100} = 0.1 \text{ g}$$

In this experiment, the ratio of PVA: Pd = 1.2 (wt./wt.)

$$\text{PVA that used in this experiment} = 1.2 \times \frac{1}{99} = 0.0121 \text{ g}$$

$$\text{Thus, we have to pipette the PVA solution} = \frac{10 \times 0.0121}{0.1} = 1.21 \text{ ml}$$

➤ Calculation for preparation of 0.1M of NaBH₄

$$\text{Solution 1000 ml consisted of NaBH}_4 = 0.1 \text{ mol}$$

$$\text{Solution 10 ml consisted of NaBH}_4 = \frac{0.1 \times 10}{1000} = 0.001 \text{ mol}$$

Therefore, we have to weight NaBH₄ = 0.001 × 37.83 = 0.0378 g diluted in 10 ml of volumetric flask with DI-water

The ratio of NaBH₄: Pd = 5:1 (mol/mol)

$$\text{So that, Pd } \left(\frac{1}{99 \times 106.42} \right) \text{ mol required NaBH}_4 = \frac{5}{99 \times 106.42} = 4.746 \times 10^{-4} \text{ mol}$$

$$\begin{aligned} \text{NaBH}_4 \text{ 4.7458 mol obtained from 0.1M NaBH}_4 &= \frac{4.746 \times 10^{-4} \times 1000}{0.1} \text{ ml} \\ &= 4.746 \text{ ml} \end{aligned}$$

In this experiment, we used 2.688 ml of PdCl₂ stock solution, 1.21 ml of PVA (1% wt. aqueous solution), and 4.746 ml of 0.1M NaBH₄ to reduced PdCl₂ solution for 1 g of TiO₂ support.

APPENDIX E

CALCULATION FOR PREPARATION OF 1%Pd/TiO₂ CATALYSTS BY
INCIPIENT WETNESS IMPREGNATION METHOD

Preparation of 1%Pd/TiO₂ catalysts by the incipient wetness impregnation method are shown as follows:

Reagent: - Titanium dioxide (TiO₂)
 - Palladium nitrate hexahydrated (Pd (NO₃)₂.6H₂O)
 Mw =338.52 g/mol

Example Calculation for the preparation of 1%Pd/TiO₂

Based on 100 g of catalyst used, the composition of the catalyst will be as follows:

| | | | |
|------------------|---|-------|--------|
| Palladium | = | 1 g | |
| Titanium dioxide | = | 100-1 | = 99 g |

For 3 g of TiO₂

Palladium required = $3 \times \left(\frac{1}{99}\right)$ = 0.0303 g

Palladium 0.0303 g was prepared from Pd (NO₃)₂.6H₂O and molecular weight of Pd is 106.42

$$\begin{aligned} \text{Pd (NO}_3)_2 \cdot 6\text{H}_2\text{O required} &= \frac{\text{Mw of Pd(NO}_3)_2 \cdot 6\text{H}_2\text{O} \times \text{Pd required}}{\text{Mw of Pd}} \\ &= (338.52/106.42) \times 0.0303 = 0.0964 \text{ g} \end{aligned}$$

Since the pore volume of the TiO₂ support is 0.4 ml/g. Thus, the total volume of impregnation solution which must be used is 1.2 ml for 3 g of TiO₂. The DI-water is added until equal pore volume to dissolve palladium nitrate hexahydrated.

APPENDIX F

CALCULATION OF THE CRYSTALLITE SIZE

Calculation of the crystallite size by Debye-Scherrer equation

The crystallite size was calculated from the half-height width of the diffraction peak of XRD pattern using the Debye-Scherrer equation.

From Scherrer equation:

$$D = \frac{K\lambda}{\beta \cos\theta} \quad (\text{B.1})$$

- Where
- D = Crystallite size, Å
 - K = Crystallite-shape factor = 0.9
 - λ = X-ray wavelength, 1.54056 Å for CuK α
 - θ = Observed peak angle, degree
 - β = X-ray diffraction broadening, radian

The X-ray diffraction broadening (β) is the pure width of a powder diffraction free from all broadening due to the experimental equipment. Corundum was used as a standard sample to observe the instrumental broadening. The X-ray diffraction broadening (β) can be obtained by using Warren's formula.

From Warren's formula:

$$\beta = \sqrt{B_M^2 - B_S^2} \quad (\text{B.2})$$

- Where
- B_M = The measured peak width in radians at half peak height.
 - B_S = The corresponding width of the standard material.

Example: Calculation of the crystallite size of TiO_2

$$\begin{aligned} \text{The half-height width of peak} &= 0.13^\circ \text{ (from figure B.1)} \\ &= (2\pi \times 0.13)/360 \\ &= 0.00227 \text{ radian} \end{aligned}$$

The corresponding half-height width of peak of corundum = 0.000329 radian

$$\begin{aligned} \text{The pure width} &= \sqrt{B_M^2 - B_S^2} \\ &= \sqrt{0.00227^2 - 0.000329^2} \\ &= 0.00225 \text{ radian} \end{aligned}$$

$$\beta = 0.00225 \text{ radian}$$

$$2\theta = 25.32^\circ$$

$$\theta = 12.66^\circ$$

$$\lambda = 1.54056 \text{ \AA}$$

$$\begin{aligned} \text{The crystallite size} &= \frac{0.9 \times 1.54056}{0.00225 \cos 12.66} = 631.58 \text{ \AA} \\ &= 63.2 \text{ nm} \end{aligned}$$

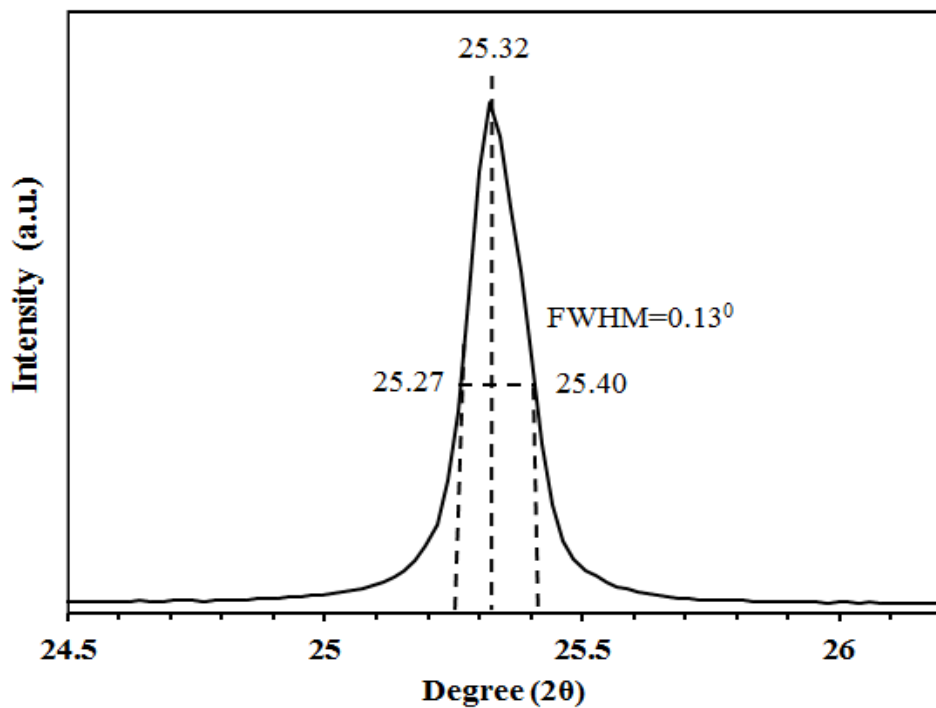


Figure B.1 The measured peak of TiO₂ for calculation the crystallite size.

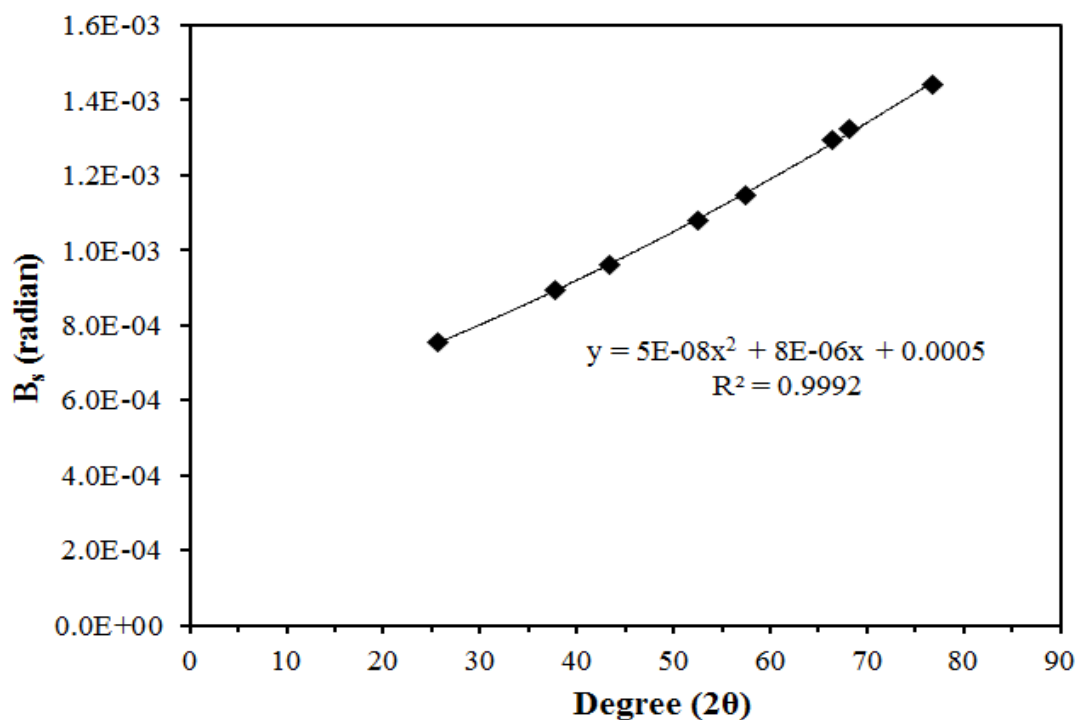


Figure B.2 The plot indicating the value of line broadening due to the equipment.

The data were obtained by using corundum as a standard

APPENDIX G

CALCULATION OF LATTICE PARAMETERS

The lattice parameter calculation based on Bragg's law

From Bragg's law:

$$d = \frac{n\lambda}{2\sin\theta} \quad (\text{C.1})$$

where

d is d spacing (Å)

n is integer (1)

λ is X-ray wavelength, 1.54056 Å for CuK α

θ is Observed peak angle (radian) In case of cubic phase

$$d = \frac{n\lambda}{2\sin\theta} = \frac{a}{\sqrt{h^2 + k^2 + l^2}} \quad (\text{C.2})$$

Example: Calculation of the d-spacing of TiO₂

An interesting diffraction peak is the (101) plane occurred at the 2θ of 25.32°

$$\text{Or } \theta = 25.32^\circ / 2 = 12.66^\circ$$

$$\theta = 0.221 \text{ radian} \quad (\text{C.3})$$

Therefore, the d-spacing is calculated by substitution (C.3) into (C.1) and estimated a value from equation (C.2)

$$d = \frac{1.54056}{2 \sin(0.221)} = 3.515 \text{ Å} = 0.3515 \text{ nm}$$

$$\text{From (C.2)} \quad a = d \times \sqrt{2} = 0.3515 \times \sqrt{2} = 0.4971 \text{ nm}$$

Calculated lattice parameters (a, b) from the TiO₂ (200) plane

$$2\theta = 48.06^\circ$$

$$\theta = 48.06^\circ / 2 = 24.03^\circ = 0.419 \text{ radian}$$

Therefore, the d-spacing is calculated by substitution (C.3) into (C.1) and estimated a value from equation (C.2)

$$d = \frac{1.54056}{2 \sin(0.419)} = 1.8915 \text{ \AA} = 0.18915 \text{ nm}$$

From (C.2)

$$d = \frac{n\lambda}{2\sin\theta} = \frac{a}{\sqrt{h^2+k^2+l^2}}$$

$$d = \frac{a}{\sqrt{2^2+0^2+0^2}}$$

$$a = 2xd = 2 \times 0.18915 = 0.3783 \text{ nm} = 3.7830 \text{ \AA}$$

In case of tetragonal phase ($a=b, \neq c$)

$$\frac{1}{d^2} = \frac{h^2+k^2}{a^2} + \frac{l^2}{c^2} \quad (\text{C.4})$$

$$c = \sqrt{\frac{1}{\left(\frac{1}{d^2} - \frac{1}{a^2}\right)}} \quad (\text{C.5})$$

Substituted $d=0.3515 \text{ nm}$, $a= 0.3783 \text{ nm}$ in equation (C.5)

$$c = \sqrt{\frac{1}{\left(\frac{1}{0.3515^2} - \frac{1}{0.3783^2}\right)}}$$

$$c = 0.9508 \text{ nm} = 9.510 \text{ \AA}$$

Therefore, the tetragonality $\left(\frac{c}{a}\right)$ was calculated as following;

$$\frac{c}{a} = \frac{9.510}{3.783} = 2.51$$

APPENDIX H

CALCULATION FOR METAL ACTIVE SITES AND DISPERSION

Calculation of the metal active sites and metal dispersion of the catalyst measured by CO adsorption is as follows:

Calculation of metal active site

| | | |
|---|---|-------------------------------|
| Let the weight of catalyst used | = W | g |
| Integral area of CO peak after adsorption | = A | unit |
| Integral area of 75 μ l of standard CO peak | = B | unit |
| Amounts of CO adsorbed on catalyst | = B-A | unit |
| Volume of CO adsorbed on catalyst | = $75 \times [(B-A)/B]$ | μ l |
| Volume of 1 mole of CO at 30°C | = 24.86×10^6 | μ l |
| Mole of CO adsorbed on catalyst | = $[(B-A)/B] \times [75/24.86 \times 10^6]$ | mole |
| Molecule of CO adsorbed on catalyst | = $[3.02 \times 10^{-6}] \times [6.02 \times 10^{23}] \times [(B-A)/B]$ | molecules |
| Metal active sites | = $1.82 \times 10^{18} \times [(B-A)/B] \times [1/W]$ | molecules of CO/g of catalyst |

Calculation of %metal dispersion

Definition of % metal dispersion:

$$\text{Metal dispersion (\%)} = 100 \times \frac{\text{molecules of Pd from CO adsorption}}{\text{molecules of Pd loaded}}$$

In this study, the formula from Chemisorb 2750 Operator's Manual can be used for determining the % metal dispersion as follows:

$$\%D = S_f \times \left[\frac{V_{\text{ads}}}{V_g} \right] \times \left[\frac{M_w}{\%M} \right] \times 100\% \times 100\% \dots \dots \dots (1)$$

Where

| | | |
|-----------|---|---|
| %D | = | %metal dispersion |
| S_f | = | stoichiometry factor, (CO on Pd* =1) |
| V_{ads} | = | volume adsorbed (cm ³ /g) |
| V_g | = | molar volume of gas at STP = 22414 (cm ³ /mol) |
| Mw | = | molecular weight of the metal (a.m.u.) |
| %M | = | %metal loading |

Example: %Dispersion of 1%Pd/TiO₂(I)-R40

- Calculation Volume Chemisorbed (V_{ads})

$$V_{ads}(\text{cm}^3) = \left[\frac{V_{inj}}{m} \right] \times \sum_{i=1}^n \left(1 - \frac{A_i}{A_f} \right) \dots\dots\dots(2)$$

Where:

| | | |
|-----------|---|--|
| V_{inj} | = | volume injected (cm ³) = 0.075 cm ³ |
| m | = | mass of sample (g) |
| A_i | = | area of peak i |
| A_f | = | area of last peak |

To replace values in equation (1) and (2);

$$\begin{aligned}
 V_{ads} &= \left[\frac{0.075}{0.0235} \right] \times \left[\left(1 - \frac{0.010}{0.143} \right) + \left(1 - \frac{0.142}{0.143} \right) \right] \\
 &= 0.345 \text{ cm}^3 \\
 \%D &= 1 \times \left[\frac{0.345}{22414} \right] \times \left[\frac{106}{1} \right] \times 100\% \times 100\% \\
 &= 16.4\%
 \end{aligned}$$

So that %Pd dispersion is 16.4%

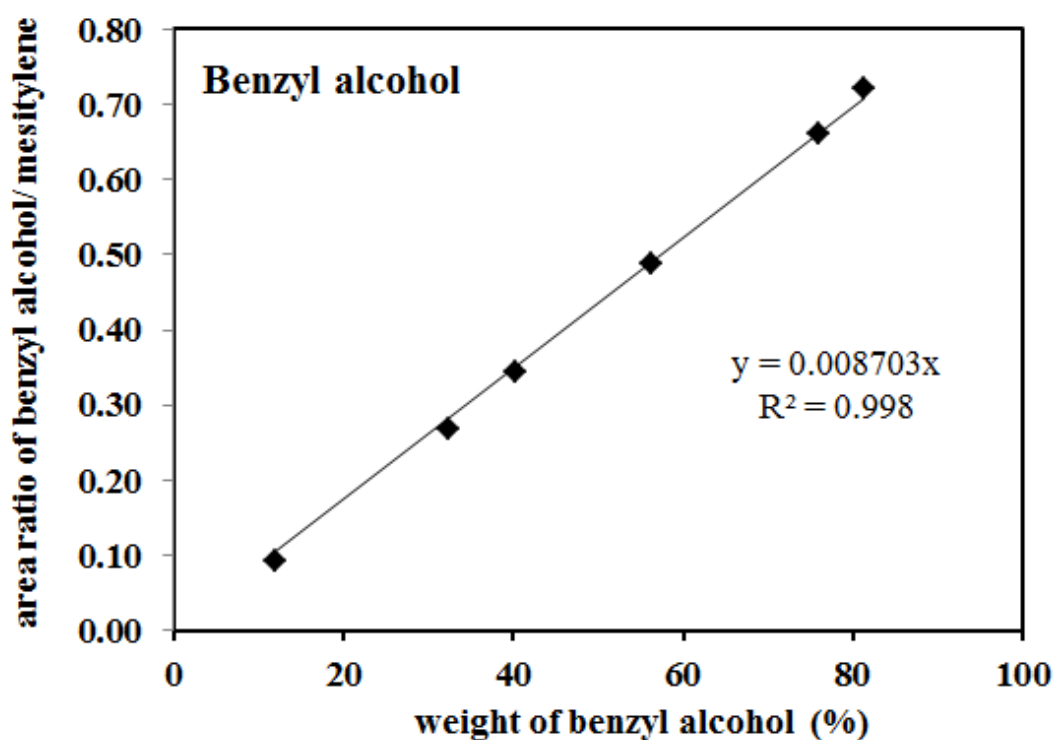
APPENDIX I

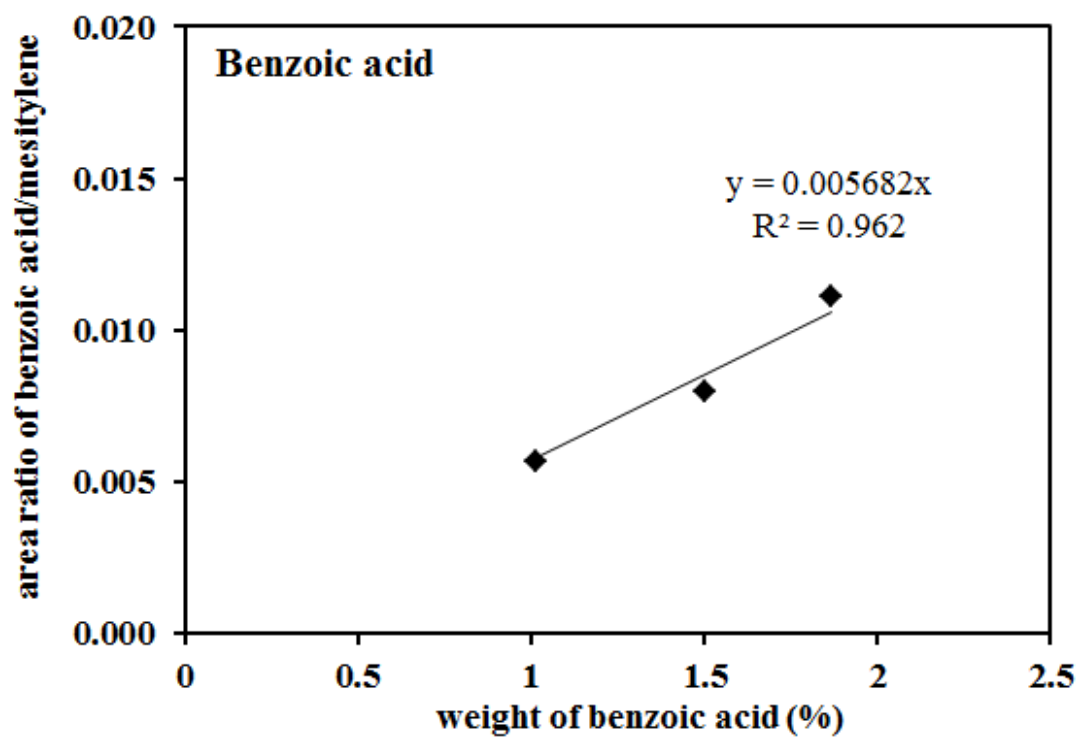
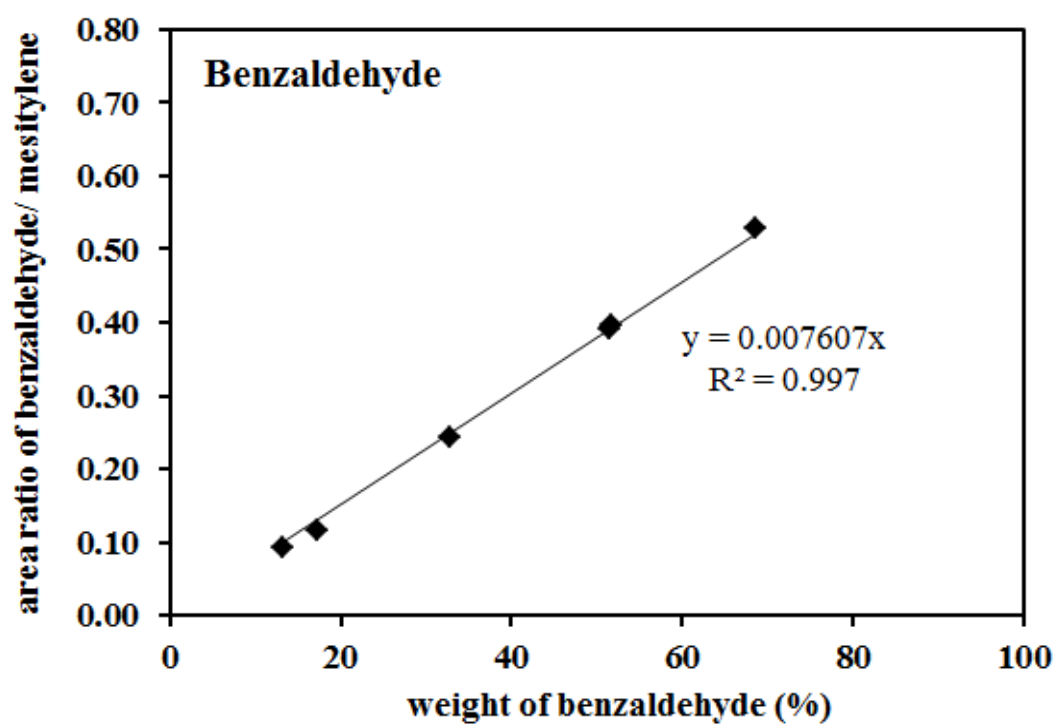
CALCULATION OF BENZYL ALCOHOL CONVERSION AND BENZALDEHYDE
SELECTIVITY

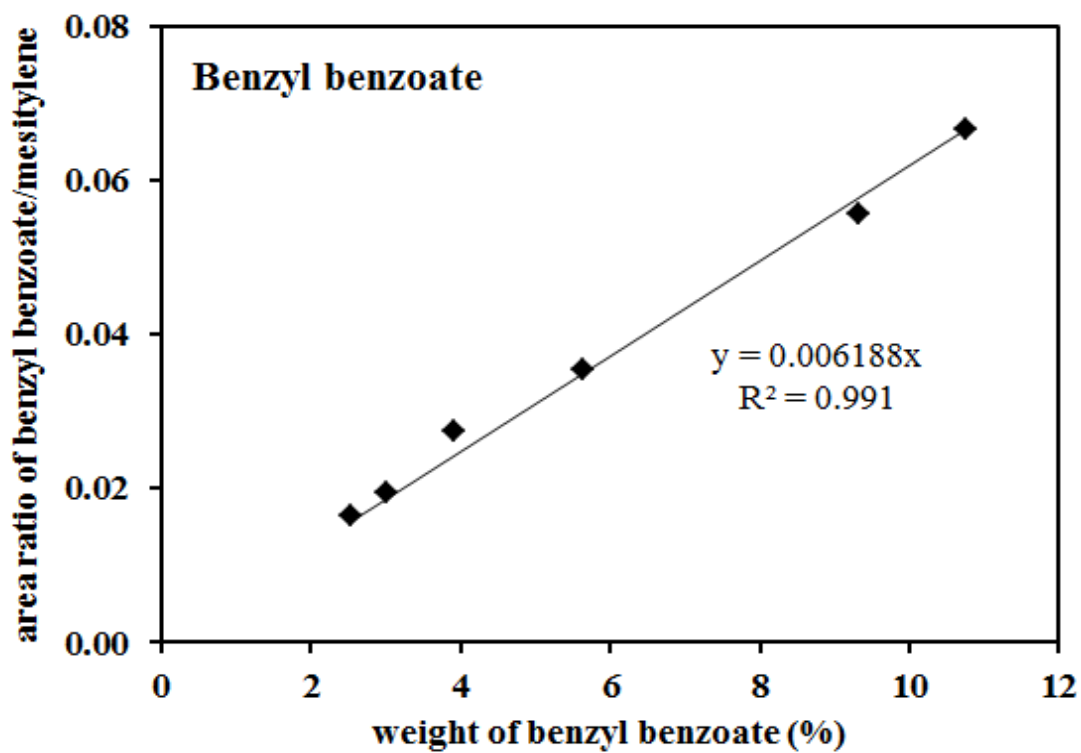
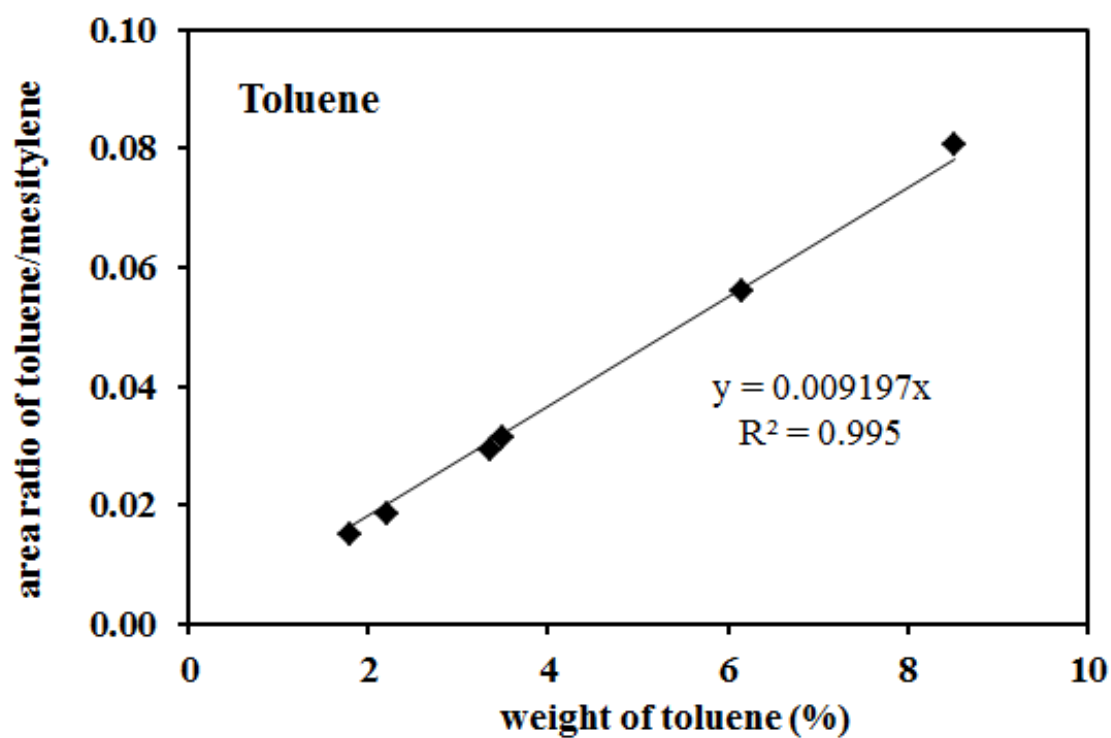
In this experimental, we used mesitylene as an internal standard for GC analysis. The calibration curves of benzyl alcohol (BA) and all products are demonstrated. In addition, the conversion of benzyl alcohol and selectivity of benzaldehyde are shown as following:

$$\% \text{ conversion of BA} = \frac{\text{wt.\% of BA in feed} - \text{wt.\% of BA in product}}{\text{wt.\% of BA in feed}} \times 100$$

$$\% \text{ selectivity of benzaldehyde} = \frac{\text{wt.\% of benzaldehyde}}{\text{total wt.\% of all products}} \times 100$$







APPENDIX J

CALCULATIONS OF ALKYNES CONVERSION AND ALKENES SELECTIVITY

The catalytic performance of liquid-phase selective hydrogenations of alkyne was evaluated in term of alkyne conversion and alkene selectivity. In this research, alkyne molecules are 3-hexyn-1-ol and phenylacetylene. The consequence desired products are cis-3-hexen-1-ol and styrene, respectively.

$$\% \text{ conversion of alkyne} = \frac{\text{mole of alkyne in feed} - \text{mole of alkyne in product}}{\text{mole of alkyne in feed}} \times 100$$

$$\% \text{ selectivity of alkene} = \frac{\text{mole of desired product (alkene)}}{\text{mole of total products}} \times 100$$

APPENDIX K

LIST OF PUBLICATIONS

1. Patcharaporn Weerachawanasak, Piyasan Praserthdam, and Joongjai Panpranot, "Liquid-Phase Hydrogenation of Phenylacetylene Over the Nano-sized Pd/TiO₂ Catalysts", *Journal of Nanoscience and Nanotechnology*, 14 (4) (2014), 3170-3175.
2. Patcharaporn Weerachawanasak, Graham. J. Hutchings, Jennifer K. Edwards, Simon A. Kondrat, Peter J. Miedziak, Piyasan Praserthdam, and Joongjai Panpranot, "Surface functionalized TiO₂ supported Pd catalysts for solvent-free selective oxidation of benzyl alcohol", *Catalysis Today* (accepted)
3. Jarutphon Sittikun, Yuttanant Boonyongmaneerat, Patcharaporn Weerachawanasak, Piyasan Praserthdam, Joongjai Panpranot, "Pd/TiO₂ catalysts prepared by electroless deposition with and without SnCl₂ sensitization for the liquid-phase hydrogenation of 3-hexyn-1-ol", *Reaction Kinetics Mechanisms And Catalysis*, 111 (2013), 123-135.
4. Napaporn Tiengchad, Okorn Mekasuwandumrong, Chayanin Na-Chiangmai, Patcharaporn Weerachawanasak, Joongjai Panpranot, "Geometrical confinement effect in the liquid-phase semihydrogenation of phenylacetylene over mesostructured silica supported Pd catalysts" *Catalysis Communications*, 12 (10) (2011), 910-916.
5. Patcharaporn Weerachawanasak, Piyasan Praserthdam, and Joongjai Panpranot, "Surface functionalized TiO₂ supported Pd catalysts for solvent-free selective oxidation of benzyl alcohol", *Oral presentation in the framework of the*

Catalysis on Advanced Materials symposium, IMRC (XXII International Materials Research Congress) at Cancun, Mexico, August 11-15, 2013.

6. Patcharaporn Weerachawanasak, Piyasan Praserthdam, and Joongjai Panpranot, “Effect of Pd dispersion on the strong metal-support interaction in Pd/TiO₂ catalysts” Poster presentation in *RGJ-Ph.D. Congress XIV at Pattaya, Chonburi, April 5-7, 2013.*



VITA

Miss Patcharaporn Weerachawanasak was born on July 13th, 1982 in Nakhonsawan, Thailand. She received the Bachelor's Degree in Chemistry Science from Kasetsart University in April 2005 and Master's Degree in Chemical engineering, Chulalongkorn University in May, 2008. She entered the doctor of Engineering program in Chemical engineering at Chulalongkorn University.

